EROSIONAL DRAINAGE NETWORK:

DEVELOPMENT AND ANALYSIS

UNDER SIMULATED RAINFALL

By

AYODELE O. OGUNLELA

Bachelor of Science in Agricultural Engineering
University of Ibadan
Ibadan, Nigeria
1980

Master of Science
Iowa State University
Ames, Iowa
1985

Submitted to the Faculty of the
Graduate College of the
Oklahoma State University
in partial fulfillment of
the requirements for
the Degree of
DOCTOR OF PHILOSOPHY
December, 1989

EROSIONAL DRAINAGE NETWORK:

DEVELOPMENT AND ANALYSIS

UNDER SIMULATED RAINFALL

Thesis Approved:

Bruce Wilson

Thesis Adviser

Dan W. Green

Charles E. Pugh

C. Harman

Arlin D. Wiebe

Norman N. Durham

Dean of the Graduate College

PREFACE

This thesis reports on the study of the effects of rainfall intensity and soil profile condition on drainage network development in a laboratory environment. Rainfall was artificially applied at two levels (relatively high and low levels) on soil surfaces of two different roughness conditions. Drainage basin parameters were obtained for each situation. The results obtained for the different situations were analyzed and compared for statistical significance. The research involved the development of procedures for identifying rills (channels) from point elevation data.

Acknowledgement is due to the following who contributed immensely to the success of this work:

Dr. Bruce N. Wilson, my major advisor, for his guidance, encouragement, and constant readiness to help at all times.

Dr. C. Tom Haan, Dr. Jan Wagner, Dr. Charles E. Rice and Dr. Arlin D. Nicks, members of my graduate committee, for their help and guidance throughout the course of this study.

Dr. David R. Thompson, for allowing the use of university facilities.

Chris Rice, Maolin Zheng, Randy Richardson and Bill Brown, for their help in plot preparation and data collection.

Wayne Kiner, Mark Appleman, Mark Marston, Robert Harrington, Robert Harshman, Bruce Lambert and Gordon Couger, for their help at various phases of the research.

Shirley Motsinger, for typing the dissertation.

My wife, Laide, and daughters, 'Bunmi and Tolu, for their patience and support throughout the course of this study.

TABLE OF CONTENTS

LIST OF TABLES

LIST OF FIGURES

CHAPTER I

INTRODUCTION

Soil erosion may be defined as the detachment and transportation of soil particles by wind or water. Closely associated with erosion is sedimentation. Sedimentation occurs when the sediment load exceeds the transport capacity of the flow. Net sediment yield is therefore a function of erosion and sedimentation processes. While wind erosion may be of concern in some areas, water erosion is of greater concern in most parts of the world.

Soil erosion and sedimentation have adverse effects on agricultural productivity and on water quality in fluvial systems. Plant nutrients and fine particles are selectively removed, causing poor soil tilth and reduction in soil productivity. Sediment transport results in stream pollution. Sediment carries soil-absorbed chemicals which pollute the water and result in degradation of water quality. Different researchers (Beasley et al., 1980; Tubbs and Haith, 1981) have addressed the problem of nonpoint-source pollutants in agricultural runoff. They recognized the importance of sediment transport in this problem. Also, sediment deposition in reservoirs, stream channels and other conveyance structures reduces their capacity, thus reducing

the efficiency of these structures in their intended usage.

Soil erosion and sedimentation problems sometimes require costly solutions. The restoration of the value of an eroded agricultural land requires increased production inputs of fertilizers, mechanization and management practices. Sediment removal from public water supplies, reservoirs, stream channels and other conveyance structures is costly. Erosion-related costs have been estimated to be between $3.2 to $13 billion per year in the United States (Clark et al., 1985).

An important component in the erosion process is rill erosion. Schwab et al. (1966) have identified rill erosion as the most common form of erosion. The United States Department of Agriculture (USDA, 1985) listed inadequate knowledge of the mechanisms of erosion as one of the problems of predicting soil erosion. USDA (1985) further stressed the need for the development of predictive equations for rill erosion as distinct from those of interrill erosion. There is therefore a need for more specific investigation into rill erosion.

Rill erosion results from a concentration of overland flow and involves soil removal from small channels (rills). The development of these drainage channels (rill network) is a major feature of the erosion and sedimentation processes. The size and extent of these channels depend on the magnitude of flow concentrations, the nature of the soil,

topographic features, and other hydraulic and hydrologic variables.

The drainage characteristics of large river systems have been investigated for many years (Davis, 1895; Hadley and Schumm, 1961; Carlston, 1963). A major problem in these studies is isolating a particular variable of interest because of complex interrelationships among hydrologic, hydraulic and topographic variables. Laboratory experiments provide a means of alleviating this problem. Experiments can be conducted under controlled conditions and the effects of certain variables can be isolated and investigated. Also, a laboratory provides suitable environment for instrumentation systems that cannot be efficiently operated in the field.

The research objectives of this study were:

1. To gather point elevation data for analysis of network development in a laboratory-controlled environment;
2. To determine flow paths and drainage networks from point elevation data;
3. To analyze the effects of rainfall intensity and soil profile condition on drainage network development.

CHAPTER II

LITERATURE REVIEW

Introduction

In Chapter I, the importance of the soil erosion problem was emphasized. Two approaches used in erosion studies are experimentation and modeling. Researchers have used both approaches to gain a better understanding of the erosion process. The effects of different factors on soil erosion have been investigated and instrumentation systems have been developed to facilitate erosion research.

In this chapter, pertinent literature is reviewed. The topics to be covered include empirical soil erosion studies, erosion modeling, soil surface description, instrumentation, interpolation techniques, geomorphic studies and parameter variability.

Empirical Soil Erosion Studies

Over the years, many studies have been conducted to determine the effects of different factors on erosion. Since rainfall and runoff drive soil detachment and transport, factors that affect hydrologic and hydraulic processes also affect the erosion process. As shown by Park et al. (1981), additional factors relating to soil

characteristics and surface and geographic conditions are also important. A summary of empirical studies to quantify these factors is given in this section.

Zingg (1940) investigated the effects of degree and length of slope on soil loss by runoff. The results of various researchers were grouped and analyzed. To enable comparison, the different results were coded (since the test conditions differed), and equations of the following forms were obtained:

$$X = C_1 S^m \tag{2.1}$$

$$X = C_2 L^n \tag{2.2}$$

where

X = total soil loss (in weight units),

S = land slope (in percent),

L = horizontal length of land slope (feet),

C_1, C_2 = constants, and

m, n = exponents.

Considering both S and L as independent variables in their relation to soil loss, their effects were combined to produce the equation

$$X = C S^m L^n \tag{2.3}$$

where

C = a constant of variation, and the other terms are as previously defined.

$$C = f(K) \tag{2.4}$$

$$m = f(K,L) \tag{2.5}$$

$$n = f(K,S) \tag{2.6}$$

where K represents the infiltration rate, physical properties of the soil, intensity and duration of the rain, and other factors. Average values of m and n were proposed as 1.4 and 1.6 respectively.

In their series of studies on soil erosion, Ellison and Ellison (1947) expressed soil detachment due to surface flow as

$$D_1 = f(D_2, D_3) \tag{2.7}$$

where

D_1 = soil detachment,

D_2 = the soil's detachability, and

D_3 = the detaching capacity of the flow.

To simulate natural soil conditions, Meyer and Monke (1965) developed an experimental apparatus which included a slope table, soil bed, sediment hopper, and glass beads. Their aim was to determine the basic relationships between soil erosion and different factors such as particle size, slope steepness and length, which were studied at different levels. An equation of the following form was obtained:

$$e_r = C_{LSD} S^m L^n D^p \tag{2.8}$$

where

e_r = runoff erosion,

S = slope steepness,

L = slope length,

D = particle diameter,

C_{LSD} = constant coefficient, and

m,n,p = exponents.

From their data, values for m, n and p were 3.5, 1.9 and -0.5 respectively.

Meyer (1965) reported on laboratory studies on erosion. It was observed that soil erosion by runoff occurred predominantly by rilling, which corresponds to accepted concepts. The results also indicated that there were critical values of slope steepness and length below which no appreciable erosion occurred. Soil erosion by runoff was therefore expressed as

$$e_r = C_s(S-S_c)^m;\ S > Sc \qquad (2.9)$$

$$e_r = C_L(L-L_c)^n;\ L > Lc \qquad (2.10)$$

where

m, n = exponents,

C_s, C_L = coefficients, and

S_c, L_c = critical values of the slope S and length L, respectively.

Meyer et al. (1975) conducted field studies to investigate the effects of flow rate and canopy on rill erosion. The results suggested there was a critical flow rate below which no appreciable rill erosion occurred. The

presence of a canopy decreased rill erosion and effectively eliminated interrill erosion.

To study the physical characteristics of rill and interrill eroded soils, Young and Onstad (1978) used 1.52m by 4.52m laboratory plots with preformed rills on three soils and with simulated rainfall. Highly-aggregated soils were found to be less vulnerable to interrill erosion while those low in organic matter were more susceptible to rill erosion. Young and Onstad (1978) acknowledged that the nature and extent of rills are influenced by slope length and steepness, random and oriented microtopography, the quantity and rates of surface runoff, and soil properties.

In a field study, Foster et al. (1982) observed that freshly-tilled soil was more susceptible to rill erosion than an exposed, previously-deposited sediment. This is to be expected since the tillage operation (immediately before the tests) reduces the soil's ability to withstand the erosive forces of runoff. The results also indicated a linear relationship between rill erosion and discharge rate. Foster et al. (1982) further observed that the geomorphic characteristics of the rills were similar to those of rivers.

Gilley et al. (1986) investigated the effects of slope length on runoff rate, runoff velocity, sediment concentration and soil loss rate from residue-covered plots. Runoff rate, runoff velocity and soil loss rate were found to increase with downslope distance. Sediment concentration

and soil loss rate along the entire slope length were also found to decrease with crop residue rate.

Flanagan et al. (1986) studied the effects of storm pattern on runoff, infiltration, erosion and nutrient losses. Storm pattern was found to have a significant influence on these variables (runoff, etc.), which were also affected by the previous storm type.

Foster et al. (1984a, 1984b), in their laboratory studies on rill hydraulics, examined the nonuniformity in rill cross-section and profile and the nonuniformity of hydraulic variables along a rill's boundary. In these studies, the authors utilized a full-scale fiberglass, fixed bed replica of a rill formed on an erosion plot by runoff from simulated rainfall.

In the first part of the study, velocity relationships in rills were investigated (Foster et al., 1984a). Equations were developed to relate velocity of flow in rills with other hydraulic variables of discharge, slope, and hydraulic radius. The following equations were developed from their data:

$$V = 16.0Q^{0.28}S^{0.48} \qquad (2.11)$$

where

V = velocity in m/s,

Q = discharge rate in m^3/s, and

S = slope in m/m.

Also,

$$V = 121R^{0.73}S^{0.79} \qquad (2.12)$$

where

R = average hydraulic radius for the rill in meters.

The other symbols are as previously defined. Their work also suggested the use of normal distribution to describe velocity distribution along a rill's boundary.

Shear stress relationships in rills were investigated in the second part of the study (Foster et al., 1984b). The results indicated great variation in shear stress with time and space. The Pearson Type III (3-parameter gamma) distribution was found to fit the observed, moderately-skewed data whereas the log-normal distribution was found to better describe highly-skewed data. The authors indicated the possibility of improving rill erosion estimates from stochastic models that consider the spatial and temporal variations of flows in rills.

The Universal Soil Loss Equation (USLE) (Wischmeier and Smith, 1978) is an empirical erosion equation developed to estimate the average annual soil loss from an area (usually agriculture lands). The equation (USLE) is given as

$$A = RKLSCP \qquad (2.13)$$

where

A = average annual soil loss,

R = rainfall erosion index. R indicates the potential of rainfall to erode the soil,

K = soil erodibility factor (compares the soil-loss to that from a 72.6 ft. (22.6m) length field under identical condition),

S = slope-steepness factor (compares the soil-loss to that from a field of 9-percent slope),

C = cover-management factor (compares the soil-loss to that from a field in tilled, continuous fallow condition), and

P = support practice factor (compares soil-loss for a given support practice such as contouring, stripcropping or terracing to that for up and down the slope farming). The USLE lumps rill and interrill erosion together, and it does not account for deposition within the watershed. Also, USLE does not estimate soil loss from single storms.

Foster et al. (1977) modified the R-factor in USLE to obtain an improved erosivity factor for a single storm (Rm).

$$Rm = R_{rainfall} + Rrunoff \qquad (2.14)$$

$$Rm = aEi_{30} + bVQp^{d} \qquad (2.15)$$

where

E = total storm energy

i_{30} = the storm's maximum 30 min. rainfall intensity

V = runoff volume

Q_p = peak runoff

a, b, d = constants

(a ≈ 0.5; b ≈ 0.35; d ≈ 1/3 for Ei_{30} in N/hr, V in mm and Q_p in mm/hr)

Williams (1975) also modified Equation (2.13). The modification uses a runoff erosivity factor instead of the rainfall erosivity factor R to obtain

$$A = g(VQp)^{h}KLSCP \qquad (2.16)$$

where

g, h = constants (g ≈ 95; h ≈ 0.56)

A = soil loss in tons

V = runoff volume in acre-ft

Qp = peak runoff in cubic feet per second. The terms are as previously defined.

Working from the sediment continuity equation

$$D = \frac{dG}{dx} \qquad (2.17)$$

where

D = detachment rate (wt/area/time) at a point,

G = sediment load per unit width (wt/width/time) and

x = distance,

Foster and Wischmeier (1974) evaluated the topographic factor (LS) in the Universal Soil Loss Equation (USLE) for irregular slopes to obtain

$$A = RCP \sum_{i=1}^{n} \frac{K_i S_i \, (l_i^{m+1} - l_{i-1})^{m+1}}{l \, (72.6)^m} \qquad (2.18)$$

where

l = slope length (in feet)

m = slope-length exponent

(usually assumed equal to 0.5)

n = number of segments of uniform characteristics

The other variables are as defined in the USLE. Equation (2.18) also accounts for the non-uniformity of the soil erodibility factor K in each slope segment.

Wilson (1986) proposed a method for estimating the topographic factor (LS) in USLE. The method uses as input data topographic maps from which estimates of slope length, shape and gradient are developed. Frequency distributions of slope steepness, slope length and LS values are also produced from this method.

A device that has been widely used in field and laboratory erosion studies is rainfall simulator. This device has been used to quantify USLE parameters (Simanton et. al. 1985). The simulators are especially useful for field studies in areas where natural rainfall is unreliable. Also, with rainfall simulators the impact of different rainfall sequences can be examined in the laboratory or on the field in a relatively short period of time. This is due to the high degree of control over simulator operation.

The simulator may be a nozzle-type (e.g. Neibling et al., 1981; Moore et al., 1983) or a drop-former type (e.g., Onstad et al., 1981). In all rainfall simulator designs, attempts are made to duplicate natural rainfall characteristics which include its drop size distribution and drop impact velocities. Additional design considerations include reproducibility of storm patterns, portability and low cost (Moore et al., 1983).

Erosion Modeling

In recent years, use of modeling techniques in soil erosion research and in the design of soil conservation practices has increased as the result of more sophisticated computing systems and the need for greater information in making complex engineering, business, and agriculture decision. Meyer et al. (1976), in discussing soil erosion concepts, stressed the usefulness of erosion models developed from basic principles in evaluating land-use alternatives. An overview of erosion models is given in this section.

Meyer and Wischmeier (1969) simulated the erosion process by considering (1) soil detachment by rainfall, (2) transport by rainfall, (3) detachment by runoff,and (4) transport by runoff as its separate but related components. Four submodels representing the four major components were developed.

Detachment by rainfall (D_R) was expressed as

$$D_R = S_{DR} A_I I^2 \tag{2.19}$$

where

S_{DR} = constant, representing soil effect,

A_I = area of the increment, and

I = maximum 30-minute rainfall intensity.

The detachment by runoff, D_F, was assumed to be proportional to the square of the velocity. D_F on a slope increment was computed as the average of the detachment capacities at the start and end of the increment. The transportation capacity of rainfall (T_R) was expressed as

$$T_R = S_{TR} SI \tag{2.20}$$

where

S_{TR} = soil effect (assumed constant)

S = slope steepness, and

I = rainfall intensity

The transport capacity of runoff, T_F, was expressed as

$$T_F = S_{TF} S^{5/3} Q^{5/3} \tag{2.21}$$

where

S_{TF} = a soil term (assumed constant),

S = slope steepness, and

Q = flow rate.

Contributions from rainfall and runoff were considered in evaluating the total detachment and transport capacity. The limiting factor which controls erosion is the lesser of the total detachment and transport capacity. The authors indicated the need for improved mathematical relationships and incorporation of additional components into the model.

Foster and Meyer (1975) developed a mathematical model to simulate upland erosion from fundamental principles. The erosion process was separated into rill and interrill erosion. The continuity equation for mass transport and a sediment load-flow detachment interrelationship form the basis of the model. The authors indicated the need to fully develop most of the relationships used in the model.

Rohlf and Meadows (1980) simulated rill formation during the overland runoff-erosion process. The model was based on a water-sediment continuity equation and channel boundary shear relationships. The model underpredicted both the sediment discharge and the eroded rill area.

Foster (1982) provided basic information and factors for modeling soil erosion. Equations describing the fundamental relationships in the soil erosion process were presented and their limitations emphasized. To describe the erosion-sedimentation process, a continuity equation of the following form was adopted:

$$\frac{\partial q_s}{\partial_x} + \rho_s \frac{\partial (cy)}{\partial_t} = D_r + D_L \qquad (2.22)$$

where

q_s = sediment load (mass per unit width per unit time),

x = distance along the slope,

ρ_s = mass density of the sediment particles

c = concentration of the sediment in the flow (volume sediment per volume flow),

y = flow depth,

t = time,

D_r = rill erosion rate (mass per unit time), and

D_L = delivery rate of sediment from interrill areas (mass per unit time).

Assuming semi-steady sediment movement, the above equation reduces to

$$\frac{dq_s}{d_x} = D_r + D_L \qquad (2.23)$$

The assumption of semi-steady sediment movement simplifies the process, thus reducing the complexity of the model. In many situations, this assumption may not be realistic and the unsteady form of continuity (i.e., Equation (2.22)) should be used.

As shown by Equation (2.22), Foster (1982) divided erosion into rill and interrill components. This is a good approach because the two types of erosion are caused by different hydrologic processes (rainfall for interrill erosion, and runoff for rill erosion). Rill erosion was expressed as (Foster, 1982)

$$D_{rc} = a(\tau - \tau_{cr})^b \qquad (2.24)$$

where

D_{rc} = rill erosion detachment capacity rate (mass per unit total surface area per unit time)

τ = the flow's shear stress assuming broad shallow flow, and

τ_{cr} = a critical shear stress.

The actual detachment rate (D_r) is not always equal to the detachment capacity rate (D_{rc}) due to the presence of sediment in the flow (Hirschi and Barfield, 1986). D_r and D_{rc} are related by the equations (Hirschi and Barfield, 1986)

$$D_r = (1 - \frac{G_f}{T_c}) D_{rc} \qquad (2.25)$$

$$D_r = (1 - \frac{G_f}{T_c}) a(\tau - \tau_c)^b \qquad (2.26)$$

where G_f is the flow sediment load and T_c is the flow sediment transport capacity. The other terms are as previously defined.

Equation (2.24) is for gross rill erosion (erosion in many single rills lumped together), and also on the assumption that rill erosion and flow are uniformly distributed across the slope. In reality, erosion and flow

concentrations in a field are greater in some rills than in others. The assumption of uniform distribution, however, introduces great modeling convenience.

Assuming τ_{cr} to be zero and analyzing some field data, the rill erosion equation was derived as (Foster, 1982)

$$D_{rc} = 83.7\ K_r\ \tau^{1.5}\ C_r \qquad (2.27)$$

where

D_{rc} = rill erosion detachment capacity rate (kg/m^2 of total area · h),

τ = average shear stress assuming broad shallow flow (N/m^2),

K_r = soil erodibility factor for rill erosion ($kg \cdot h/N \cdot m^2$), and

C_r = a cover-management factor for rill erosion.

The interrill soil detachment was expressed as (Foster, 1982)

$$D_L = m \cdot C_i\ K_i\ I_{eff}^2\ S_i \qquad (2.28)$$

where

c_i = a cover-management factor for interrill detachment,

K_i = soil erodibility factor for interrill erosion,

I_{eff} = modified rainfall intensity based on the percent canopy cover,

m = constant,

S_i = interrill slope steepness factor,

$$S_i = 2.96\ (\text{Sin}\ \theta)^{0.79} + 0.56, \text{ and} \qquad (2.29)$$

θ = slope angle.

Foster (1982) also mentioned different situations encountered in the "real world," and discussed the degree of ease or difficulty in modeling these situations. The degree of simplicity or complexity of a model depends on the objectives of the modeler, the situation being modeled, available resources (data, degree of sophistication of the computing system, etc.), and a host of other factors.

Wilson (1986) utilized minimization principles in modeling rill erosion. The minimization of energy dissipation rate was with respect to the suspended sediment load rate. Evaluation of the model was through sensitivity analysis which indicated its sensitivity to variations in Manning's "n" with sediment load rate.

Moore and Burch (1986a) developed physically-based analytical functions to predict the effects of topography on erosion and deposition. The model was tested using hypothetical landscapes and an experimental catchment at Wagga Wagga, Australia. The results indicated the importance of slope length and steepness, and hillslope shape on soil loss and deposition on a hillslope or catchment.

Hirschi and Barfield (1986) developed a physically-based, research-oriented erosion model called KYERMO. The model was developed with special emphasis on steep slopes. The authors' objective was to isolate important subprocesses in the overall erosion process to facilitate further

research and understanding of the erosion process. The model consists of four major components: (1) runoff generation, (2) runoff routing, (3) sediment generation, and (4) sediment routing components.

A sensitivity analysis of the KYERMO model was conducted (Hirschi and Barfield, 1986). This indicated the importance of the detachment equation coefficient, the critical tractive force, and Manning's n. Also, the analysis indicated the inappropriateness of the Universal Soil Loss Equation (USLE) LS-factor for use on steep slopes. The maximum erosion rate was obtained for some intermediate number of rills per unit width that depended on the flow and plot conditions. The predictive capabilities of the model were adequate (compared to existing erosion models and field data). However, the authors indicated that additional development of the model is required (1) to increase its capabilities to handling more than 10 slope increments, (2) to provide better means of estimating rill detachment parameter values, and (3) to recognize stochasticity in the rilling process.

Sayler and Fornstrom (1986) used a critical tractive force approach in modeling erosion in irrigation furrows. Field observations and measurements were taken to determine the effects of various soil parameters on the critical tractive force. A correlation analysis was performed on the data to develop critical tractive force models. Results from this study indicated that the largest increases in

tractive force were created by decreases in furrow width and that tractive force increased with furrow roughness and slope.

Novak (1985) derived predictive equations for soil losses by rill erosion by assuming the rills were in equilibrium with the maximum overland flow occurring within the period of interest. The equations were physically-based and are more applicable to long-term soil-loss estimates from relatively undisturbed areas.

Soil Surface Description

Soil surface topography significantly affects hydrologic, hydraulic and erosion processes. A number of indices has been used to describe the soil surface roughness (Currence and Lovely, 1970; Lehrsch et al., 1988b).

Currence and Lovely (1970) applied different tillage operations on different plots. The tillage operations included plowing, plowing and disking, and power rotary tillage. Soil surface height (distance from level datum to the soil surface) measurements were taken after the tillage operations. The indices used to describe the soil surface roughness included the standard deviation of the original, uncorrected surface heights (z_{ij}), the standard deviation of the corrected heights (z'_{ij}), and the natural logarithmic transformation of heights (e'_{ij}). z'_{ij} was expressed as (Currence and Lovely, 1970)

$$z'_{ij} = z_{ij}-(\bar{z}._j-\bar{z}..)-(\bar{z}_i.-\bar{z}..)-(\bar{z}..) \qquad (2.30)$$

where

z'_{ij} = corrected height reading in the i^{th} row and j^{th} column,

z_{ij} = original height reading in the i^{th} row and j^{th} column,

$\overline{z.j}$ = average of readings in the j^{th} column,

$\overline{z_i.}$ = average of readings in the i^{th} row, and

$\overline{z..}$ = over-all average,

and e'_{ij} was expressed as

$$e'_{ij} = \ln z_{ij} - \overline{(\ln z.j} - \overline{\ln z..)} - \overline{(\ln z_i.} - \overline{\ln z..)} \qquad (2.31)$$

where

ln = natural logarithm,

$\ln z_{ij}$ = transformed height reading in the i^{th} row and j^{th} column,

$\overline{\ln z.j}$ = average of the transformed readings in the j^{th} column,

$\overline{\ln z_i.}$ = average of the transformed readings in the i^{th} row, and

$\overline{\ln z..}$ = over-all average of transformed readings

Lehrsch et al. (1988b) evaluated eight roughness parameters for describing soil surface roughness with an aim of selecting the best parameter. The parameters evaluated included maximum peak height (PKHT), a micro-relief index (MI), peak frequency (FREQ), and the product of the micro-relief index and peak frequency (MIF). The micro-relief index was defined as the area per unit transect length between the measured surface profile and the least-squares regression line through all measured positions of the transect (Lehrsch et al., 1988b). Other parameters evaluated were maximum depression depth, FREQ/PKHT, MI/PKHT, and MI/FREQ.

From the tests performed, Lehrsch et al. (1988b) chose the common logarithm of MIF as the best descriptor of soil surface roughness. This parameter was selected due to its sensitivity to rainfall effects and its consistency in responding to simulated rainfall. In addition, MIF can be measured relatively precisely and can also account for spatial dependency (Lehrsch et al., 1988b).

A common representation of the soil surface topography is obtained by drawing contour lines of the surface. This is partly due to the fact that contour maps enable a quick visualization of the topographic data. Morse (1968) discusses the use of a mathematical model in analyzing contour maps. Certain requirements were set by the author to facilitate the analysis. An appropriate scale and contour interval when drawing contour maps are important.

Zevenbergen and Thorne (1987) emphasized the importance of choosing an appropriate grid mesh distance when analyzing soil surface topography. They acknowledged that the choice of an appropriate grid mesh depends on the variation of slope and aspect, and on the precision of the elevation data. Using too large grid mesh distances might lead to missing important information on the topography while too small a grid mesh distance requires excessive, precise data giving only minor surface features.

Spectral analysis has been widely used in characterizing soil surface roughness (Currence and Lovely, 1970; Merva et al., 1970; Podmore and Huggins, 1980; Wu et al., 1980). This method is especially applicable to surfaces with periodic variations caused by tillage tool marks.

Julian (1967), Merva et al. (1970), Newland (1975), and Haan (1977) give some theoretical insights into the spectral analysis techniques. Its application is not limited to soil surface description. It can also be used in analyzing hydrologic events or other phenomena where periodicities may be present (e.g., Duck and Burggraf, 1986). The spectral density function helps in determining which frequencies explain the variance of the soil surface. Periodicities in the surface can be modeled using Fourier series, which can be expressed as (Bath, 1974)

$$H(s) = a_o + \sum_{k=1}^{\infty} (a_k \text{ Cos } kws + b_k \text{ Sin } kws) \qquad (2.32)$$

where

a_o = constant

a_k, b_k = Fourier coefficients

w = angular frequency

$w = 2\pi f = 2\pi/P$ (2.33)

f = frequency

P = period

Currence and Lovely (1970) used spectral analysis to analyze the soil surface roughness created by different tillage operations. The roughness caused by tillage implements was distinguished from random roughness by spikes in the periodogram.

Podmore and Huggins (1980) examined the roughness and other hydraulic characteristics of seven different surfaces. Spectral analysis was applied in the study. The authors concluded that, for the surfaces investigated, the spectra showed an overriding influence of random roughness, which suggested the possibility of characterizing roughness of those surfaces by only using the variance.

Instrumentation

In recent years there has been rapid development of instrumentation systems for measuring soil surface profiles. This is due in part to the greater emphasis placed on soil surface topography in the erosion process. In this section the equipment for measuring soil surface profiles will be discussed.

Hirschi et al. (1984) summarized important attributes of some soil surface profilers, ranging from pin displacement units (e.g. Curtis and Cole, 1972; Moore and Larson, 1979; McCool et al., 1981; Radke et al., 1981), height transducers (e.g. Currence and Lovely, 1970; Mitchell and Jones, 1973; Podmore and Huggins, 1981), to "non-contact" profile-measuring devices (e.g. Harral and Cove, 1982; Romkens et al., 1982). The pin displacement units and height transducers are "contacting" profile measuring devices in the sense that they make physical contact with the soil during a measuring session. They both have essentially the same mode of operation (moving the pin or probe from a reference height to the soil surface). However, while many pins are involved in the pin displacement unit only a single probe is used in the height transducer. Sources of error in the "contacting" soil profile measuring devices include the tendency of the pins to penetrate into soft soil and possible deformation or rupture of soil clods. In addition, soil profilers in this category generally require more time for the operation.

The "non-contacting" soil profilers are relatively more recent developments. They are generally more sophisticated than the "contacting" profilers. During operation, the non-contacting profilers do not come in contact with the soil surface. In the remainder of this section specific works related to soil profiler developments ("contacting" and "non-contacting") will be discussed. Those that fall in the

pin displacement category will be discussed first, followed by height transducers and then the "non-contacting" category.

Curtis and Cole (1972) developed a profile gage for measuring soil loss from surface-mined areas. Differences in soil profile readings from one date to another gave a measure of soil loss or deposition. McCool et al. (1981) reported on the development of a portable photographically recording rill meter. The authors listed the uses of the meter as including the collection of data on the effects of slope and climatic variables on rill erosion, and quantifying the magnitude of rill erosion on runoff plots. McCool et al. (1981) pointed out a major limitation of the device as the time lag between data collection and data availability.

Radke et al. (1981) designed and constructed a lightweight, battery-operated rillmeter. The meter used steel pins for soil surface contact with the pin displacement sensed electronically. Other design requirements were that the device had a vertical resolution of 1mm over a 25cm range with a measuring capability of over 300 surface elevations in less than 1 min. The authors mentioned the unreliability of the sensing switches as the major shortcoming of the meter. This was attributed to the varying field weather conditions. Hirschi et al. (1984) developed two similar surface profile meters of different

sizes and pin spacings. The surface heights were measured electronically and stored on magnetic disk.

Schafer and Lovely (1967) developed a soil surface profile meter, with an aluminium tripod as its support. The profiler had the capability of rapidly and automatically taking a large number of point elevation readings. This device falls into the "height transducer" category. The profile measuring device of Mitchell and Jones (1973) consisted essentially of a carriage-probe unit, a power supply-control unit and a recording unit. In this device, the carriage-probe unit was made of aluminium. The profiler could measure 1,225 points in approximately 1 1/2 hr.

Henry et al. (1980) designed and constructed a portable, battery-powered soil profiler. In this device, a linear potentiometer was connected to the probe for sensing the soil surface elevation. In Podmore and Huggins' (1981) soil profile meter a linear variable differential transformer (LVDT) was used as the sensing element. Podmore and Huggins (1981) reported two primary problems with the probe tip configuration used in their soil surface meter. These were the lateral deflection of the probe when in contact with irregular-shaped soil particles, and penetration of the probe into the soil.

Khorashahi et al. (1985) developed a "non-contacting" optical device for measuring soil surface elevations for erosion studies. The profiler consisted of a laser, a digital camera and a mechanical drive system for horizontal

movement. A control board was used to interface the camera with a microcomputer. Data collection rate was 100 height measurements every 2 1/2 minutes. This rate of data gathering was affected by data display, motor speed, rate of data transfer to the microcomputer, and software efficiency (Khorashahi et al., 1985).

Khorashahi et al. (1985) also performed an error analysis of their device to find the magnitude of the measurement error and to identify areas for possible error reduction. The accuracy of the elevation measurements was within $\pm$1.95mm. The authors reported the sources of errors affecting the height measurements as including rod deflection and light reflectivity of the soil surface (which could result in missing data). The error sources affecting the repeatability of horizontal movements were motor steps, gear slippage, chain vibration and ball bearing misalignment (Khorashahi et al., 1985).

Interpolation Techniques

Interpolation is essentially a point estimation process. This technique has been widely used in different fields of study and its general usage include (Rhind, 1975): the production of map output as contours, hillshading, etc., the calculation of some property of the surface at a given position; the computation of some property of a sub-area or sub-volume under a surface; and in computing parametric descriptions of global surface characteristics.

In discussing interpolation techniques, Rhind (1975) emphasized the need to choose an appropriate interpolation method for the problem at hand. In this respect, the form and size of the input data are important considerations. Rhind (1975) also listed different interpolation methods including zone partitioning, global fitting, gridding, contour-chasing methods, and multi-quadric analysis. He acknowledged that gridding is the most common of the interpolation techniques.

McLain (1976) described a method for smooth interpolation between random data points in two or more dimensions. The plane is partitioned into triangles by connecting neighboring data points. For each data point, the coefficients (a's) of the polynominal approximation

$$f(x,y) = a_1 + a_2x + a_3y + a_4x^2 + a_5xy + a_6y^2 \qquad (2.34)$$

were computed using the point of interest and its five nearest neighbors; where

x, y = x- and y- coordinates, respectively

f (x, y) = function value at (x,y)

The final approximation at the vertex of each triangle was obtained from

$$F = \sum_{i=1}^{3} \rho_i f_i = \rho_1 f_1 + \rho_2 f_2 + \rho_3 f_3 \qquad (2.35)$$

where:

f_i = value of the initial approximation (Equation 2.34) at each of the three vertices in the triangle.

ρ_i = weighting factors, expressed as (McLain, 1976)

$$\rho_i = d_i^n/(d_1^n + d_2^n + d_3^n) \quad (2.36)$$

$$d_i = l_i x + m_i y + q_i \quad (2.37)$$

l_i, m_i, q_i = coefficients

n = constant

McLain (1976) indicated the suitability of the method for graphical applications.

The use of triangular network in surface interpolation has also been discussed by Mark (1975). In that study (Mark, 1975), different terrain storage methods were compared in terms of digitation techniques, computer data-storage and retrieval methods, and assumptions about the surface behavior between data points. The differences between surface-specific sampling (selecting points with special significance in the topography, e.g. peaks and pits) and surface-random sampling (point selection criteria independent of the surface) were highlighted. Gold et al. (1977), Peucker et al. (1978) and Fowler and Little (1979) discussed the use of the Triangulated Irregular Network (TIN) in contour mapping. This network (TIN) represents a surface as a set of non-overlapping contiguous triangular facets, of irregular size and shape (Fowler and Little, 1979). The triangular network analyses are generally more

complex than in the rectangular networks. The remainder of this section will focus on gridding techniques, specifically rectangular (regular) grids.

Rectangular gridding techniques are needed in several instances, such as in the estimation of missing data points and in the conversion of unevenly spaced points into regular grid. Also, overlapping in some data collection systems may be corrected for by gridding. In addition, some data-analysis techniques require data in gridded forms thus necessitating the use of a gridding method. Rhind (1975) listed some gridding techniques including distance-weighted means and kriging.

In distance-weighted means the estimate at a grid point is obtained as the weighted mean of its neighboring points. The weight assigned to a neighboring point is expressed as a function of its distance to the grid point. The closer this neighboring point is to the grid point the higher the weight. The inverse distance weighting and inverse squared distance weighting are common applications of this procedure. Delfiner and Delhomme (1973) reported a distance-weighted mean estimation method where the weighting function was of the form:

$$\beta = \begin{cases} \dfrac{R^2 - d^2}{R^2 + d^2}, & d \leq R \\ 0, & d > R \end{cases} \qquad (2.38)$$

where

d = distance of the neighboring point to the grid point.

R = radius of the neighborhood centered at the grid point.

Kriging is an estimation technique that has been widely used in different fields of study. The term "kriging" was derived from the name D.G. Krige, a geologist who developed the technique and used it to estimate gold reserves. For best results, the kriging estimates are required to be unbiased, and with minimum variance of errors (optimality).

The kriging estimator is a linear estimator (Bras and Rodríguez-Itube, 1985), and it considers the following in the estimation process (Delhomme, 1978):

1. Distances between the estimated point and the data (sample) points.

2. Distances between the data (sample) points; and

3. The structure of the variable under study (through the variogram).

There are three major methods associated with kriging--each more suited to a particular situation, and all involving basically the same principles: (1) universal kriging, (2) ordinary kriging, and (3) cokriging. Universal kriging is applicable to nonstationary random fields and processes (Delfiner and Delhomme, 1973; Chirlin and Wood, 1982; Bras and Rodríguez-Iturbe, 1985; Bárdossy et al., 1987) and is generally more complex than the other kriging techniques. Ordinary kriging is applicable when the

processes involved are assumed to be stationary--i.e., with constant expectation or mean (Delfiner and Delhomme, 1973; Delhomme, 1978; Yost et al., 1982b; Bárdossy and Bogárdi, 1983; Bras and Rodríguez-Iturbe, 1985). Cokriging (Meyers, 1982; Carr et al., 1985; Yates and Warrick, 1987) may be used when highly-correlated variables are involved in the estimation process.

Journel and Huijbregts (1978) and Bras and Rodríguez-Iturbe (1985) gave mathematical development of the kriging equations. The semivariogram (commonly called variogram) (Yost et al., 1982a; Delhomme, 1978; Warrick and Meyers, 1987) is an important component in the kriging equations. Kriging analyses usually assume that an appropriate semivariogram has been developed for the problem at hand. The semivariogram development for the "stationary" case is based on the "intrinsic hypothesis" (Delhomme, 1978)

$$E[Z(\vec{c} + \vec{h}) - Z(\vec{c})] = 0 \qquad (2.39)$$

$$Var[Z(\vec{c} + \vec{h}) - Z(\vec{c})] = 2\gamma(\vec{h}) \qquad (2.40)$$

where

Z is a random variable, E is the Expectation operator and $\gamma(\vec{h})$ is the semivariogram.

$\vec{c}_i$ = coordinate (x_i, y_i) of data point i

$\vec{h} = \vec{h}(\vec{c}_{i+1}, \vec{c}_i)$ = (vector) difference between the points $\vec{c}_{i+1} = (x_{i+1}, y_{i+1})$ and $\vec{c}_i = (x_i, y_i)$

The semivariogram is expressed from Equation (2.40) as

$$\gamma(\vec{h}) = 1/2 \text{ Var } [Z(\vec{c} + \vec{h}) - Z(\vec{c})] \tag{2.41}$$

Writing $Z_\Delta = Z(\vec{c} + \vec{h}) - Z(\vec{c})$ (2.42)

$$\gamma(\vec{h}) = 1/2 \text{ Var } [Z_\Delta] \tag{2.43}$$

Now, the variance is the second moment about the mean, or

$$\text{Var}[Z_\Delta] = E[Z_\Delta - \mu_{Z\Delta})^2] = E[Z_\Delta{}^2] - (E[Z_\Delta])^2 \tag{2.44}$$

where

$\mu_{Z\Delta} = E[Z_\Delta]$ = population mean of the random variable Z_Δ

Using Equations (2.39) and (2.42),

$$E[Z(\vec{c} + \vec{h}) - Z(\vec{c})] = E[Z_\Delta] = 0 \tag{2.45}$$

$$\text{Var}[Z_\Delta] = E[Z_\Delta{}^2] \tag{2.46}$$

Thus, the semivariogram for the "stationary" case could be expressed as

$$\gamma(\vec{h}) = 1/2 \; E[Z_\Delta{}^2] = 1/2 \sum_{i=1}^{n} Z_{\Delta i}^2 \rho_i \tag{2.47}$$

where

Z_Δ = elevation value $Z(\vec{c} + \vec{h}) - Z(\vec{c})$

ρ_i = "discrete probability" or "relative-frequency" for $Z_{\Delta i}$

The kriging system of equations for the "stationary" case could be expressed as (Bras and Rodríguez-Iturbe, 1985)

$$\sum_{j=1}^{n} \beta_j \gamma(\vec{c}_i - \vec{c}_j) + \alpha = 1/D \int_D \gamma(\vec{c}_g - \vec{c}_i) d\vec{c} \qquad (i = 1,2, ..., n) \qquad (2.48)$$

$$\sum_{i=1}^{n} \beta_i = 1 \qquad (2.49)$$

where

β_i = weighting factors

α = Lagrange multiplier

D = region for the estimation

The other terms are as previously defined.

Geomorphic Studies

Geomorphology deals with the study of the features of land surfaces. This branch of science has three major practical applications (Schumm, 1983):

1. Evaluating existing land surface conditions,
2. Predicting future land surface conditions both with constant and changing environmental conditions, and
3. Interpreting the past (retrodiction).

This section is divided into three parts. First, studies dealing with the general aspects of geomorphology will be discussed, followed by studies dealing specifically with drainage network extraction and drainage basin morphometry.

General Geomorphic Studies

The discussion in this section commences with the problem of channel initiation/definition. This problem is of paramount importance in nearly all geomorphic studies. According to Knighton (1984); channel initiation involves two related problems: (1) determining the processes whereby water movement becomes sufficiently concentrated to cut a recognizable channel, and (2) identifying the conditions under which the initial cut is maintained and enlarged to form a permanent channel. This concept is reasonable and is popularly accepted in different scientific circles.

Rogers and Singh (1986) presented a theoretical basis for channel initiation, using a critical shear stress approach. This approach was based on the premise that drainage channels are formed when the shear stress of the flowing water is sufficient to move surface soil. The authors indicated that the amount of runoff available to move sediment is a function of geologic and climatic characteristics. The shear stress of the flowing water could be expressed as

$$\tau = \gamma RS \qquad (2.50)$$

where

τ = shear stress (force per unit area)

γ = specific weight of water

S = channel slope

R = hydraulic radius of the channel

$$R = A/P \tag{2.51}$$

A = channel cross-sectional area

P = wetted perimeter

The resistance to motion, offered by the soil particles is (Rogers and Singh, 1986)

$$r = (\gamma_s - \gamma)\ V/A_s \tag{2.52}$$

where

r = intensity of resistance to movement (force per unit area)

γ_s = specific weight of soil particle

V = volume of the particle

A_s = surface area of the particle

For a sphere,

$$V/A_s = (1/6)d \tag{2.53}$$

where d is the diameter of the sphere.

Thus, for irregular particles,

$$V/A_s = kd \quad \text{(Rogers and Singh, 1986)} \tag{2.54}$$

where k is a shape factor which is approximately 0.04 to 0.8.

By assuming a steady and uniform flow, the shear stress required to initiate sediment movement is given as (Rogers and Singh, 1986)

$$\gamma RS = (\gamma_s - \gamma)kd \qquad (2.55)$$

where the terms are as previously defined.

A major disadvantage in the above-mentioned approach to channel initiation is the difficulty in determining the parameters involved. Also, the approach neglects friction and cohesion between soil particles. These are actually significant in sediment detachment. Furthermore, researchers like Lavelle and Mofjeld (1987) have questioned the existence of critical stresses for incipient motion and erosion. This stems from the difficulty in defining incipiency of particle motion.

Wilberg and Smith (1987) derived an expression for the critical shear stress of noncohesive sediment from the balance of forces on individual particles at the bed surface. Uniform and heterogeneous sediments were considered in the analysis. Wilson and Barfield (1986) developed a detachment algorithm for noncohesive sediment. The algorithm was based on the probability of turbulent detachment forces exceeding the submerged weight of particles.

Moore and Burch (1986b) considered sediment incipient motion using the critical unit stream power concept. The unit stream power, P, is defined as the time rate of potential energy dissipation per unit weight of water, i.e.

$$P = \frac{dY}{dt} = \frac{dx}{dt}\frac{dY}{dx} = vs \qquad (2.56)$$

where

Y = elevation above a datum (i.e. the potential energy per unit weight of water)

x = longitudinal distance

t = time

v = flow velocity in the longitudinal direction

s = energy gradient (s can be approximated by the slope of the soil surface or channel bed)

The results from Moore and Burch's (1986b) analyses suggested that P_{CR}/η, the critical unit stream power for rill initiation (P_{CR}) divided by the kinematic viscosity (η), may be a unique value that is independent of soil type. In the remaining parts of this subsection, laboratory and field experiments relating to general geomorphology, will be summarized.

Schumm and Khan (1972) studied the effects of slope and sediment load on channel patterns using a large concrete recirculating flume. Results from the experiments indicated the existence of threshold values of slope and/or sediment-load above which channel patterns are significantly altered.

Moss et al. (1980) investigated the interactions between flowing water and natural, loose, sandy detritus in flumes, using small discharges over a large range of slopes. They observed that small rills transported little sand at slopes below 0.01, with the transporting power greatly increased in the slope range 0.01 to 0.04 which resulted in the formation of channel systems. The transporting

potential of the small rills became enormous by a slope of 0.3. Moss et al. (1980) also noted that the processes in the small channels were similar to those of rivers. Moss et al. (1982) studied the formation of small channels in overland flow. The significance of such channels was emphasized from the study.

Spomer and Hjelmfelt (1986) measured concentrated flow erosion channels on conventional and conservation-tilled watersheds. More concentrated flow channels were found in the conventionally-tilled watershed. Spomer and Hjelmfelt (1986) indicated the need for more information on techniques to better define and measure concentrated flow erosion. They further indicated the usefulness of photogrammetric procedures in delineating interrill and rill erosion. Such procedures (photogrammetry) have also been used in determining Universal Soil Loss Equation (USLE) parameters (Morgan et al., 1980).

To account for sedimentation processes in the Dry Creek Drainage Basin, Nebraska, Spomer et al. (1986) used historic and contemporary erosion measurements on channels, gullies and rangeland, including computed erosion rates from cropland. Such information is particularly useful in model verification and in improving conservation designs. Rogers and Singh (1986) collected and analyzed data relating drainage density, infiltration capacity, runoff volume, and sediment yield for small drainage basins located on different geologic formations. They acknowledged the close

interaction between geology and hydrology and its effect in analyzing runoff from a watershed.

Allen (1986) related drainage density to runoff and sediment yield. The study was conducted on a group of watersheds in the United States Southern Plains. Remote sensing techniques were used in obtaining the drainage density values. Allen (1986) described in detail the procedures used to obtain the drainage densities in the study. This was in realization that the drainage density value is influenced by the scale of the base map or aerial photo, the magnification of the viewing instrument, and the definition of an initial channel.

Allen (1986) also reported discontinuity of watercourses on some watersheds. Two such situations were given: (1) when gullies eroded midway up hillslopes with no connections to the channel below, and (2) channels losing their identity through deposition, and thus becoming nonfunctioning. In such situations, the length of the upstream channel was used as the determining factor for channel inclusion in the analysis. If the upstream channel length was greater than the nonchannelized length, the upstream channel was included in the channel system. The upstream channels were excluded from the analysis when their cumulative length was less than the length of the intervening nonchannelized portion. In both cases the nonchannelized portion was excluded from the channel system. Allen also found higher correlation between runoff and

sediment yield versus drainage density when gullies and microchannels were included in the analysis. His work clearly demonstrates the need to adequately describe the procedures used in channel definition/identification in a study.

Drainage Network Extraction

A drainage basin or watershed has been described as a well-defined topographic and hydrologic entity that is regarded as a fundamental spatial unit (Knighton, 1984). It is an area limited by a drainage divide and occupied by a drainage network (Schumm, 1983). Shreve (1966) described a drainage network (or channel network) as consisting of the channels upstream of an arbitrarily chosen channel cross section or outlet of the network. In this sub-section, studies dealing with the extraction of drainage network from the features of the land surface are summarized.

Peucker and Douglas (1975) utilized the notion of surface-specific points and lines in identifying potential stream and ridge features from terrain elevation data. Some of the features coded were peaks, pits, passes, ridges and ravines. Two major assumptions were made in the study: (1) every point on the surface could be classified on the basis of an analysis of its neighbors, and (2) the surface has a smooth neighborhood correlation (i.e. the surface is "topographically well behaved"). Peaks were regarded as local maxima along ridge-lines, pits as local minima along

ravine-lines, and passes as occurring where ridge-lines and ravine-lines crossed. Peucker and Douglas remarked that the developed procedures were sensitive to encoding "noise".

In extracting structural information from digitized data, Toriwaki and Fukumura (1978) adopted the use of two local features: the connectivity number (CN) and coefficient of curvature (CC). Precise definitions and properties of CN and CC are given in the paper. The connectivity number, CN, at an element (i,j) essentially provides information on how many connected components exist in the neighborhood of (i,j). Each element of such connected components must have an elevation value greater than or equal to that of (i,j). The structural information extracted using this method included peaks, pits, passes, ridge lines and ravine lines. Fischler et al. (1981) also described a method for delineating roads and other linear structures in aerial imagery.

Mark (1984) reported a study on automatically delineating drainage networks from digital elevation models. Two algorithms were described in the paper: one was based on Peucker and Douglas' (1975) work where concave and convex features were marked as potential stream and ridge regions, respectively, and the other was based on runoff concentration simulation whereby those cells receiving surface runoff above a predetermined threshold were declared to be the drainage network. The essential roles of data acquisition methods and processing were discussed. The

second method of runoff concentration simulation was based on the reasonable assumption that drainage channels represent points at which runoff concentration is great enough that fluvial processes dominate over slope processes.

O'Callaghan and Mark (1984) developed a technique for extracting drainage networks from gridded elevation data. The technique could extract only the major drainage paths, and was similar to that described by Mark (1984) where drainage channels were formed from runoff concentration above a predetermined threshold. O'Callaghan and Mark (1984) defined a digital elevation model (DEM) as "any numeric or digital representation of the elevation of all or path of planetary surface, given as a function of geographic location." Jenson (1985) also developed an algorithm to extract drainage networks from digital elevation data. The algorithm consisted of three major steps: (1) the identification of drainage cells, (2) grouping the drainage cells, and (3) linking groups of drainage cells. The drainage cell identification process was implemented as a 3 by 3 cell moving window and was based on the premise that an area with a V-shaped elevation profile would channel water, and should therefore be part of the drainage network.

Band (1986) described an approach by which drainage basin structures could be automatically extracted, mapped and encoded from elevation data. The approach dwelled on previous works from related areas (e.g. Peucker and Douglas, 1975; O'Callaghan and Mark, 1984), combined with original

methods. The Peucker and Douglas' (1975) algorithm was applied in the network construction. Upward concave points were marked as potential stream points while convex points were marked as potential ridge points. The ridge image was considered an approximation to the drainage divides.

In processing the data, Band (1986) used a 3 x 3 pixel window, depicting the set of pixels to the East, North, West and South of the central pixel as the four-connected neighbors while the eight pixels surrounding the central one were regarded as the eight-connected neighbors. The following procedures were used to obtain the drainage lines: The pixel of highest elevation was flagged from the set consisting of the central pixel and those to its East, South and South-East. After one sweep of the matrix, the unmarked pixels were regarded as the drainage courses. Ridge lines were found in a similar way. These techniques led to the extraction of a set of segments that could serve as a basis to grow and connect the rest of the drainage system. The author claimed that the techniques worked very well in rugged terrain with well-incised streams and sharp divides.

Band (1986) also labelled channel segment ends as downstream or upstream nodes. Drainage from the downstream nodes occurred to successively lower pixel until another stream segment was encountered. This implied a "maximum descent" algorithm whereby the next pixel chosen was (Band, 1986)

$$P_i/\Delta P_i = \max(\Delta P_1, \Delta P_2, \Delta P_3, \Delta P_4, \Delta P_5, \Delta P_6, \Delta P_7, \Delta P_8) \quad (2.57)$$

where

$$\Delta P_i = P_o - P_i \qquad (2.58)$$

P_o is the pixel at the center of the 3 x 3 pixel window, and P_i (i = 1,2,.....8) are its eight neighbors.

To generate the divided network, Band (1986) considered the set of drainage area pixels (A) as the complement of the set of stream network pixels (S). The set of divide pixels (D) was considered a subset of A. The properties of D (e.g. D is a four-connected) greatly facilitated its extraction. The final steps in Band's algorithm consisted of building a topologic code that described the stream networks; and giving a unique numerical label to each link and associated drainage area. The row and column coordinates and a topologic code were recorded at each node. A source node was coded L-1, where L is the number of links joining at the node. The algorithms were assembled into a computer program called STREAMS (STreams and Ridge Edge Analysis and Mapping System). The program was tested with data from the Glendora, California quadrangle which covers the western portion of the Sam Dimas Experimental Forest. The results showed a fairly close correspondence between the automatically extracted networks and those from topographic maps.

In delineating drainage basin elements from digital elevation data, Palacios-Vélez and Cuevas-Renaud (1986) defined a drainage channel from the slope perspective. In that study, channels were regarded as lines of convergent

slopes. For channel identification, paths of steepest slope were analyzed in a downstream direction while for ridge identification, paths of steepest slope were analyzed in an upstream direction. The contributing area to any point in the channel network was taken as the locus of all points in the watershed, whose paths of steepest slope pass through the given point.

Drainage Basin Morphometry

Drainage basin morphometry refers to the quantitative description of a drainage basin. Gardiner (1974) listed several uses of morphometric analysis, including its use: in regional geomorphological studies to gain some impression of an area before performing detailed field work; as a predictive tool, in studies to indicate hydrologic response; as a descriptive tool, in studies of land evaluation and in comparative regional studies; and as an analytical tool in studies of drainage basin dynamics and landscape evolution.

The drainage basin is usually described in terms of the order of streams within the basin, their number, frequency, lengths, and pattern, drainage area, drainage density, etc. Horton (1945) distinguished between drainage pattern and drainage composition. While drainage pattern refers to the manner of distribution of a given set of tributary streams within the basin, the drainage composition implies the numbers and lengths of streams and tributaries of different sizes or orders, regardless of their pattern (Horton, 1945).

Horton further indicated that drainage composition has a high degree of hydrologic significance, whereas drainage pattern alone, although highly significant in relation to geologic control of drainage systems, has but little hydrologic significance.

Another insight into morphometric studies is the relation between large and small basins. Working from the relation of channel number to channel length for several drainage basins, Leopold et al. (1964) concluded that, in general, large basins are geometrically similar to small basins with regard to relations of orders, numbers of streams, and stream lengths. A premise for drainage basin analysis is that of empiricity. This was adequately summarized by Jarvis (1977) who stated that: "In the absence of a definitive network growth model of physical laws, drainage network analyses are necessarily empirical and inductive". In the remaining parts of this subsection, studies and discussions relating to drainage basin analysis are summarized.

An important aspect in drainage network analysis is that of stream ordering. Gardiner (1974) lists several stream ordering procedures including those of Horton, Strahler, Shreve, Gregory and Walling, Walsh, Scheidegger, and Woldenberg. Two of the most commonly used ordering procedures will be briefly discussed, namely Horton's and Strahler's stream ordering procedures. In Horton's system of ordering (Horton, 1945) first order streams are those

with no tributaries. Second order streams have as tributaries only first order streams. Third order streams receive as tributaries only first and second order channels while fourth order streams receive first, second, and third order channels as tributaries; etc. With this system of ordering, the main stream has the highest order.

Strahler's ordering procedure is essentially a modification of Horton's procedure. Rodríguez-Iturbe and Valdés (1979) summarized Strahler's stream ordering procedure as follows: (1) First order streams are channels originating at a source. (2) When two streams of order q join, a stream of order q + 1 is created. (3) When two streams of different orders join, the channel segment immediately downstream has the higher of the orders of the two combining streams.

Morisawa (1957) compared streams obtained from contour crenulations and from bluelines on topograpghic maps, to those obtained from actual field measurements. The conclusion from that study was that, at least for small watersheds, the contour method was preferred over that from using bluelines from topographic maps. This was due to the fact that the blue lines on the topographic maps were inserted only where water was found during map preparation, thus possibly excluding some seasonal channels. Eyles (1966) also computed drainage basin parameters from Malayan maps and from aerial photographs.

Mark (1983) conducted extensive field surveys of drainage networks within drainage basins located in Northeastern Kentucky. In this paper, different methods of extracting drainage network from topographic maps were discussed, including contour crenulation method. Mark also stressed the need for the researcher to fully understand the processes and guidelines under which the study maps were prepared, before drawing conclusions on map-derived basin attributes.

Parameter Variability

Great variability with time and space exists in parameters involved in soil- and water- related processes. This is largely due to the heterogeneity of the soil medium, which creates additional complexity in studies involving these processes. Under controlled conditions, the effects of soil heterogeneity on these processes are minimized. Performing experiments under controlled conditions is often necessary in order to investigate the effects of certain variables on soil-related processes. Studies dealing with parameter variability will be summarized in this section. Although it is recognized that hydrology, soil erosion/soil properties, and geomorphology are interrelated areas of study, this section is being divided into those subtopics (hydrology, etc.) mainly for convenience.

Hydrology

In this subsection, studies relating to parameter variability in hydrologic processes are summarized. Freeze (1980) analyzed rainfall-runoff processes on a hillslope using a stochastic approach. The analysis was aimed at determining the influence of spatial stochastic properties of hillslope parameters on the statistics of the resulting runoff events. Freeze used Monte-Carlo simulation methods to generate stochastic values for saturated hydraulic conductivity and for storm rainfall properties.

Sharma et al. (1980) studied the surface hydrologic variability of a watershed in terms of the parameters of Philip's infiltration equation. The Philip's 2-parameter infiltration equation is given as

$$I = St^{1/2} + At \qquad (2.59)$$

where

I = the cumulative infiltration at time t, and

S and A = the parameters

Twenty-six sites on a grassland watershed in the Washita River Basin, located in the Southern Great Plains of the United States, were chosen for the infiltration study. The concept of similar-media was used in scaling the data.

Results of the Sharma et al. (1980) tests indicated random distribution of the parameters S and A over the watershed. The log-normal distribution was found to fit

data for S, A, and I (at a given time) better than the normal distribution. Jaynes and Clemmens (1986) described a method for incorporating the effects of spatial variability of infiltration rates into border irrigation models.

Parameter variability is usually considered by fitting the observed data to probability distributions. Haan (1977) gave mathematical procedures for transforming uncertainty in parameter estimation to uncertainty in predicting the process response. Haan and Wilson (1986) applied this approach to the estimation of runoff frequencies from probability distributions of rainfall and other factors affecting runoff.

Soil Erosion/Soil Properties

Parameter variability pertaining to soil properties and erosion in field and laboratory studies are discussed in this subsection. This discussion commences with the question that often arises in soil studies: the question of the number of samples required to adequately represent (or estimate the mean of) a soil property. This question is particularly germane since the extent to which a certain soil property varies affects the number of samples required to adequately represent its mean.

Warrick and Nielsen (1980) presented results from different sources on the values of estimated mean, standard deviation and coefficient of variation (CV) for some basic soil properties. They classified the soil properties as

those with (1) low variation (e.g. bulk density), (2) medium variation (e.g. particle size fractions), and (3) high variation (e.g. saturated hydraulic conductivity). For soil parameters in the low-variation group, relatively small sizes are required in estimating the mean while for those in the high-variation group, much larger sample sizes are required. Assuming independent samples, and that the sample is large enough that the Central Limit Theorem applies; the number of samples necessary to be within d units of the mean $(1-\alpha)$ 100% of the time is (Warrick and Nielsen, 1980)

$$n = \theta_\alpha^2 \sigma^2 / d^2 \qquad (2.60)$$

where

θ is the soil property of interest (e.g. Bulk density)

θ_α = normalized deviate

$$\theta_\alpha = \frac{\theta - \mu}{\sigma} \sim N(0, 1) \qquad (2.61)$$

μ = mean

σ = standard deviation

α = confidence level

$(1 - \alpha)$ 100% = confidence interval (CI)

Included in the Warrick and Nielsen (1980) paper is a summary of the approximate number of samples required to estimate mean values of some soil properties (computed from the results from different sources, using Equation 2.60). For bulk density, the required sample size was estimated as 2 (for estimation within 10% of the mean, and at $\alpha = 0.05$).

While acknowledging the fact that the Central Limit Theorem does not apply for a sample size of 2, Warrick and Nielsen (1980) maintained that many fewer samples are needed to estimate bulk density than the other soil parameters. They further stated that while the sample sizes shown in the paper for the different parameters do not transfer directly to other fields, same relative values should be expected among the parameters.

The soil surface configuration is usually described in terms of its roughness (soil surface roughness). Zobeck and Onstad (1986) discusses the effects of various factors, including tillage, rainfall, runoff, and soil texture, on random roughness. Random roughness is defined as the standard error of individual elevations after oriented roughness has been removed. The study indicated that tillage and rainfall had the most pronounced effects on random roughness, with random roughness decreasing exponentially with increasing rainfall. A simple model was proposed to predict changes in random roughness with rainfall and tillage operations. Lehrsch et al. (1988a) determined the spatial variability of soil surface roughness parameters using a semivariogram analysis.

The processes mentioned in the preceding subsection and paragraph (rainfall, runoff, infiltration, etc.) bear great relevance to soil erosion studies in their direct and indirect effects on erosion processes. Another factor of considerable importance is soil erodibility. This factor

measures the degree of vulnerability or susceptibility of the soil to erosion (Hudson, 1981). It is a highly-variable factor and has been the subject of research by many workers.

Dickinson et al. (1982) conducted studies to investigate possible seasonal variations in soil erodibility. The methods used included (1) Wischmeier's nomographic estimate of soil erodibility, (2) laboratory soil-loss determinations, and (3) surface soil shear strength measurements, all evaluated under a range of soil and seasonal conditions. Their results indicated seasonal variations in soil erodibility. This variation was influenced by antecedent soil water content, soil texture, and soil density. In addition, surface soil shear strength values were found to vary seasonally with soil characteristics. A strong, negative correlation between soil erodibility and seasonal surface soil shear strength was obtained from their study.

Mutchler and Carter (1983) also conducted a study to determine the variation in soil erodibility during the year. For their study, data from erosion plots at Holly Springs, MS (6 years) and Morris, MN (10 years) were used. Periodic variation in soil erodibility was observed. The average monthly soil erodibility (K_m) was expressed as

$$K_m = K.K_c \qquad (2.62)$$

where

K = average annual soil erodibility (from the

Universal Soil Loss Equation), and

K_c = variability coefficient. K_c was expressed as a cosine function of the form

$$K_c = 1 + a\text{Cos}\ \theta \qquad (2.63)$$

Data from Holly Springs, MS, and Morris, MN, (Mutchler and Carter, 1983) resulted in the following equation for Holly Springs:

$$K_c = 1 + 0.6903\ \text{Cos}[(t - 2.147)2\pi/12], \qquad (2.64)$$

and for Morris:

$$K_c = 1 + 0.6508\ \text{Cos}\ [(t - 4.456)\ 2\pi/12] \qquad (2.65)$$

where t is the time in months (for example, Jan.1≡1.0; Jan. 15≡1.5; Feb. 1≡2.0; April 15≡4.5)

The results showed that for the Holly Springs data, soil erodibility ranged from a low of 0.31K on August 5 to a high of 1.69K on February 4. This result is compatible with the findings of Dickinson et al. (1982), who obtained highest erodibility values in early spring conditions for Ontario, Canada soils. Mutchler and Carter (1983) also expressed hope that normal air temperature data could be used in approximating soil erodibility variation. The average annual soil erodibility (K) is also involved in the computation.

Alberts et al. (1986) used rainfall simulation to investigate the temporal variation of soil erodibility. Two soils, located about 400m apart and with similar cropping

and management history, were used in the study. Statistical methods were used in the evaluation. The results indicated a highly significant variation between years and a highly significant interaction between year and soil. Their research further indicated the importance of climatic and soil factors in influencing runoff and erosion processes.

The soil erodibility factor (K) in the Universal Soil Loss Equation (USLE) considers both rill and interrill erosion. However, consideration of the separate processes of rill and interrill erosion involves the use of different erodibility factors (K_r for rill erosion and K_i for interrill erosion). Foster (1982) suggests that for a soil that seems especially vulnerable to rill erosion, K_r should be increased from K (USLE K) by 1/3, or decreased from K by 1/3 for a soil that does not seem vulnerable to rill erosion. Likewise, K_i should be decreased by 1/3 from K for a soil that seems especially vulnerable to rill erosion, or increased by 1/3 from K for a soil that does not seem vulnerable to rilling.

Bryan and Luk (1981) conducted laboratory experiments to investigate soil erosion variation under simulated rainfall using three soil types. Rainfall intensity and duration, slope angle and length, surface cover and soil type, some of the major factors affecting soil-loss and runoff, were held constant during the tests. Variability was assessed in terms of the coefficient of variation.

Although most of the controlling factors were held constant, Bryan and Luk's (1981) test results indicated variability in soil-loss and surface runoff. This was described as inherent soil-loss variability. The effects of random variation were also recognized. Bryan and Luk (1981) indicated that the extent of the variability obtained in that study might be specific to the conditions under which the experiments were performed. They concluded that soil-loss variability, like soil erodibility, was essentially a relative property.

Geomorphology

The discussion in this subsection centers on the random walk model application to rill network development. The random walk model is a fundamental premise for drainage network development, which, in essence, considers channel network development as being random, but following an average or a most probable form for a given set of conditions. Leopold et al (1964) gave a brief discussion on this model.

Scheidegger (1967) applied random walk principles to the formation of drainage patterns into an intramontane trench. In that application, Scheidegger assumed that the landforms under consideration were solely formed by fluvial erosion. Similarity between the network developed from the random walk model and the actual network, was found.

Seginer (1969) applied the combination of random walk model and random roughness model in drainage network construction. In the random walk model the drainage directions out of elementary areas were assigned at random, while the roughness heights of the elementary areas were assigned at random in the random roughness model. The random roughness model yielded values of primary probabilities (i.e. probabilities which could be used in the construction of a random walk model).

Summary

Soil erosion problems are of great concern in most areas of the world. Factors affecting the rate of erosion include rainfall intensity, slope length and steepness, surface condition, soil characteristics, and other hydraulic and hydrologic variables.

The development of drainage channels is an important feature in the erosion process. The drainage basin or watershed composes of these channels which develop randomly but following an average or a most probable form for a given set of conditions. In drainage basin studies the procedures used in determining the basin parameters must be adequately described.

CHAPTER III

INTERPOLATION AND CHANNEL IDENTIFICATION ALGORITHMS

Introduction

In this chapter the theoretical developments for elevation estimation and channel identification used in the study are discussed. Topics included under elevation estimation are the derivation of interpolation equations, definition of neighborhood zones, finding neighborhood zones, and handling empty neighborhood zones. Flow paths and channels are identified using the algorithm developed by Couger et al. (1989). A description of this algorithm is also given.

Elevation Estimation

An important component in this study is the development of procedures for interpolating elevation values (2-dimensional interpolation) from large data sets. The procedures developed below are being used in lieu of the more sophisticated kriging technique because thousands of data points are involved in the computation. Kriging is too computationally extensive to be effective for this type of problem.

Derivation of Interpolation Equations

The derivation of equations to be used in the interpolation procedures will be based on points randomly spaced in two dimensions (x- and y-directions) around the point of interest (Figure 1). Adaptation of this method to special cases [e.g. constant x and random y] is easily accommodated.

Consider a grid point G surrounded by sample (data) points i = 1, 2, 3, . . ., n within a region D (n is the number of sample or data points).

Let, $z_i = z(x_i, y_i)$ = elevation value at the point (x_i, y_i)

$\hat{z}_i$ = estimate of z_i,

Z = random variable (elevation),

$\hat{Z}$ = estimate of Z.

We recognize that

z is the value taken by Z,

$\hat{z}$ is the value taken by $\hat{Z}$,

$\hat{Z}$ is an estimator while $\hat{z}$ is an estimate.

The subscript g will be used when referring to the grid point, while the subscript s will be used when referring to the sample (or data) point.

Consider now Figure 1 where the estimate $\hat{z}_g$ at G is to be obtained by a weighted-average procedure as

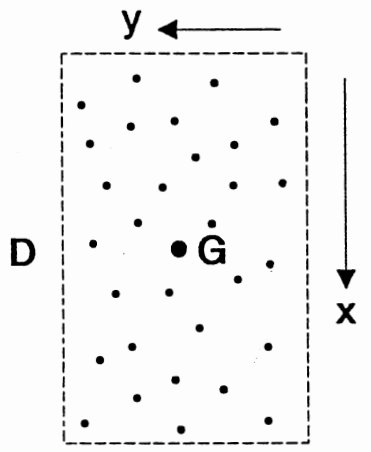

Figure 1: Grid Point G, Surrounded by Sample (data) Points

$$\hat{z}_g = \frac{\eta_1 z_{s1} + \eta_2 z_{s2} + \eta_3 z_{s3} + \cdots + \eta_n z_{sn}}{q} \tag{3.1}$$

where

$$q = \sum_{i=1}^{n} \eta_i \tag{3.2}$$

and where η_i is a weighting coefficient for z_{si}, the elevation value at sampling point i (i = 1, 2, 3, $\cdots$, n).

By letting

$$\frac{\eta_i}{q} = \lambda_i \quad (i = 1, 2, 3, \cdots, n) \tag{3.3}$$

Equation (3.1) becomes

$$\hat{z}_g = \sum_{i=1}^{n} \lambda_i z_{si} \tag{3.4}$$

Similarly, the estimator $\hat{z}_g$ could be written as

$$\hat{z}_g = \sum_{i=1}^{n} \lambda_i z_{si} \tag{3.5}$$

where $\hat{z}_g$ is a linear estimator.

The weighting factor λ_i will be expressed as a function of the distance d_i

$$\lambda_i = f(d_i) \tag{3.6}$$

where d_i is the distance between the grid point (G) and the data (or sample) point i.

$$d_i = [(x_g - x_i)^2 + (y_g - y_i)^2]^{1/2} \tag{3.7}$$

where

(x_g, y_g) = coordinates of the grid point G

(x_i, y_i) = coordinates of the data (or sample) point i

By substituting Equation (3.6) into Equation (3.5) one obtains

$$\hat{Z}_g = \sum_{i=1}^{n} \lambda_i Z_{si} = \sum_{i=1}^{n} f(d_i) Z_{si} \tag{3.8}$$

From Equations (3.3) and (3.2),

$$\sum_{i=1}^{n} \lambda_i = \frac{1}{q} \sum_{i=1}^{n} \eta_i = \frac{\sum_{i=1}^{n} \eta_i}{\sum_{i=1}^{n} \eta_i} = 1 \tag{3.9}$$

Thus, Equation (3.8) is comparable to the "Expected value" of Z which is defined as

$$E(Z) = \sum_{i=1}^{n} f_z(Z_i) . Z_i \tag{3.10}$$

where $f_z(Z_i)$ is the "probability value" for Z_i. Equation (3.10) is presented to tie the theory in this section with kriging theory given in Chapter II.

The problem is now reduced to determining the appropriate function, $f(d_i)$. The function should take into consideration the physical nature of the problem.

For $\hat{z}_g$ computation, the influence of a sample (or data) point i on the grid point G decreases as the distance d_i between the sample point and the grid point increases; i.e. the weighting factor λ_i should be inversely related to the distance d_i. Thus, a general expression for λ_i is

$$\lambda_i = f(d_i) = \frac{(1/d_i^k)}{\sum_{i=1}^{n} \{(1/d_i^k)\}} \tag{3.11}$$

where k is an exponent.

By substituting Equation (3.7) into Equation (3.11), one obtains

$$\lambda_i = \frac{\{1/[(x_g - x_i)^2 + (y_g - y_i)^2]^{k/2}\}}{\sum_{i=1}^{n} \{(1/[(x_g - x_i)^2 + (y_g - y_i)^2]^{k/2}\}} \tag{3.12}$$

Considering the large data size involved, using k = 2 in Equation (3.12) will greatly reduce computer processing time since it eliminates the need for a square-root determination, and also reduces the number of exponentiation operations. Therefore k = 2 will be used in determining λ_i.

Using k = 2, Equation (3.12) can be simplified as

$$\lambda_i = \frac{\{1/[(x_g - x_i)^2 + (y_g - y_i)^2]\}}{\sum_{i=1}^{n} \{1/[(x_g - x_i)^2 + (y_g - y_i)^2]\}} \tag{3.13}$$

The elevation estimate at the grid point G ($\hat{z}_g$) is then obtained by substituting λ_i into Equation (3.4);

$$\hat{z}_g = \sum_{i=1}^{n} \frac{\{z_{si}/[(x_g - x_i)^2 + (y_g - y_i)^2]\}}{\sum_{i=1}^{n} \{1/[(x_g - x_i)^2 + (y_g - y_i)^2]\}} \tag{3.14}$$

where z_{si} is the elevation value at sampling point i.

Writing

$$S = \sum_{i=1}^{n} \{1/[(x_g - x_i)^2 + (y_g - y_i)^2]\} \tag{3.15}$$

Equation (3.14) can be written as

$$\hat{z}_g = \frac{1}{S} \sum_{i=1}^{n} \frac{z_{si}}{[(x_g - x_i)^2 + (y_g - y_i)^2]} \tag{3.16}$$

Definition of Neighborhood Zone

The neighborhood zone of a grid point G is the zone whereby the sample (data) points within it significantly influence the elevation value at the grid point. Consider a grid point G with its neighborhood zone as shown in Figure 2, where

Δx_g = x - increment for grid points,

Δy_g = y - increment for grid points,

$C_x \Delta x_g$ = neighborhood zone limits for x, from the grid point,

$C_y \Delta y_g$ = neighborhood zone limits for y, from the grid point,

C_x, C_y = coefficients (in the x- and y-directions respectively), to be determined, and

$\frac{\Delta s}{2}$ = maximum attainable distance from the grid point G, within the neighborhood zone.

The furthest sample points from the grid point G are located at the points A, B, C and D, which specify the limits of the neighborhood zone. From Figure 2,

$$\frac{\Delta s}{2} = [(C_x \Delta x_g)^2 + (C_y \Delta y_g)^2]^{1/2} \tag{3.17}$$

It is desired to select optimum coefficients (C_x and C_y) with respect to some chosen criteria. This brings into focus certain considerations:

1. The neighborhood zone is determined from the grid resolution.

2. The farther away a sample (or data) point is from the grid point the less its influence on the elevation value at the grid point as considered in the weighting factor.

3. For a given zone area A, it is desirable to constrain or limit the perimeter (or boundary) of the neighborhood zone for computational efficiency.

Of all parallelograms with a prescribed (fixed) area (or zone) A, the one with the smallest perimeter is a square

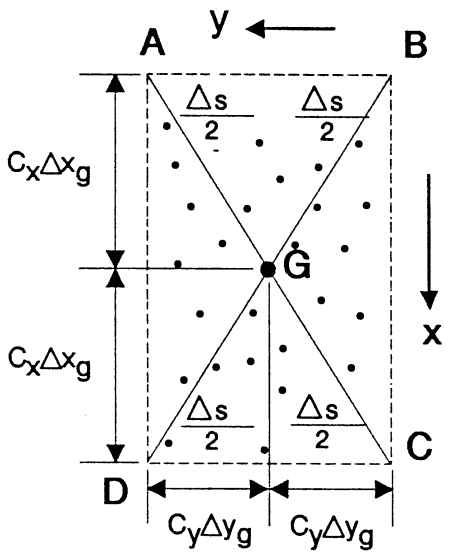

Figure 2: "Neighborhood Zone"

(see Beveridge and Schechter (1970) and Rao (1984)). Relating this to Figure 2, one obtains

$$C_x \, \Delta x_g = C_y \, \Delta y_g \tag{3.18}$$

For convenience, the ratio α_g will be defined as

$$\alpha_g = \frac{\Delta y_g}{\Delta x_g} = \frac{C_x}{C_y} \tag{3.19}$$

Since Δx_g and Δy_g are user-inputs, the ratio, α_g, can be determined, and C_x can then be obtained from Equation (3.19) as

$$C_x = (\Delta y_g \, / \, \Delta x_g) \; C_y = \alpha_g C_y \tag{3.20}$$

or C_y can be obtained as

$$C_y = C_x/(\Delta y_g \, / \, \Delta x_g) = C_x/\alpha_g \tag{3.21}$$

The coefficients C_x and C_y can be determined by Equation (3.19). The neighborhood zone for a grid point G is then a square which may be completely specified by Δx_g, Δy_g, C_x and C_y.

A simpler approach to define the neighborhood zone is to specify $\Delta s/2$ (and hence Δs), and then obtain C_x or C_y in terms of Δs. An estimate of $\Delta s/2$ will be made from the form of the input data and the grid resolution.

Substituting Equation (3.20) into Equation (3.17) and

squaring both sides of the resultant equation;

$$(\Delta s/2)^2 = \alpha_g^2 \, C_y^2 (\Delta x_g)^2 + C_y^2 (\Delta y_g)^2 = C_y^2 [\alpha_g^2 (\Delta x_g)^2 + (\Delta y_g)^2] \tag{3.22}$$

Using $\alpha_g = \Delta y_g / \Delta x_g$ yields

$$C_y = \frac{\Delta s}{2[(\Delta y_g)^2 + (\Delta y_g)^2]^{1/2}} \tag{3.23}$$

or

$$C_y = \frac{\Delta s}{2^{3/2}(\Delta y_g)} \tag{3.24}$$

Equation (3.24) is then substituted into Equation (3.20) to obtain C_x.

Finding the Neighborhood Zone

When thousands of data points are involved, an efficient algorithm is required to determine the neighborhood zone. An algorithm to accomplish this task is discussed here. It uses knowledge of the organization or storage arrangement of the input data to improve its efficiency. The algorithm is therefore limited to the particular instrumentation system discussed in Chapter IV.

Data Format

If the elevation points from the instrumentation were stored in a completely random fashion, then the algorithm

would have to check every single point to determine whether it falls in the neighborhood zone. For the many data points gathered in this study, such an algorithm would require excessive computer time. Fortunately, the data system gathers and stores points in a systematic fashion such that a smaller searching zone can be specified.

A schematic of the data gathering movement is given in Figure 3. The equipment starts at the furthest upsloped location and moves across the plot from y_{st} to y_{fin} gathering elevation data at an approximate spacing to Δy_s. The equipment then moves down the plot a distance of Δx_s. Data are now gathered across the plot from y_{fin} to y_{st}. These steps are repeated down the plot as shown in Figure 3.

If the data collection system worked perfectly, the data would be stored as a grid with Δx_s spacing in the x-direction and Δy_s spacing in the y-direction. Unfortunately the data gathering system does not work perfectly. Gaps in the data are possible. Thus, to search for the neighborhood zone in the lines of data a range around the points of interest is needed to account for missing data points. This logic is given separately for the first row (i=1) and subsequent rows ($i \geq 2$).

First Row (i=1)

For the first "pass" in the y-direction, the grid point j is approximately located at the position

$$P_{gj} = |INT((y_g(j) - y_{st})/\Delta y_s)| \qquad (3.25)$$

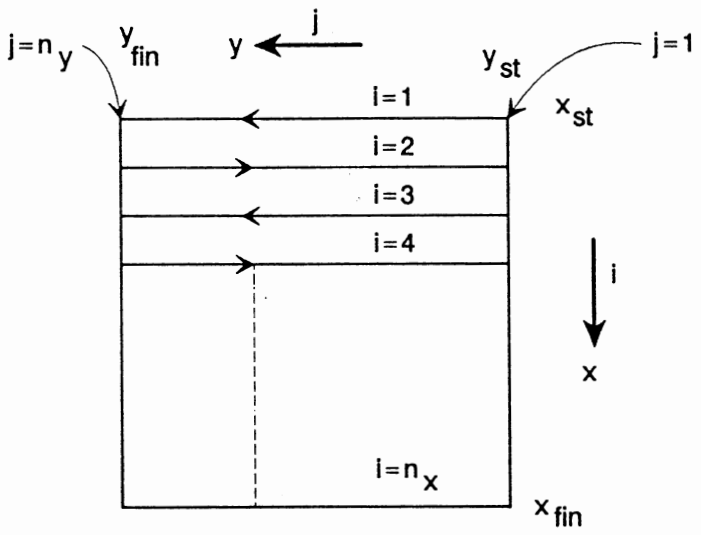

Figure 3: Data Format

where

$y_g(j)$ = y-value at grid point j

y_{st} = starting value for y

Δy_s = approximate input-data spacing in the y-direction

For i=1, the location of the lower limit of the searching zone is given as,

$$L_{p1} = P_{gj} - P_{L1} \tag{3.26}$$

where P_{L1} is defined as

$$P_{L1} = |INT((1+f)c_y \Delta y_g/\Delta y_s)| \tag{3.27}$$

where f is a neighborhood zone extension factor to account for possible gaps in the data file and other terms are as previously defined.

Similarly, the location of the upper limit of the searching zone is given as,

$$U_{p1} = P_{gj} + P_{L1} \tag{3.28}$$

where P_{L1} is as previously defined by Equation (3.27). If L_{p1} is less than 1, it is set to 1. If U_{p1} is greater than n_t, the total number of data points in the input data file, U_{p1} is then set to n_t.

Subsequent Rows ($i \geq 2$)

For subsequent "passes" in the y-direction, the limits of the searching zone (their locations in the dataset) are

estimated in a similar manner as above. Even rows require careful considerations because of the complex patterns that data are stored as shown in Figure 4. The location of the grid point j in the dataset for odd rows is estimated as

$$P_{gp} = ((i-1)n_{1y}) + P_{gj} \tag{3.29}$$

and for even rows as

$$P_{gp} = ((i-1)n_{1y}) + P_e\left(\frac{j}{\alpha qg}+1\right)+\left|INT\left(\frac{y_g(j) - y_e\left(\frac{j}{\alpha qg}+1\right)}{\Delta y_s}\right)\right| \tag{3.30}$$

where

$y_g(j)$ = y-value at grid point j

$\alpha qg = |INT(\Delta y_q/\Delta y_g)|$, for $\Delta y_g < \Delta y_q$, (3.31)

$\alpha qg = |INT(\Delta y_g/\Delta y_q)|$, for $\Delta y_g > \Delta y_q$, (3.32)

Δy_q = y-increment for equipment movement,

y_e = an important y-value for the i, even case (Figure 4),

P_e = approximate position (or location) of y_e in the dataset

n_{1y}= approximate number of data points for one complete "pass" in the y- direction.

There are n_{qy} y_e's where n_{qy} is the number of movements of the data gathering equipment for each pass in the y-direction, or

$$n_{qy} = |INT((y_{fin} - y_{st})/\Delta y_q)| \tag{3.33}$$

The equation for P_{gp} for the i, even cases [Equation (3.30)] was developed in recognition of the data-flow

pattern in the negative y-direction shown in Figure 4.

The locations of the limits of the searching zone in the lines of data (for $i \geq 2$) are very similar to those previously given by Equations (3.26) and (3.28). Once again, if L_p is less than 1, it is set to 1. If U_p is greater than n_t, the total number of data points in the input data file, U_p is then set to n_t. The value of f used should be large enough to eliminate errors in not finding data points.

Empty Neighborhood Zone

The "empty neighborhood zone" refers to a situation where a grid point has no datapoints within its specified neighborhood zone. The elevation value for such a grid point is then estimated from the values at its neighboring grid points.

Consider a grid point in Figure 5, at P, with an empty neighborhood zone. Its elevation value is to be estimated from the eight neighboring grid points.

The neighboring grid points (1) through (8) are considered on a one-by-one basis. The possibility exists that some of those points (1 to 8) may have empty neighborhood zones. Therefore, treating each point separately, the algorithm first checks if the point has an empty neighborhood zone. If the zone is not empty the program goes directly to include the grid point in the computation process. If the zone is empty the program

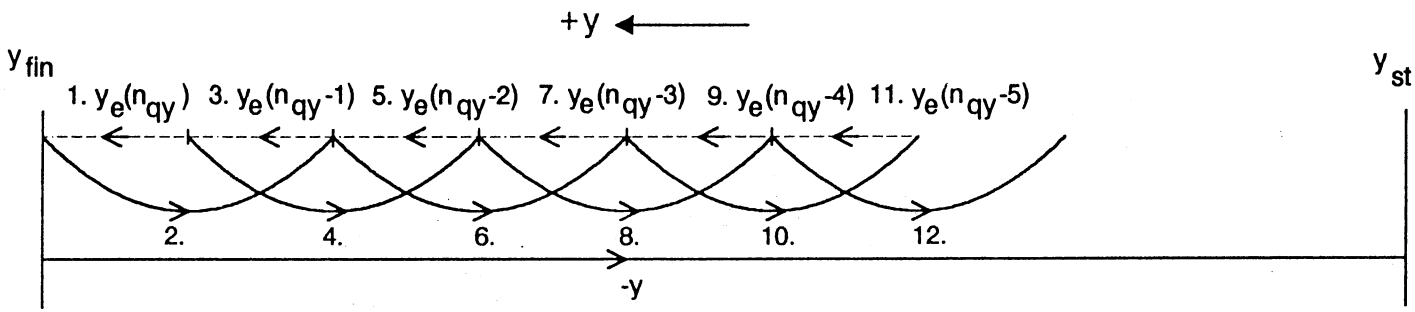

Figure 4: Data Flow Pattern for the Negative y-Direction (i, even, cases)

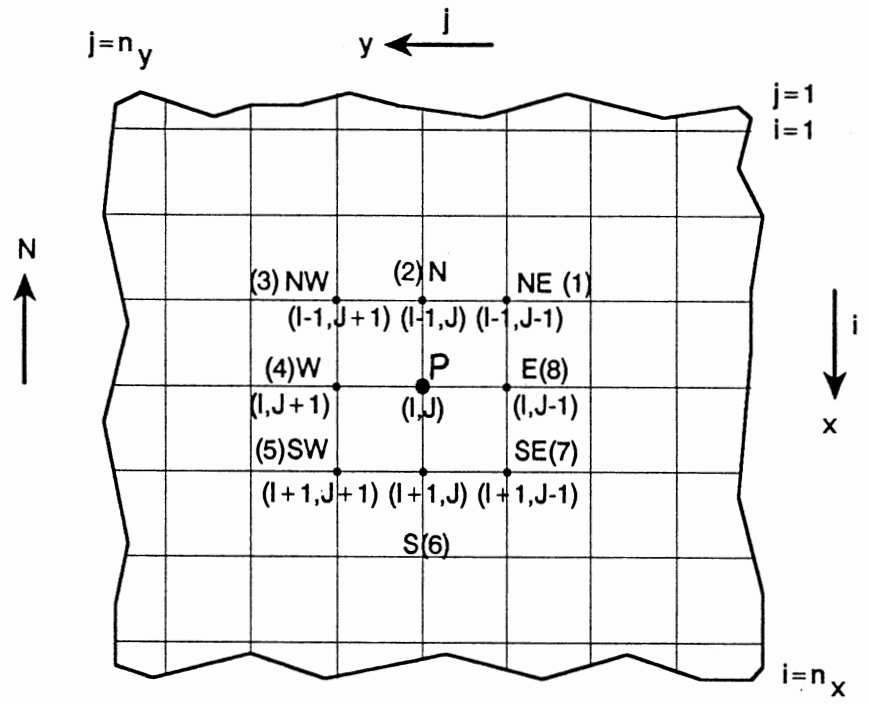

Figure 5: Grid Point, at P, with Eight Neighboring Grid Points

conducts further search as necessary with the restriction that the grid points used in the computation are no farther than 4 inches from P.

The elevation value at P is computed using Equation (3.16), where z_{si} are the elevation values at the neighboring grid points involved in the computation, n is the number of neighboring grid points involved in the computation and the subscript g refers to the point P while the subscript i refers to the neighboring points.

Channel Identification

An algorithm developed by Couger et al. (1989) is used to identify flow paths and channels. In this algorithm, flow paths are identified by assuming that water will flow to the grid point of lowest elevation. Inertia forces are neglected. The sequence of major computational steps is shown in Figure 6. These steps are discussed in greater detail later.

The program first reads in the x, y and z coordinates for each point. The data file is then iteratively examined by a recursive procedure which compares each Point P with each of the eight adjacent points shown in Figure 7 to determine if they have a lower elevation than Point P. The adjacent point with the greatest elevation difference from Point P is its outflow point. If all the adjacent points have a higher elevation than Point P, then there is no outflow and the point is a depression.

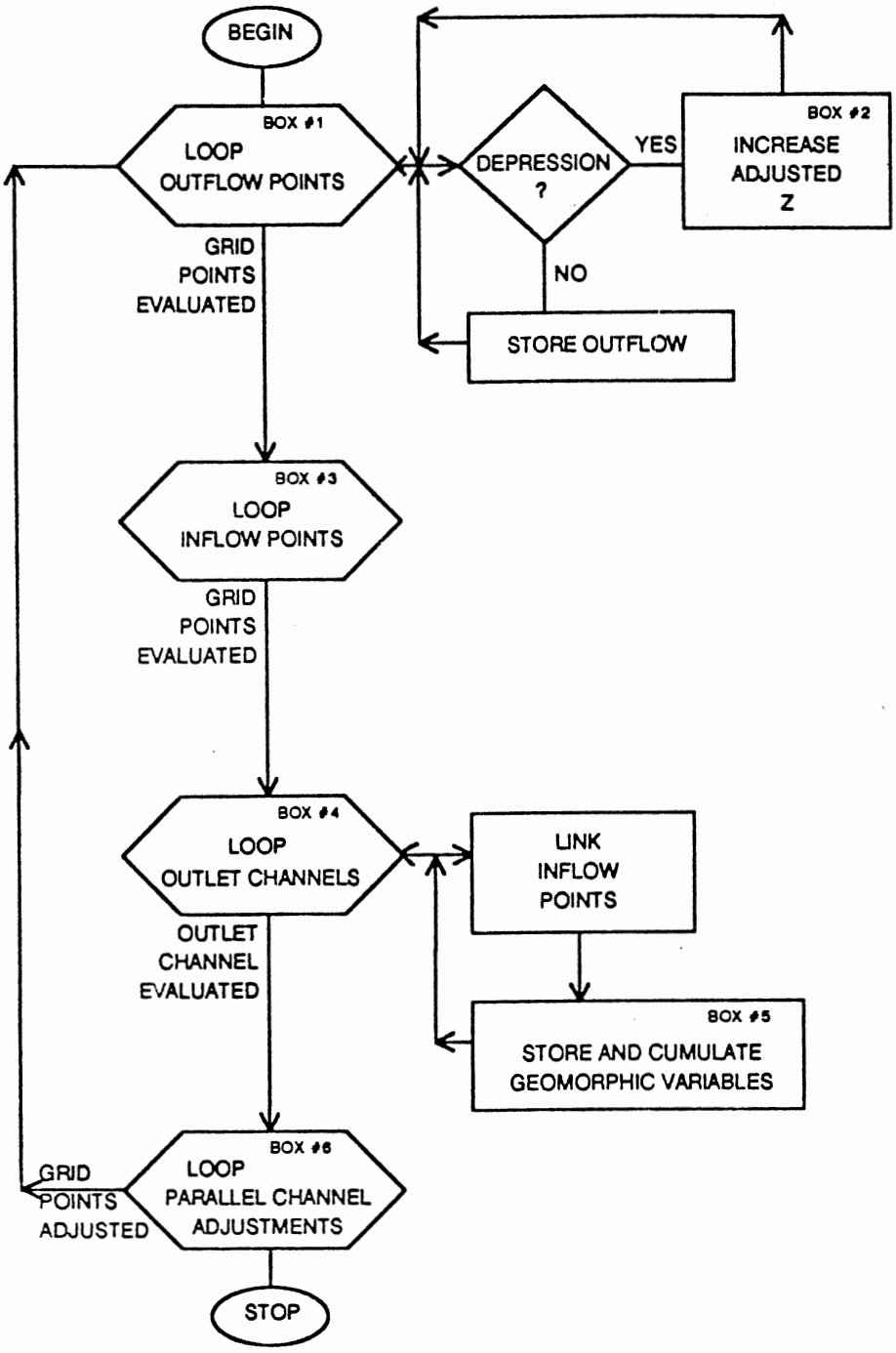

Figure 6: Flow Chart for Rill Identification

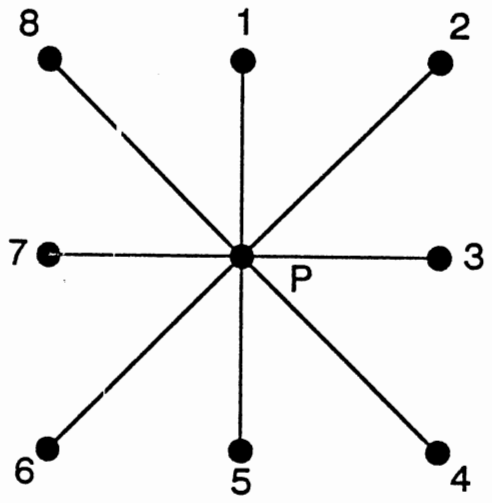

Figure 7: Inflow and Outflow Paths for Grid Point P.

Depressions are handled by adding a small incremental depth to the elevation, as though the depression were filled with water. The adjusted elevation is now compared to the adjacent points. Incremental depths are repeatedly added until outflow can occur. To implement this procedure, grid points are evaluated by selecting the outflow from the current point as the next point for evaluation. Depression filling requires that some grid points are evaluated more than once. This relatively simple approach for filling depressions will sometimes result in a meandering flow path through depressions. The algorithm assumes that all depressions eventually contribute to runoff.

After the outflow has been determined for all the grid points, each point is then examined to determine inflow points. This step is represented by Box #3 in Figure 6. There are eight adjacent points to interior grid points as shown in Figure 7. An array with eight elements is used to record whether flow is to point P by storing either a zero (no flow) or one (flow) for each adjacent point. Flow to Point P is simply determined by examining whether the outflow for the adjacent points (determined in the first pass of data) is Point P. When evaluating each grid point, the algorithm starts with the adjacent point which is directly above the point of evaluation and moves in a clockwise direction, that is, from Point 1 to Point 8 in Figure 7.

After inflow options for each grid point have been determined, it is possible to track the flow paths contributing to a given channel. The first step is to locate a channel at the outlet of the plot. This represents the base or trunk of a branching network. A recursive function is used to track the flow paths of that particular drainage network. The algorithm then locates the next channel at the outlet and repeats the process. These steps are represented by Box #4 in Figure 6.

Figure 8 will be used to describe the recursive function for tracking flow paths. Figure 8a represents the final network determined by the recursive function. Starting at Point A (base point), assume that the only inflow is the point directly above it or Point B. Therefore the path from Point B to Point A has been established. Now inflows at Point B will be considered as shown in Figure 8b. Here there are inflows from Point 2 (Point C in Figure 8a) and Point 8 (Point G in Figure 8a). Therefore, two separate branches will eventually have to be constructed at Point B. Since the algorithm works in clockwise direction from Point 1, the branch from Point 2 will be resolved first. The inflows at Point C are now considered. The first inflow point identified is flow from Point D. The algorithm then moves to this point and finds that it has no inflow points. A complete flow path of DCBA has now been established. The algorithm returns to Point C, resolves the flow path ECBA and repeats the process for the flow path FCBA. After all

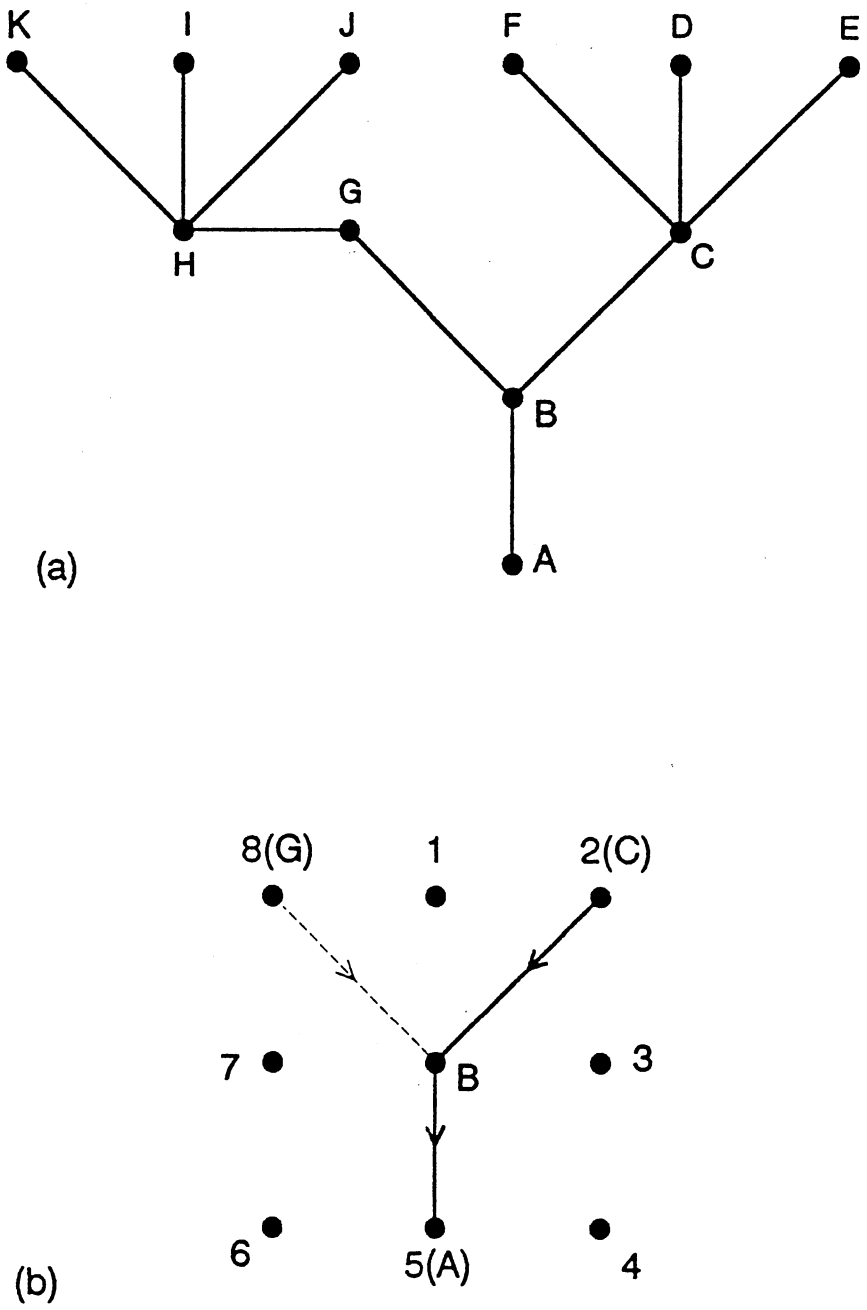

Figure 8: Schematic for Linking Flow Paths: (a) complete drainage network and (b) flow paths at Point B.

flow paths at Point C have been resolved, the algorithm returns to Point B and works on the left-hand side branch in a similar manner. Here the algorithm goes to Point G, then Point H, then Point I, then Point J and then Point K to resolve all flow paths.

Once flow paths have been determined using the algorithm described above, a system is still needed to quantify and analyze individual flow paths. To accomplish this, the network is broken down into rill orders by a method similar to that proposed by Strahler for stream orders (Morisawa, 1985). Figure 9 shows a schematic illustrating the rill ordering scheme. Rill orders are determined by examining the order of flows to the point of interest. Although there are seven possible inflows to a point, only the two inflows of highest orders are considered. If these two inflows are of the same order, the point is assigned the next larger order. If these two inflows are of different orders, the point is assigned the larger of the two possible orders. If the point has only one inflow, the order is equal to the inflow order. If the point has no inflow, the order is zero.

Rill order is established as the algorithm moves back to the starting point. For example in Figure 8a, after the flow paths above Point C have been resolved, the order for Point C can be defined. Likewise the order of Point B can only be defined after the orders of Point C and Point G are resolved. Geomorphic variables are also calculated as the

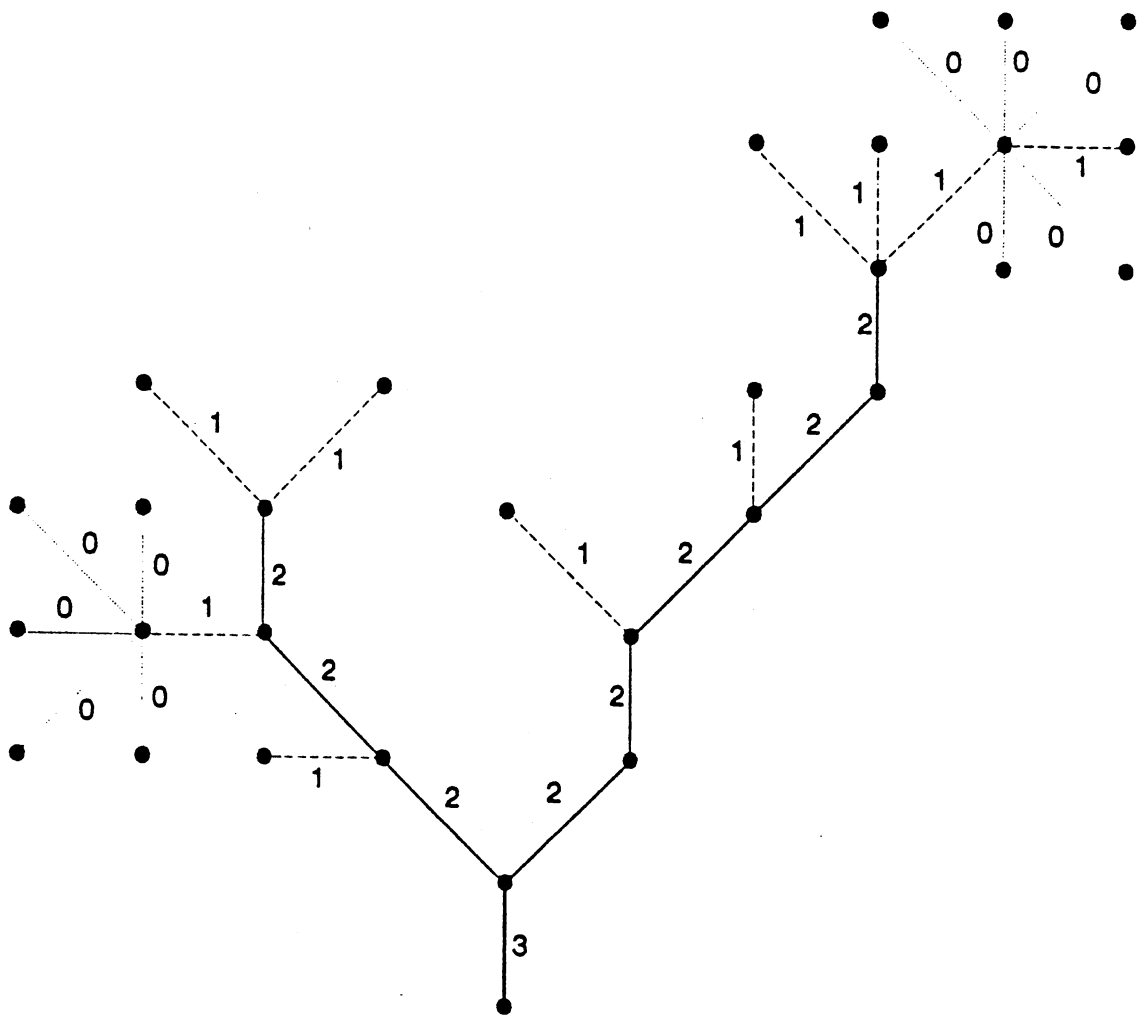

Figure 9. Example of Rill Ordering Scheme.

algorithm moves back to the starting point.

After drainage patterns have been determined for the entire plot, the rill channels are further enhanced to prevent parallel flows. This step is indicated by Box #6 in Figure 6. Parallel flows occur when two or more adjacent channels appear to be flowing downslope in parallel. Actually the algorithm has found more than one flow path in a single channel. To reduce this occurrence, the elevations corresponding to second and higher order rills are artificially lowered to force lateral flow instead of parallel flow. The procedures to identify rills are then repeated with the adjusted elevation values.

CHAPTER IV

EXPERIMENTAL PROCEDURES

Introduction

In this chapter the general experimental design of the study is first described. Equipment and methods used to gather and analyze data are then given. Procedures to quantify flow paths are also discussed.

Experimental Design

Some factors that may affect drainage network development are initial soil roughness, rainfall rate, runoff rate, soil type, slope and cover. Independent variables in the experimental design were initial soil roughness and rainfall rate. Soil type, slope and surface cover were held constant.

Two levels of soil roughness and two rainfall rates were tested for a total of four tests. For all tests, the soil cover was bare, a loamy soil was used and the slope was approximately uniform at eight percent. Laboratory tests on samples of the soil used in the experiments indicated that the soil was medium-textured with 38% sand, 40% silt and 22% clay. Also, the soil had a pH of 7.7, 1022 parts per million (ppm) of total soluble salts, 18 ppm sodium, 116

ppm calcium, 34 ppm magnesium, and a Sodium Adsorption Ratio (SAR) of 0.0.

A relatively high constant rainfall rate of 2 in/hr (5.08 cm/hr) and a relatively low constant rainfall rate of 1 in/hr (2.54 cm/hr) were used. For the high intensity the rainfall was applied for two hours while it was applied for four hours for the low intensity. Two different surface conditions called smooth and rough were considered.

Each test group consisted of two sets of topographic measurement for before and after erosion. A total of 8 topographic measurement sets of data were therefore gathered. A summary of experimental tests is given in Table I. In Table I, each run group name depicts the soil surface condition (SMOoth or ROUGH) and the rainfall level (LOW or HIGH). Also, the first three letters in each topographic data group are given. The first letter (B or A) indicates whether the data was taken Before (B) or After (A) erosion. The second letter depicts the soil surface condition: Smooth (S) or Rough (R), and the third letter depicts the rainfall level: Low (L) or High (H).

Experimental Equipment and Methods

The experiments were performed in a laboratory controlled environment using the "erosion table" located in one of the Agricultural Engineering Department's research laboratories situated at the western edge of the Oklahoma

TABLE I

SUMMARY OF EXPERIMENTAL TESTS

Run group #	Name	Rainfall rate (in/hr)	Topographic measurement sets
1	SMOLOW	1.0	BSL ASL
2	SMOHIGH	2.0	BSH ASH
3	ROUGHLOW	1.0	BRL ARL
4	ROUGHIGH	2.0	BRH ARH

State University campus. This laboratory setting (Figures 10 and 11) is well-suited for this study because of the available image processing system for recording topographic data and the ability to control environmental factors.

The erosion table is 32 ft. (≈9.8m) long and 8 ft. (2.4m) wide. It has two slope segments. One is fixed, and the other is adjustable. The fixed slope segment is at the outlet end while the adjustable slope segment is at the inlet end (Figure 11). The system is equipped with a rainfall simulator and an instrumentation component for measuring soil surface topography. A detailed description of the erosion apparatus and instrumentation system is given in Wilson and Rice (1987) and Rice et al. (1988).

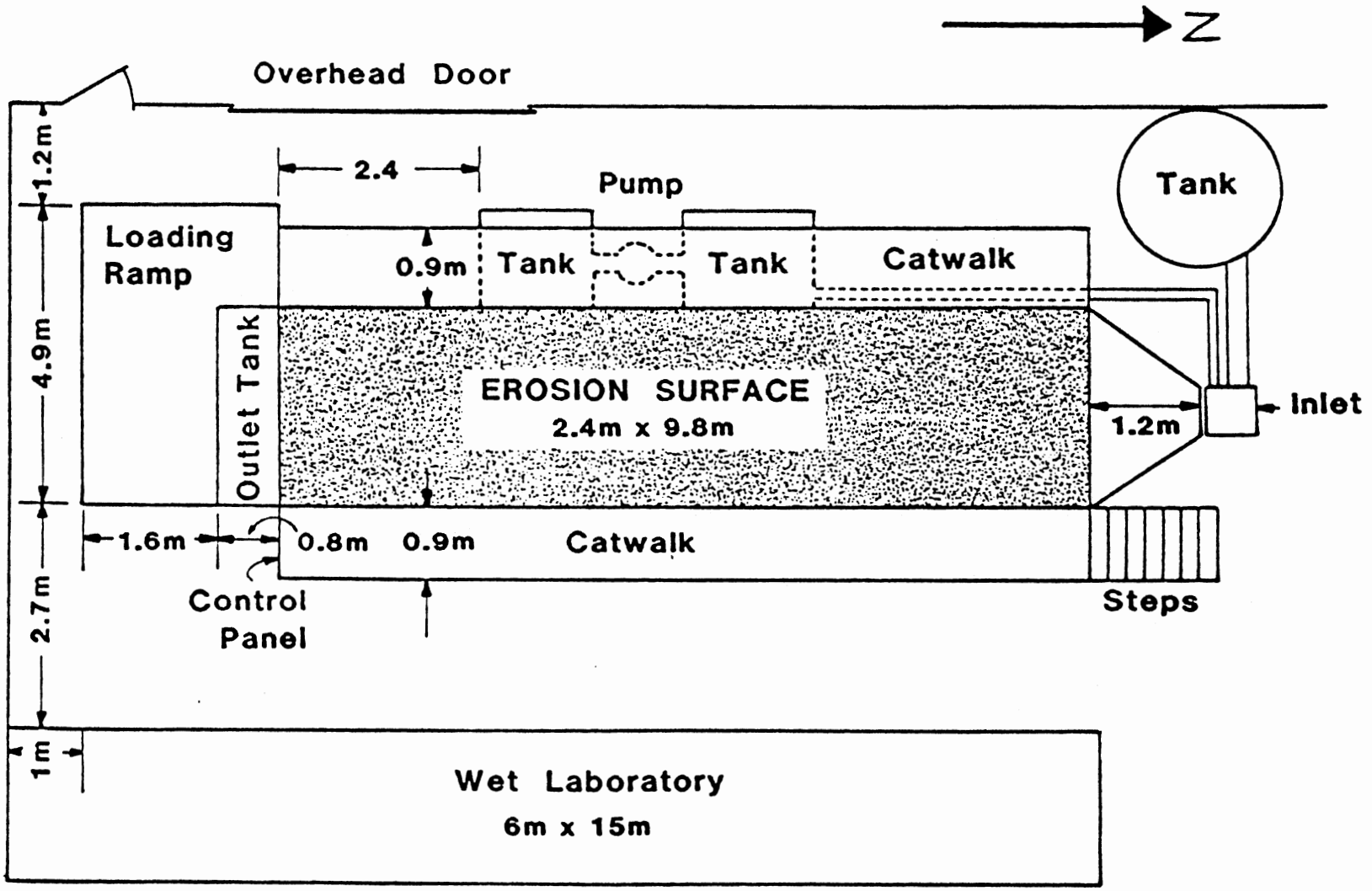

Figure 10: Layout of Erosion Apparatus.

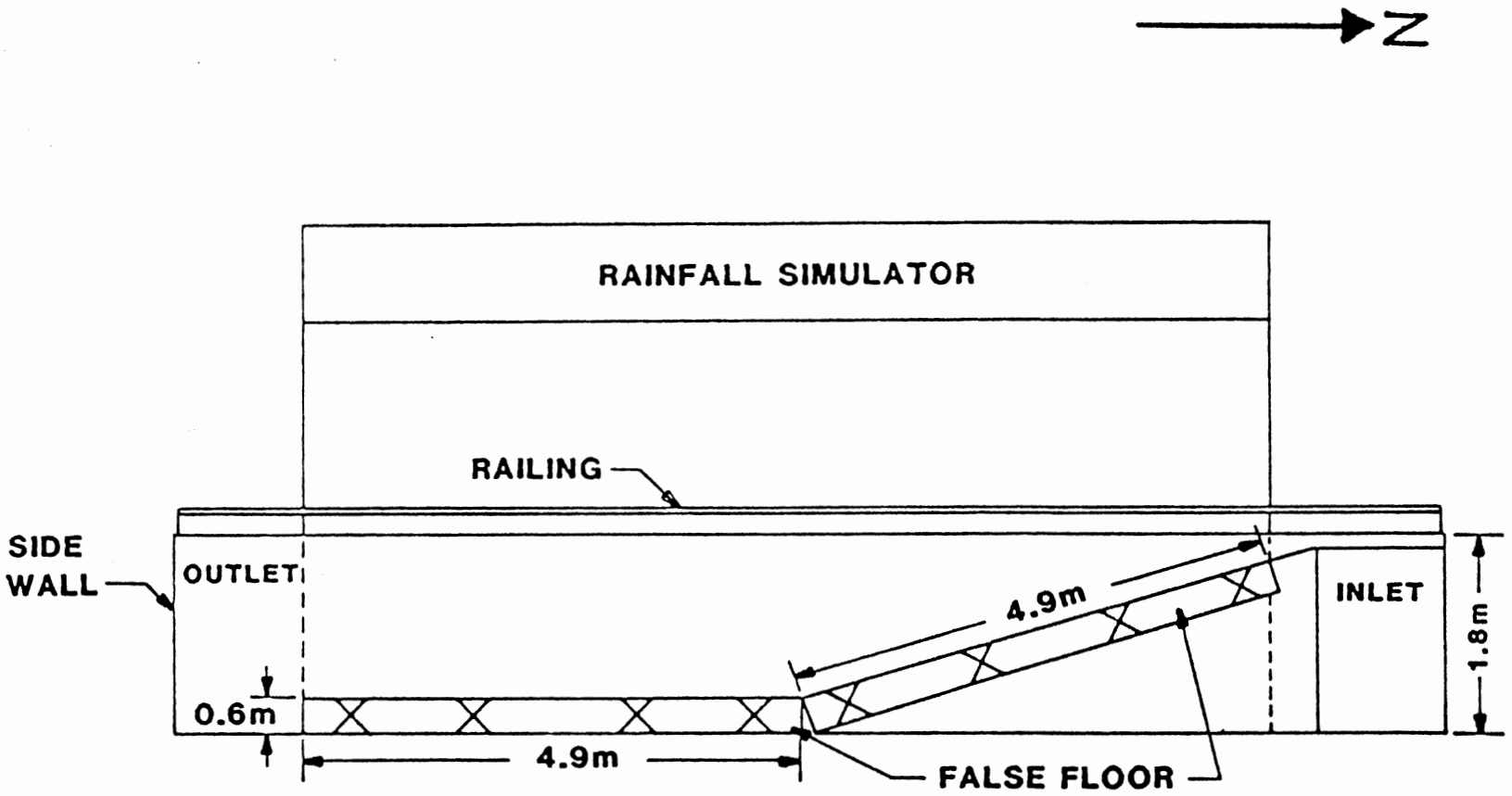

Figure 11: Side View of Erosion Table

Plot Preparation

The fixed slope segment of the erosion table was horizontal at a height of 25 in. (0.6m) above the laboratory floor. The adjustable slope segment was raised to a height of 52 in. (1.3m) at the Northmost end. The soil was then filled to the 8% slope line which had previously been marked on the table.

A loamy soil was purchased and stored outside the laboratory building. It was covered with a plastic protection to minimize weather effects. The soil was loaded onto the erosion table through a large overhead door and the loading ramp (Figure 10) using a front-end loader. Three 2 in. (5cm) perforated plastic pipes were placed beneath the soil on the table for drainage. One drainage pipe was located at each side of the erosion table and one was located in the middle.

The soil was spread on the table as it was being loaded. Soil compaction occurred during the loading process. Before each experimental test, the plot was roto-tilled up and down, and then across the plot. The additional rotary tillage across the plot was necessary to eliminate channels which were formed from the up-and-down operation. For the rough soil profile, the plot was roto-tilled only. For the smooth soil profile, the plot was roto-tilled and then raked to obtain a relatively smooth surface configuration. The rotary tillage operation was performed after most of the procedures necessary for the run

have been accomplished. This minimized disturbance to the prepared plot before the rainfall event. After the rainfall application, the plot was left to dry before being roto-tilled for the next experimental test.

Rainfall Simulator

The rainfall simulator suspended above the erosion surface is an essential component in the erosion apparatus. The simulator consists of six separate frames with each frame equipped with two oscillatory nozzles driven by a pneumatic cylinder. The six simulator frames are located approximately 5 ft. apart. They are divided into two groups, each group consisting of three frames. The vertical heights of the simulator frames can be adjusted.

Water supply for the rainfall simulator is obtained from two rectangular water tanks located under the catwalk on the western side of the erosion table (Figure 10). Overspray pans are provided beneath the nozzles to collect excess water and return it to the supply tanks.

The rainfall simulator is capable of producing rainfall with drop size distribution and impact velocities near those of natural rainfall (Wilson and Rice, 1987). The rainfall rate is controlled through a timer switch located at the Southern end of the erosion table. Different switch settings correspond to different time intervals that the oscillating nozzles discharged into the overspray pans. A short delay time implies the nozzles spend little time in

the overspray pans, thus discharging more water to the plot per unit time, and thereby increasing the rainfall intensity. Similarly, a large delay time corresponds to a lower rainfall intensity. These settings enable the simulator to deliver both uniform and varying rainfall intensities.

Calibration: Prior to the start of experimental tests, the rainfall simulator was calibrated. The main objective was to determine the extent of spatial uniformity of the rainfall application. Other objectives were to determine the rainfall intensity for a pre-set timer switch position and to determine which portions or segments of the rainfall apparatus needed adjustments (e.g. overspray pan adjustment, adjusting nozzle height to top of raingauges, etc.) before the start of experiments.

The calibration objectives were accomplished by placing raingauges in 1 ft. by 1 ft. grid and measuring the rainfall volumes. Some overspray pans were adjusted, as necessary, and the nozzle height to top of raingauges was adjusted to achieve better overlap at the center of the erosion table. The spatial uniformity of the rainfall application was determined using the uniformity coefficient and the coefficient of variation. The uniformity coefficient (Cu) is given as (Moore et al., 1983)

$$Cu = 100\left(1 - \frac{\sum_{i=1}^{n} |x_i - \bar{x}|}{n\bar{x}}\right) \quad (4.1)$$

whereas the coefficient of variation (CV) is given as

$$CV = \frac{S_d}{\bar{x}} \quad (4.2)$$

where x_i is the point reading from each raingauge, n is the number of raingauges, $\bar{x}$ is the mean and S_d is the standard deviation.

The higher the Cu, and the lower the CV, the more uniform the spatial rainfall application. A uniformity coefficient (Cu) of 74% and a coefficient of variation (CV) of 0.3 were obtained for the rainfall simulator. This compared favorably to other rainfall simulators (e.g. Moore et al., 1983).

For the experimental tests, constant rainfall intensities of 1.0 in/hr and 2.0 in/hr were used. For the relatively high rainfall intensity the rainfall simulator was operated for 2 hours while it was operated for 4 hours for the relatively low rainfall rate. The simulator nozzles were set to a height of approximately 11 ft. above the top of the soil.

Gutters: Gutters were needed to minimize "side wall/edge effects" on the erosion table during rainfall simulator operation. Water impinging on the sidewalls of

the erosion table needed to be collected in gutters (troughs) to minimize interference with rainfall pattern and drainage network development.

Two gutters were placed at the sidewalls of the erosion table, one at each sidewall. The gutters were constructed from sheet metal. For easier portability, each gutter was constructed in four 8-foot segments. The gutters had right-triangular cross-sections with top width of 3 inches and a depth of 3 inches. They were mounted on supports placed into the soil at approximately 8% slope. A flexible hose was connected to the outlet end of each gutter to avoid interference with the runoff hydrograph.

Soil, Runoff and Sediment Sampling

For each set of topographic measurements soil samples were taken at points randomly located on the plot for bulk density and moisture content determinations. Seven samples were taken before and seven after erosion. For the before erosion sampling, the soil samples were taken before the topography measurements. After taking each soil sample, the depression created from the sampling process was filled back with soil to avoid interference with the topography measurements. The sampling locations were recorded. For the after erosion sampling, the soil samples were taken after the topography measurements, and at points 5 in. to the left of the points where the before erosion soil samples were taken.

The soil sampling device had two identical cylindrical rings with an inside diameter of 2.125 in. and a height of 1.1875 in. One was used for taking the "actual" soil sample, and the other served as part of the protection for the soil sample. The soil samples used in the moisture content and bulk density determination were carefully removed from the appropriate ring. The volume of each soil sample, V_t, was that of the cylindrical ring equal to 4.21 inches^3 (69 cm^3).

The soil samples were weighed to obtain the wet sample weight, W_t, and then oven-dried to obtain the oven-dried weight, W_s. The weight of water in each sample was obtained as $W_w = W_t - W_s$. The following computations were made:

$$\text{Bulk density (Dry bulk density)}, \rho_B = W_s/V_t \qquad (4.3)$$

$$\text{Water content (dry weight basis)}, w = W_w/W_s \qquad (4.4)$$

$$\text{Volumetric water content}, \theta = w\rho_B/\rho_w \qquad (4.5)$$

where ρ_w is the density of water (= 1gm/cm^3) and other terms are as previously defined.

A collector was installed at the outlet end of the plot. This structure served the dual purpose of runoff/sediment sampling and the prevention of scouring at the outlet end of the plot. The collector was constructed from sheet metal bent at the sides to channel the flow to a single outlet. Runoff samples were taken at specified times during the runoff event. The runoff rate was computed as

the volume of water collected in a calibrated cylinder divided by the time taken to fill that volume.

Each runoff sample was poured into a pre-weighed polypropylene bottle. The bottle and runoff were weighed before oven-drying. Sediment concentration (C) was computed using the definition

$$C = \frac{W_S}{V_W + V_S} \tag{4.6}$$

which, for the density of water of 1 gm/cm^3 can be written as

$$C = (10^6)\left[\frac{W_S}{(W_W) + (W_S/G_S)}\right] \tag{4.7}$$

where V_W is the volume of water, V_S is the volume of dry soil, C is the sediment concentration (mg/L), W_S is the weight of sediment (gm), W_W is the weight of water (gm) and G_S is the specific gravity of sediment ($G_S \approx 2.65$).

Surface Topography Measurements

The soil surface topography was measured before and after each erosion test. The instrumentation system is based on image processing techniques. The key components are a camera, laser source and image processing boards. Details of the instrumentation system are given by Rice et al. (1988).

Calibration procedures were conducted prior to the start of each run. These procedures were used to convert pixel values to distance measurements. Calibration was conducted for the y (lateral) and z (vertical) directions. No calibration was necessary for the x (longitudinal) direction. The positive x, y and z directions were defined as:

x: Southward,

y: Westward and

z: Upward.

For calibration, a flat plate was used as a reference surface. The calibration in the z direction consisted of finding the laser line at the reference height and at two other heights. Calibration in the y-direction involved the use of a flat card with two parallel lines. The location of these lines was used to calibrate the system in the y direction. Here an incandescent light source was used instead of the laser light. Additional details on the calibration procedure is given by Rice et al. (1988).

Topography measurements were made using a set of programs developed by the Agricultural Engineering Department at Oklahoma State University. These programs consisted of a main program and a set of subroutines which were called as necessary by a set of commands. Key commands used in the study are given below.

1. Live: Makes the image live.
2. Filter: Performs a filtering operation on the image using a 1 x 9 convolution filter.
3. Threshold thrLevel: Performs a binary threshold operation on the image at the level thrLevel.
4. Measure: Measures surface topography.
5. Move x_d (or x_d, y_d; or x_d, y_d, z_d): Moves the camera relative to the current position by the specified distances (x_d, y_d, z_d) in the x, y or z directions. The equipment movement is powered by stepper motors.
6. Waitfor Stop: Waits for the stepper motors to stop before continuing with the operations.
7. Waitfor Stable: Waits for the camera to stabilize before continuing with the operations.
8. Locate: This command allows the user to interactively move the camera by single step increments in the x, y and z directions (Distances travelled per step in the x, y and z directions are, respectively, 0.015 in., 0.02 in., and 0.005 in.).

To correct for possible off-positioning of the equipment by possible slippage and other frictional effects, pegs were located at specified distances near the Eastern edge of the plot. When the camera reached the vicinity of a peg, the exact position of the peg was located using the Locate command. This allowed the "shift" in the x, y and z

directions to be determined, which were used in analyzing the data.

The x-coordinate of each peg was written as

$$x_{pc} = (n_p - 1)\ \Delta dp \qquad (4.8),$$

the y-coordinate as

$$y_{pc} = 0 \qquad (4.9),$$

and the z-coordinate as

$$z_{pc} = -(n_p - 1)(s)\Delta dp \qquad (4.10)$$

where n_p is the peg serial number, Δdp is the peg spacing and s is the slope.

Equation (4.10) incorporates changes in the camera height position included in the code for a system that moves downslope.

At each peg, the absolute coordinates were reset to the peg coordinates. This was done by turning off the stepper motors and specifying that the equipment move "fictitious" distances in the x, y and z directions such that the new absolute coordinates were exactly those of the peg. The stepper motors were then turned on to continue with the measurements.

The topographic data was saved for each complete movement in the y-direction. The peg datafile serial number (n_f) was related to the peg serial number (n_p) by

$$n_f = 1 + (n_p - 1) \frac{\Delta dp}{\Delta x_s} \qquad (4.11)$$

where Δx_s is data spacing in the x direction and other terms are as previously defined. The equipment movement sequence, the peg coordinates and the peg datafile serial numbers are shown in Figure 12.

Quantification of Channels

Flow paths are identified using the Couger et al. (1989) algorithm described in Chapter III. This algorithm is written to handle interior points. Plot boundary points are handled separately and depend on flow conditions. For this study, the water at top and bottom edge is free to flow off the plot; therefore, these boundary points are assigned values lower than their adjacent interior points. Conversely, water at the sides cannot flow off the plot because of plot walls. Here the boundary points are assigned values higher than their adjacent interior points.

Many studies have been conducted to quantify major river systems as discussed in Chapter II. Since rill development is also the result of detachment and transport processes, it is reasonable to examine whether geomorphic relationships may be applicable in rill networks. Three "laws" of drainage composition are considered here: Law of Stream Numbers, Law of Stream Lengths and Law of Stream Areas. In addition, drainage density and channel frequency will also be calculated for the rill networks. Definitions

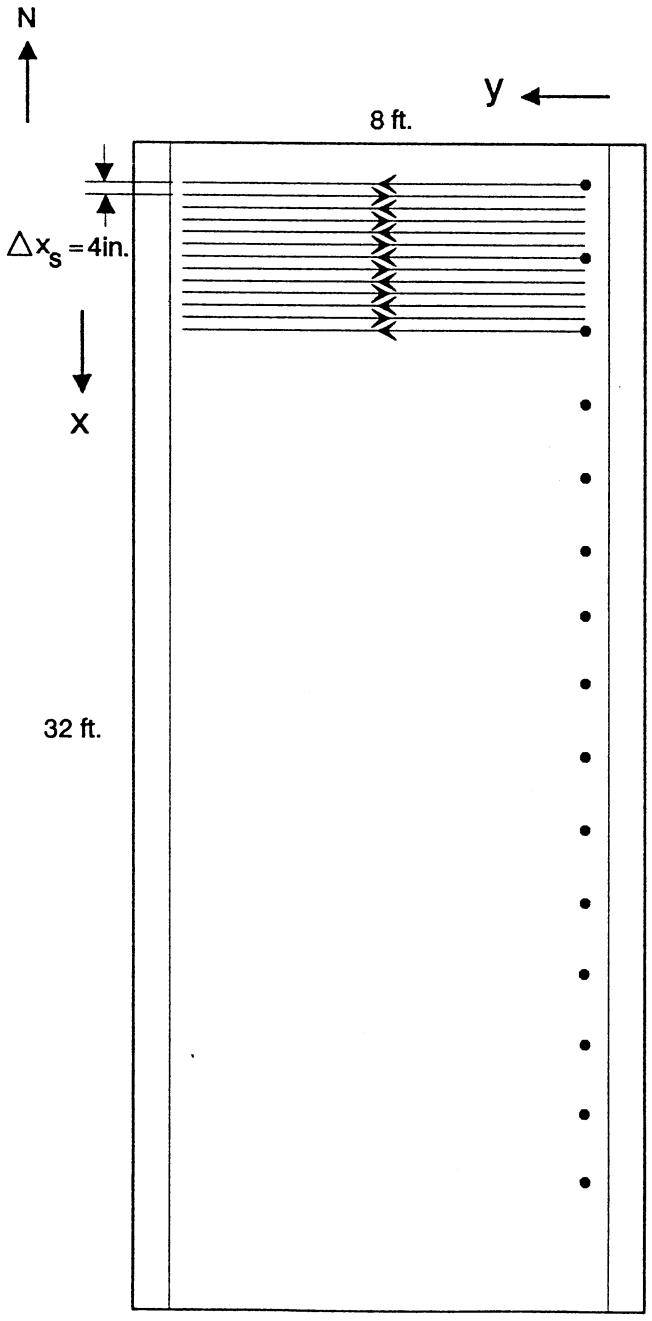

Peg #	Peg Coordinates	Peg Datafile Serial #
1	(0,0,0)	1
2	(24,0,-1.92)	7
3	(48,0,-3.84)	13
4	(72,0,-5.76)	19
5	(96,0,-7.68)	25
6	(120,0,-9.60)	31
7	(144,0,-11.52)	37
8	(168,0,-13.44)	43
9	(192,0,-15.36)	49
10	(216,0,-17.28)	55
11	(240,0,-19.2)	61
12	(264,0,-21.12)	67
13	(288,0,-23.04)	73
14	(312,0,-24.96)	79
15	(336,0,-26.88)	85

Figure 12: Equipment Movement Sequence, Peg Coordinates (in.) and Peg Datafile Serial Numbers.

of these geomorphic relationships and variables are given below (Ogunlela et al., 1989).

Rill order: indicates the position of a rill in the hierarchy of tributaries.

Rill count: number of rills for a given rill order.

The well-established relationship of the Law of Stream Numbers can be written as (Rodríguez-Iturbe and Valdés, 1979)

$$\frac{N_i}{N_{i+1}} = R_B \tag{4.12}$$

where N_i is the number of rills of order i, N_{i+1} is the number of rills of the next larger order and R_B is the bifurcation ratio.

The length of rills will be analyzed using the Law of Stream Lengths defined as (Rodríguez-Iturbe and Valdés, 1979)

$$\frac{\bar{L}_{i+1}}{\bar{L}_i} = R_L \tag{4.13}$$

where $\bar{L}_i$ is the average length of rills of order i, $\bar{L}_{i+1}$ is the average length of rills of the next larger order and R_L is the length ratio.

The drainage area of rills will be analyzed using the Law of Stream Areas defined as (Rodríguez-Iturbe and Valdés, 1979)

$$\frac{\bar{A}_{i+1}}{\bar{A}_i} = R_A \tag{4.14}$$

where $\bar{A}_i$ is the average drainage area of rills of order i, $\bar{A}_{i+1}$ is the average drainage area of rills of the next larger order and R_A is the area ratio.

Channel frequency is defined as the number of channels per unit drainage area. Mathematically, the channel frequency is calculated as

$$C_f = \frac{n_c}{A} \tag{4.15}$$

where n_c is the number of channels and A is the drainage area.

The drainage density is defined as

$$D_d = \frac{\Sigma L}{A} \tag{4.16}$$

where ΣL is the cumulative length of channels and A is the drainage area.

CHAPTER V

ANALYSIS AND DISCUSSION

Introduction

In this chapter experimental data and results are analyzed and discussed. The chapter is divided into three major sections: topographic data; soil, runoff and sediment data; and morphometric analysis. In the topographic data section, a description of and storage considerations for the topographic raw data, data reduction and gridding, and soil surface description are given. This section is followed with a presentation and discussion of results from the analysis of the soil, runoff and sediment data. The third section focuses on the drainage basin parameters for the network of rills.

Topographic Data

Raw Data: Description and Storage Considerations

A major consideration in the analysis of the topographic data was the large data sets. For each before and after measurement, the instrumentation system gathered approximately one million data points with a data spacing of

4 in. in the x direction and approximately 0.01 in. in the y direction. It took approximately 15 hours to gather these data points. For the eight topographic measurement sets, approximately eight million data points were gathered and stored.

The topographic data were stored as x, y and z data points. The data-gathering time for each measurement set could have been considerably reduced without locating the pegs near the Eastern edge of the plot. Occasional missing data were indicated in the raw data where the reflection of the laser line was not picked up by the camera.

The raw data for each measurement set occupied approximately 18 megabytes of storage space. The data were initially stored on floppy disks and later transferred to an optical storage medium as back-ups and to free the diskettes for storage for subsequent measurements. Thus, for the eight topographic measurement sets, approximately 144 megabytes of storage space were required. One obvious consequence of the large data-size is that the algorithms developed to analyze the data should be flexible and computationally efficient.

Data Reduction and Gridding

One purpose of the data reduction algorithm was simply to achieve a workable size of data without losing significant information. In addition, during the data reduction process, the missing data codes were removed, the

peg data were removed, and adjustments were made for the camera height variation and the possible off-positioning of the data collection system.

The data reduction algorithm automatically removed the missing data codes and peg heights and stored every tenth point in the data file. This later step resulted in a data spacing for the reduced data of approximately 0.13 in. in the y direction while maintaining the 4 in. spacing in the x direction. Adjustments were made in the reduction algorithm for the movement of the system in locating pegs and for the vertical movement of the camera required to keep the laser line in the field of view of the camera.

The reduced data were gridded using the interpolation procedures developed in Chapter III. The parameters used in the interpolation program are listed in Table II. All the parameters, except n_{1y}, are the same for all the data groups. For each reduced data group, an average n_{1y} was computed and used in the interpolation program.

The accuracy of the interpolation algorithm was verified by comparing statistics for the raw and grid points. The statistics computed for each transect across the plot were the mean height, maximum and minimum heights, standard deviation and coefficient of variation. The results indicated that the grid points adequately represented the raw data. The plot of the mean heights for

TABLE II

INPUT PARAMETERS FOR THE INTERPOLATION PROGRAM

(The notations are as defined in Chapter III)

Parameter	Value used
Y_{st} (in)	-2.5
Y_{fin} (in)	87.5
$4X_s$ (in)	4.0
$4Y_s$ (in)	0.13
$4X_g$ (in)	4.0
$4Y_g$ (in)	0.5
$4Y_q$ (in)	5.0
$\frac{4S}{2}$ (in)	4.5
f	6.0
n_{1y}	663 to 787

* n_{1y} was determined separately for each reduced data group.

the raw and grid points for the BSH data group is shown in Figure 13.

Soil Surface Description

Periodicities in the topographic data across the plot (y direction) were examined using the method of spectral

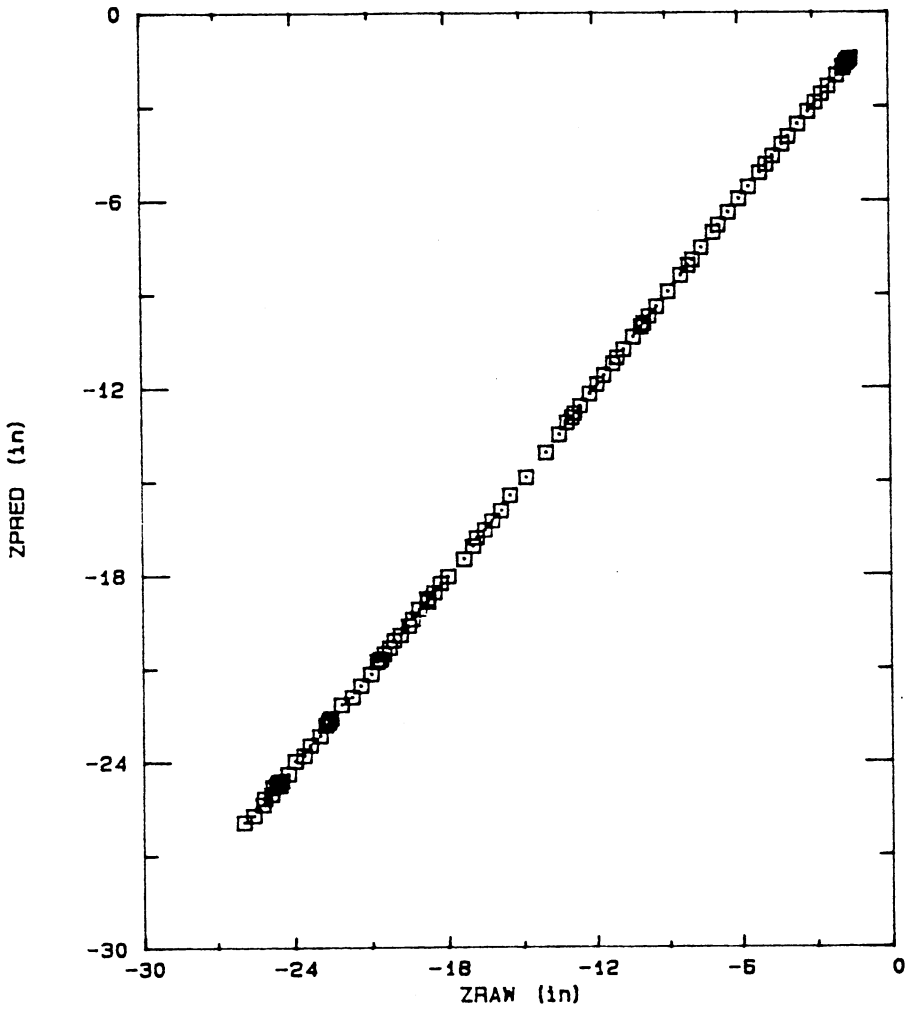

Figure 13. Observed (Raw) Mean Heights, ZRAW, and Predicted (Gridded) Mean Heights, ZPRED, for the BSH Data Group.

analysis (Haan, 1977). Three locations for a smooth surface data set (BSH) and three locations for a rough surface data set (BRL) were investigated. The three locations were taken near the top, middle and bottom of the plot. The results are shown in Figures 14 and 15. Here the frequency is in cycles/0.5 inch spacing which of course corresponds to a period of 0.5 in/cycle. A spacing of 0.5 in. was used in the y direction for the grid points.

For each data, the peak spectral density corresponded to a period of 7 1/2 ft/cycle. Thus, the peak spectral density occurred at a period (and frequency) corresponding to the width of the plot. These results indicate no significant periodicities in the topography data for each elevation trace.

In most spectral analysis, the aim is to decompose the variable of interest (elevation in this case) into deterministic and random components. The deterministic component is usually a reflection of the periodic variation in the soil surface elevation. The absence of periodicities in the data from this study indicates the predominance of the random component.

The lack of periodicities in the topography data is to be expected from the tillage operations performed on the plot. The rotary tillage operation was done up-and-down the plot and then across the plot. This sequence of tillage operations eliminated periodicities which could have resulted from the width of the tillage implement.

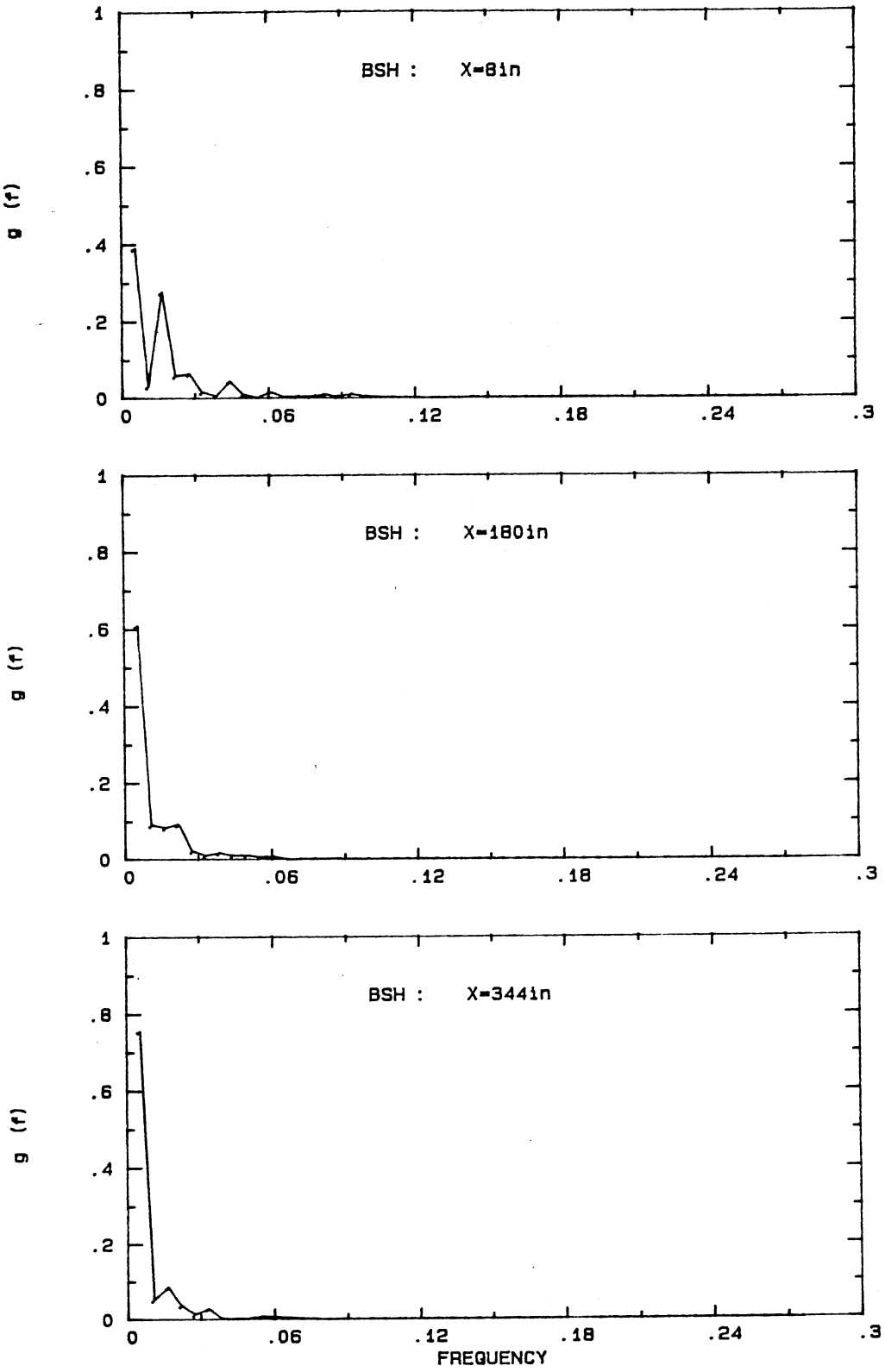

Figure 14. Spectral density function, g(f) versus frequency for a smooth surface before rainfall at the (a) top of the plot, (b) middle of the plot and (c) bottom of the plot.

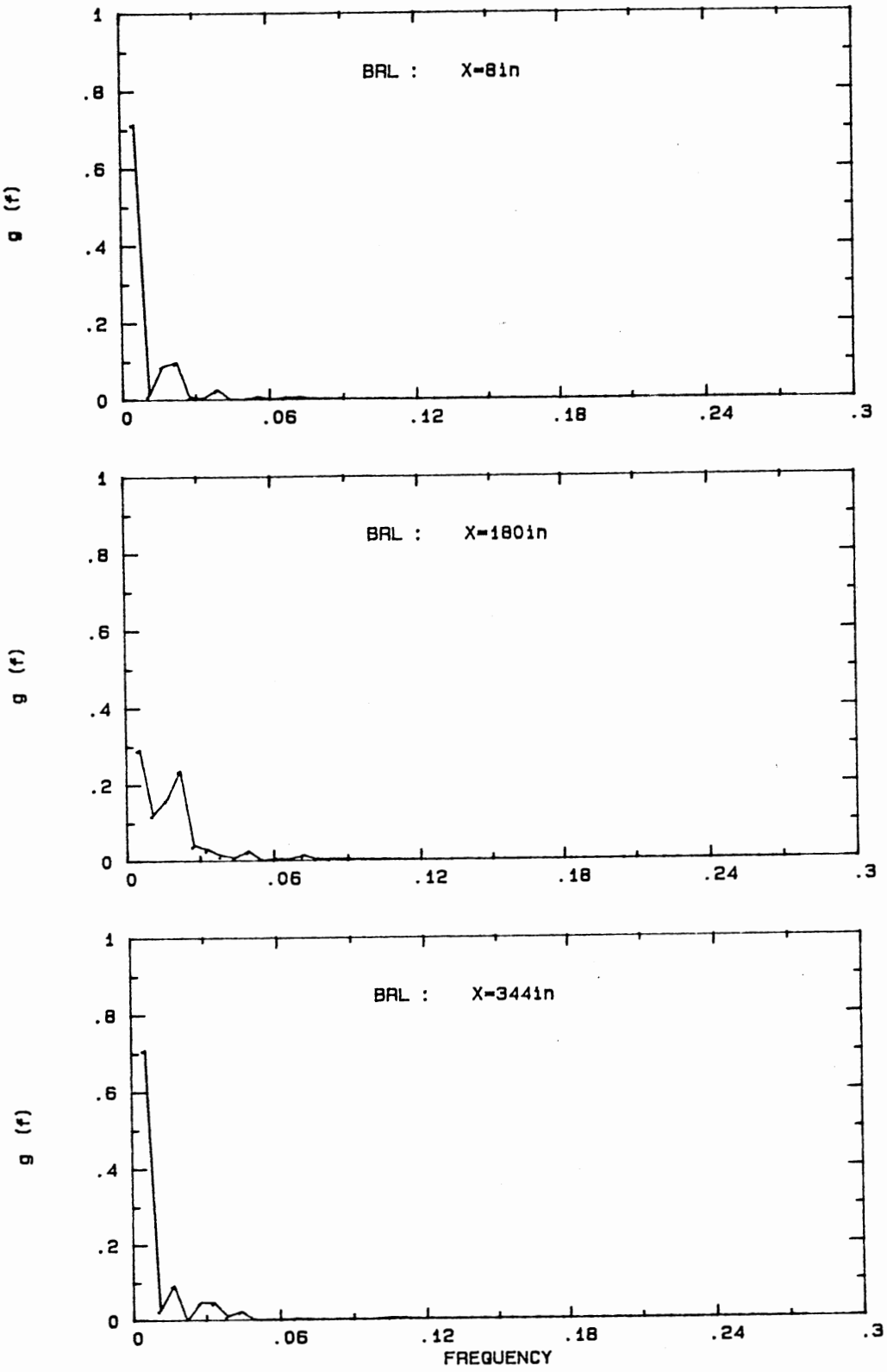

Figure 15. Spectral density function, g(f) versus frequency for a rough surface before rainfall at the (a) top of the plot, (b) middle of the plot and (c) bottom of the plot.

Descriptive statistics of surface roughness were computed for the across plot transects including the mean height, maximum and minimum heights, standard deviation and coefficient of variation. These indices of surface roughness are similar to those utilized by Currence and Lovely (1970) and Lehrsch et al. (1988a, 1988b) in their studies.

Two statistics were used to characterize the plot surface roughness. These were the mean of standard deviation (S_{dm}) and D_{vm}. D_{vm} was computed as

$$D_{vm} = \frac{\sum_{i=1}^{n} (z_{max,\ i} - z_{min,\ i})}{n} \qquad (5.1)$$

where $z_{max,i}$ and $z_{min,i}$ are the maximum and minimum elevation values, respectively, for the across plot transect and n is the number of transects. Values of these statistics for the different data groups are summarized in Table III.

For all the data groups except BSH/ASH the D_{vm} values for the after erosion measurements are lower than for the before erosion measurements. This is consistent with established scientific principles since rainfall applications smooth the soil surface thereby reducing the surface roughness. The D_{vm} values for the BSH and ASH data groups are very close, with the ASH D_{vm} value being slightly higher than for BSH. This is probably a result of other factors notably the antecedent plot condition/initial water

TABLE III

PLOT SURFACE ROUGHNESS

Topographic data set	D_{vm} from Equation (5.1) (in.)	Mean of Std. Dev. S_{dm}, in.
BSL	2.5957	0.5900
ASL	2.2360	0.5491
BSH	2.7036	0.5778
ASH	2.8489	0.6955
BRL	2.6790	0.5779
ARL	2.3905	0.552
BRH	2.9023	0.6395
ARH	2.4144	0.5738

content. The SH run had the highest initial water content of all the runs. Similar conclusions are drawn using the standard deviation mean values.

The smooth and rough soil surfaces were carefully prepared and visually appeared to be different. The plot roughness statistics (S_{dm} and D_{vm}) values for the before erosion data were compared to determine if there were any significant differences in the two surface roughness conditions. The least significant difference (lsd) procedure (Steel and Torrie, 1980) was used in the comparisons. The statistical tests were performed at the 5% level of significance. The results indicated that, for S_{dm}, there were no significant differences in the two roughness

conditions except for BSH vs. BRH; whereas for D_{vm}, there were no significant differences in the two roughness conditions except for BSL vs. BRH.

Soil, Runoff and Sediment Data

The soil samples were analyzed using the procedures discussed in Chapter IV. The mean, standard deviation, and coefficient of variation for the bulk density and moisture content data were computed for each data group. The soil bulk density exhibited a low variation within the plot. For all the data groups, the coefficient of variation for the bulk density data ranged from 0.0314 to 0.0688. The variation in initial moisture content was larger where the coefficient of variation ranged from 0.0869 to 0.3472. The lower variation for bulk density is consistent with other studies (Warrick and Nielsen, 1980).

The runoff and sediment data were also analyzed using the procedures discussed in Chapter IV. The runoff hydrographs, sedimentgraphs and load graphs for the four experimental tests are shown in Figures 16 through 19. A summary of this information and soil characteristics is given in Table IV. The total runoff volume and total sediment load were obtained by integrating flow rate and load rate curves shown in Figures 16 through 19.

A summary of runoff and sediment response is given in Table IV. With the exception of Run RH, runoff rates

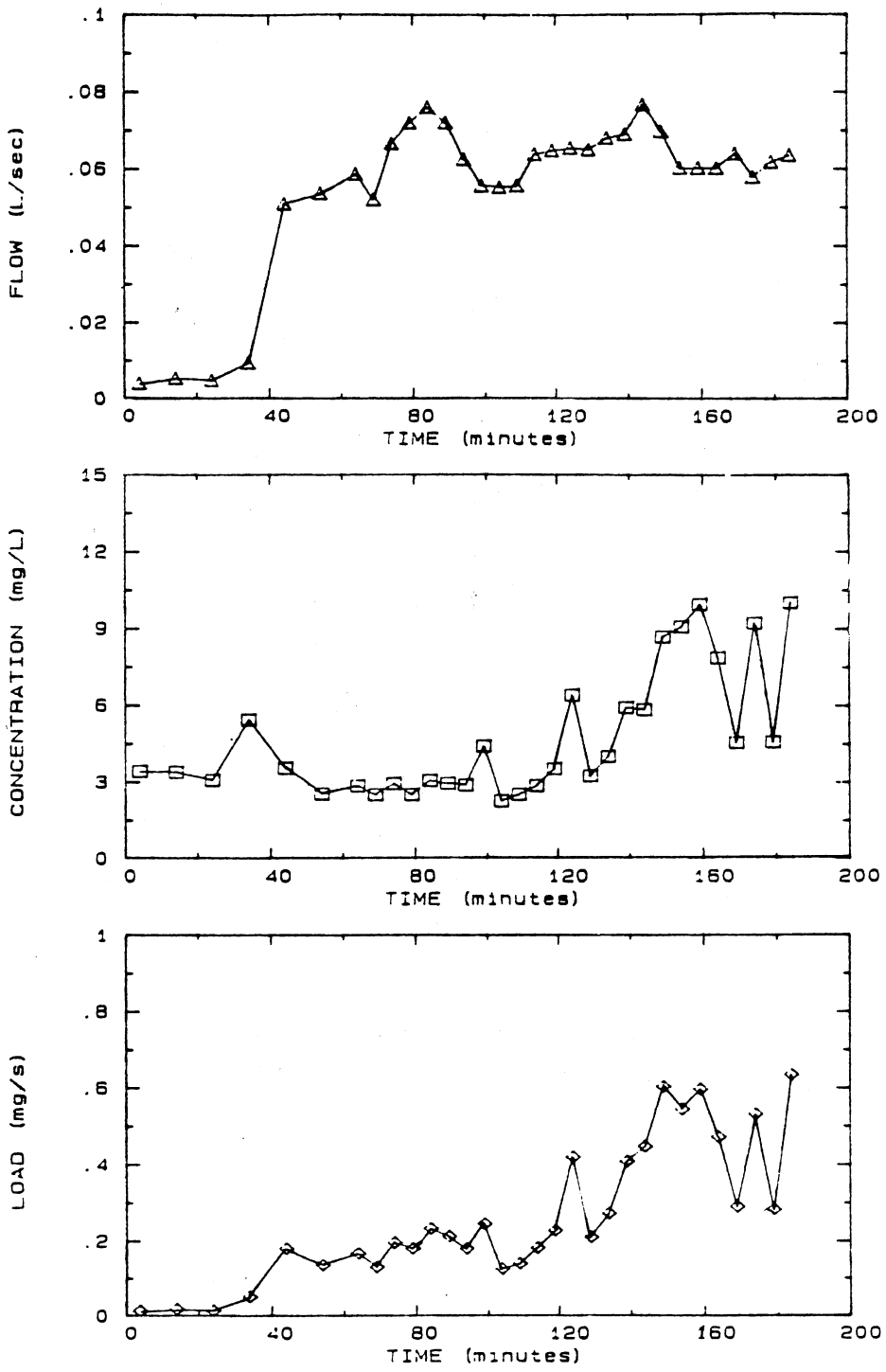

Figure 16. Hydrograph, sedimentgraph and load graph for Run SL.

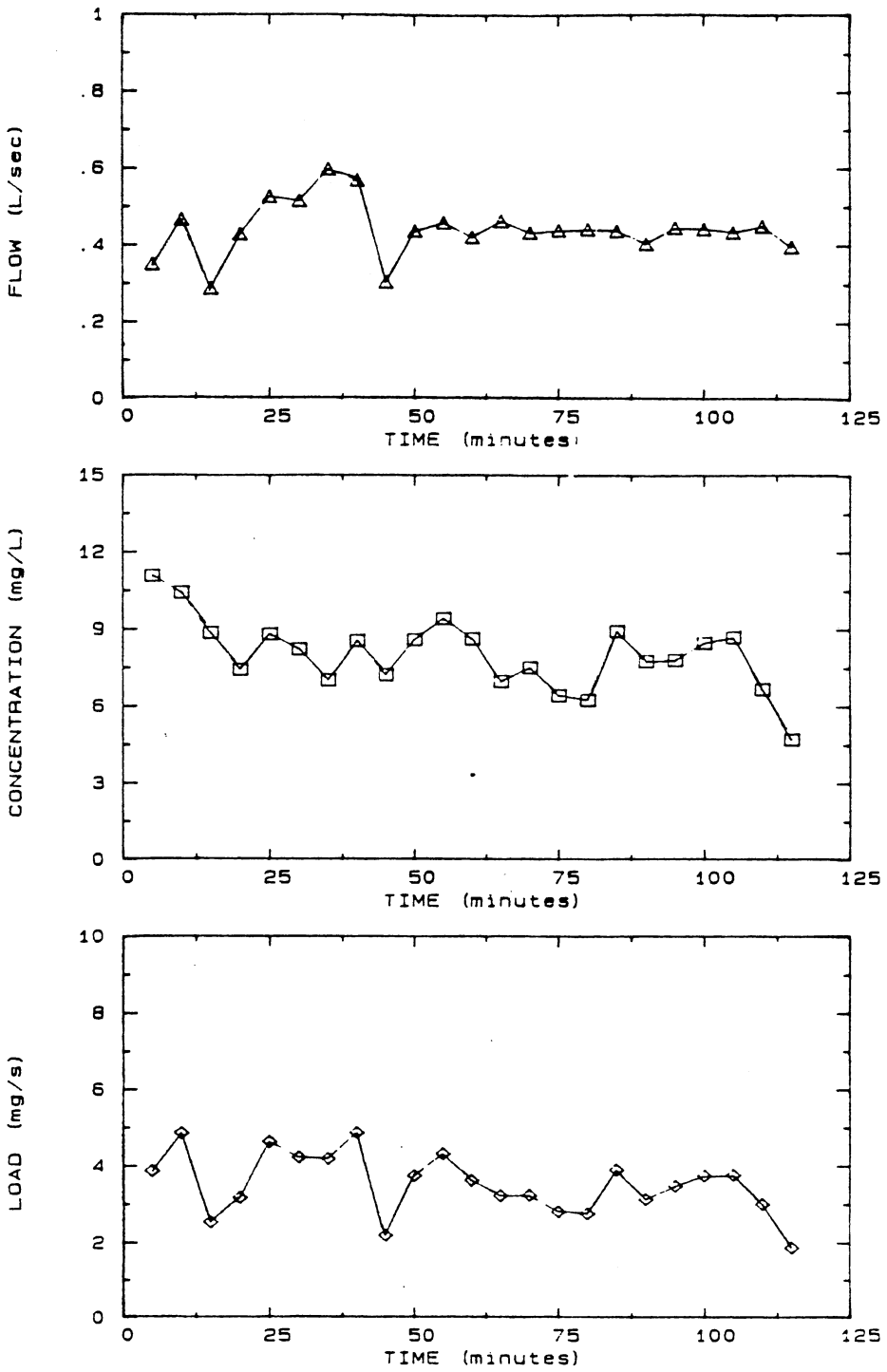

Figure 17. Hydrograph, sedimentgraph and load graph for Run SH.

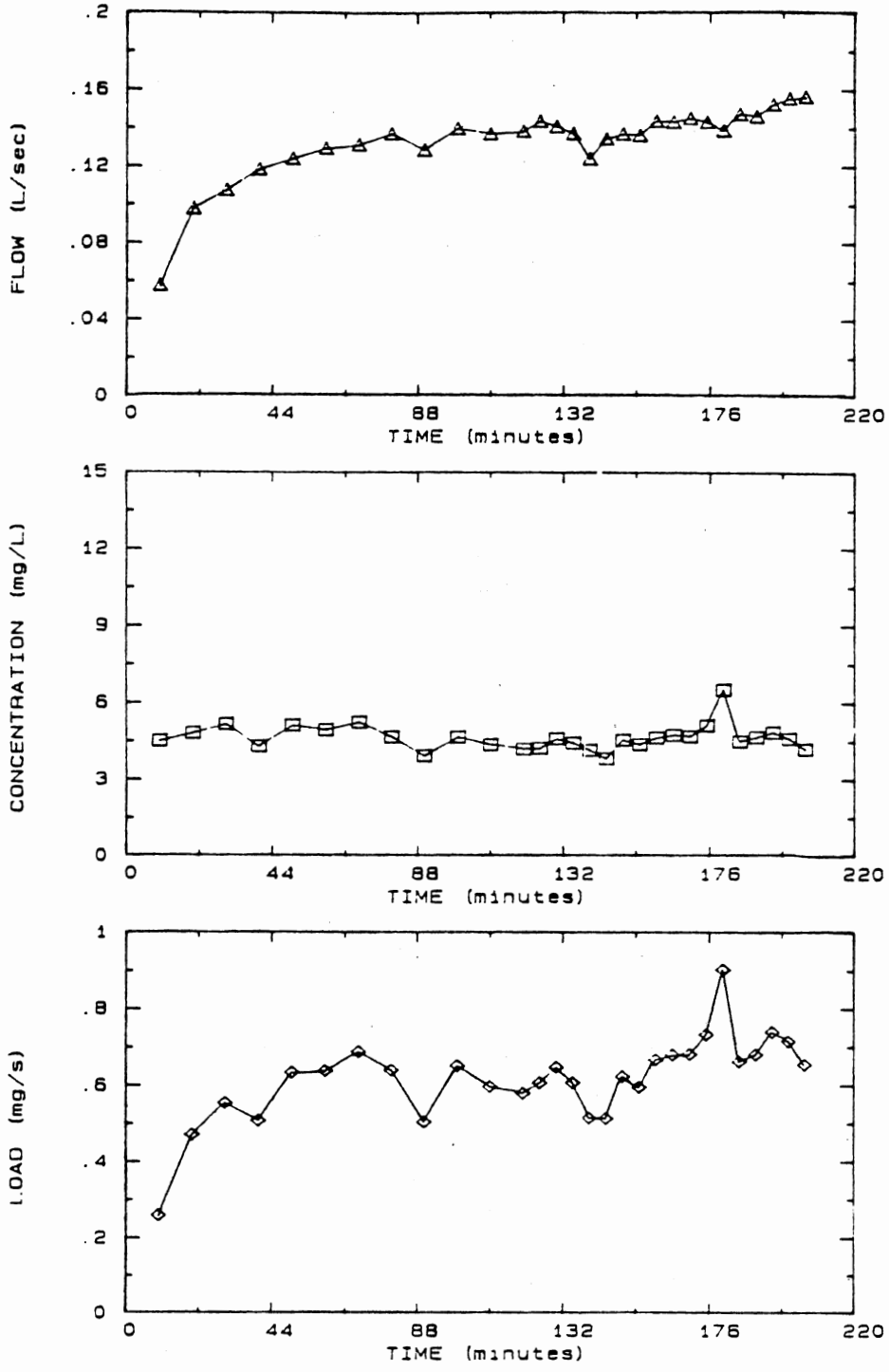

Figure 18. Hydrograph, sedimentgraph and load graph for Run RL.

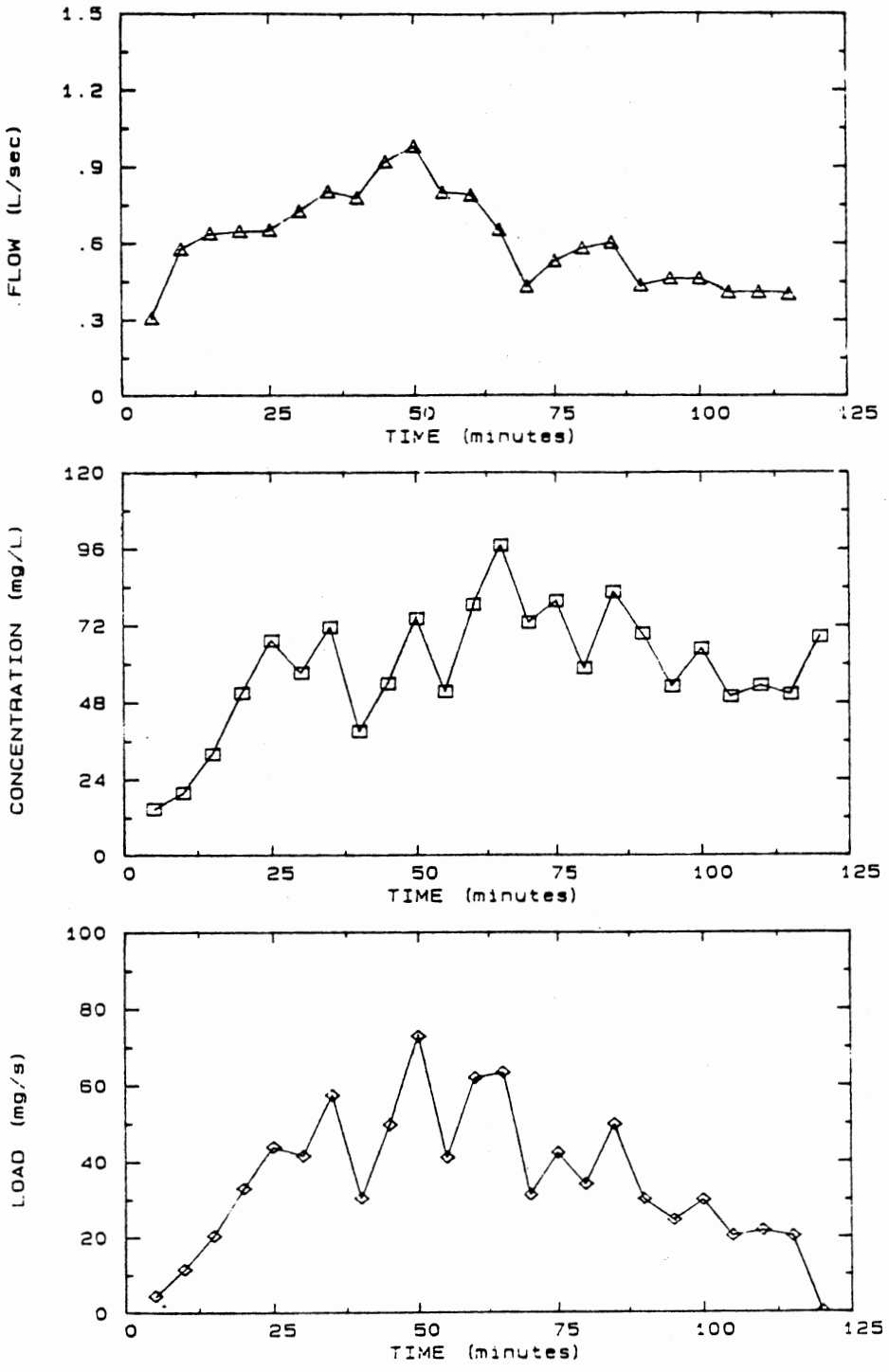

Figure 19. Hydrograph, sedimentgraph and load graph for Run RH.

TABLE IV

SUMMARY OF RUNOFF AND SEDIMENT RESULTS

Run[1] ID	Surface Condition	Rainfall[2] Rate	Rainfall Duration (Min)	Initial Water Content (cc/cc)	Bulk Density (gm/cc)	Constant Outflow Rate (L/sec)	Total Runoff Volume (Liters)	Total Sediment Yield (gm)
SL	Smooth	Low	240	0.0801	1.623[3] 1.544[4]	0.067	2223.5	2543.7
SH	Smooth	High	120	0.3060	1.638[3] 1.650[4]	0.450	2928.3	23468.8
RL	Rough	Low	240	0.2159	1.714[3] 1.729[4]	0.144	1532.7	7136.2
RH	Rough	High	120	0.1191	1.896[3] 1.676[4]	0.600	4145.7	249447.5

[1] First character (S for smooth or R for rough) for roughness, second character (L for low H for high) for rainfall condition.

[2] Low rainfall rate = 2.54 cm/hr, high rainfall rate = 5.08 cm/hr

[3] Bulk density before rainfall

[4] Bulk density after rainfall

approached reasonably constant values. Within each roughness condition, runoff volume increased with larger rainfall rates. A wetter soil may also account for some of this increase for the smooth condition. The runoff volume for Run RH was greater than the pre-set rainfall application. The reason for this is unknown. It might probably be that the actual rainfall application rate for this run was greater than 2 in./hr.

Sediment yield also increased with rainfall rate. The rough soil surface condition was more erosive than the smooth surface as indicated by the total sediment yield. This might be caused by more erosive flows resulting from the overtopping of depressions. The excessive increase in erosion for Run RH was probably the result of other factors. Prior to this run, salt crystals were noticeable at the end of the plot. This might have had a major influence on the soil erodibility.

Morphometric Analysis

The discussion in this section centers on drainage basin parameters obtained from each test. The channel identification results for the after erosion data groups are shown in Figures 20 through 23, with the drainage parameters summarized in Tables V through VIII. The geomorphic parameters are as defined in Chapter IV.

The plot boundary effects were investigated by comparing the drainage network statistics for the outlet

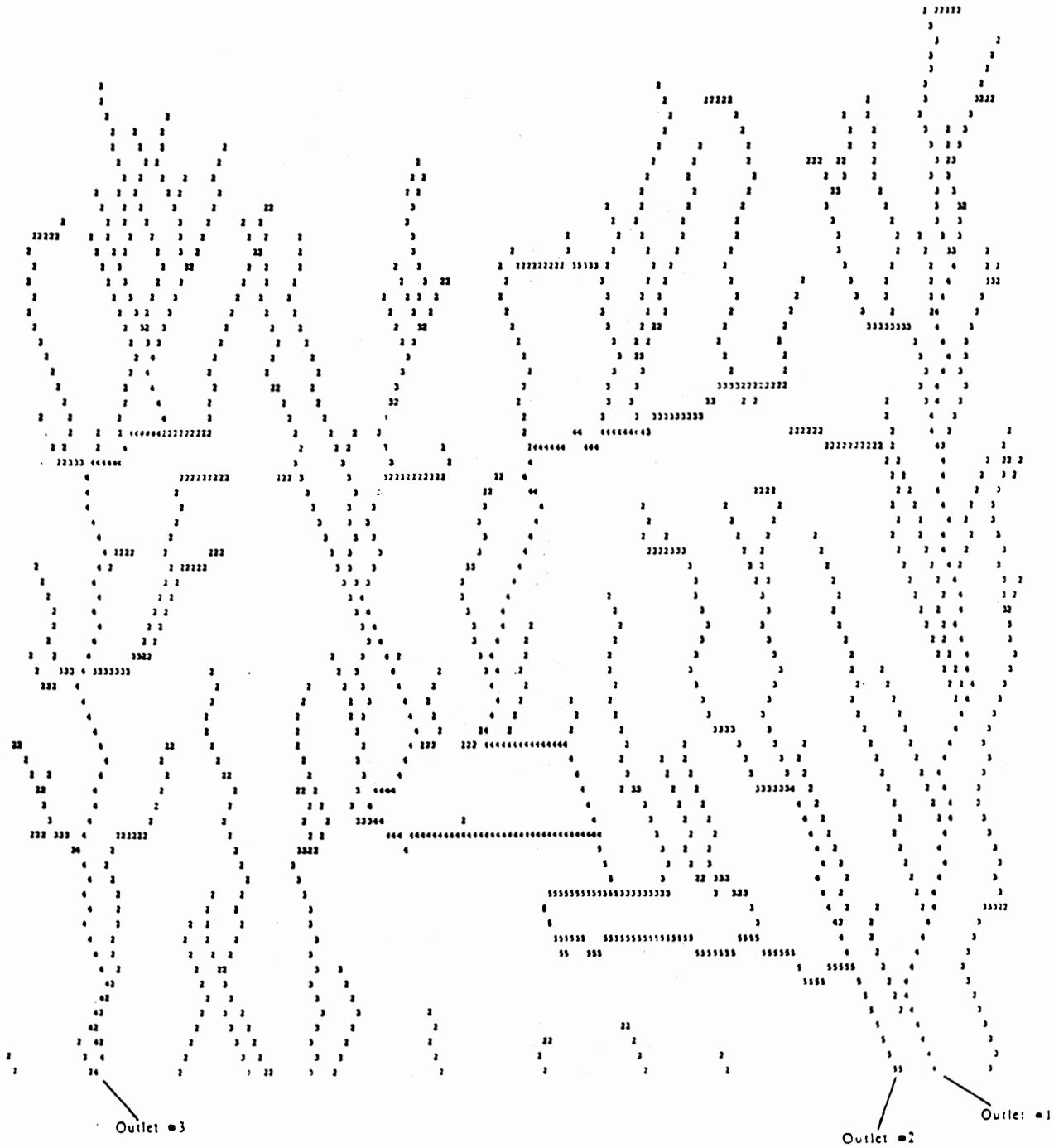

Figure 20. Rill networks for SL.

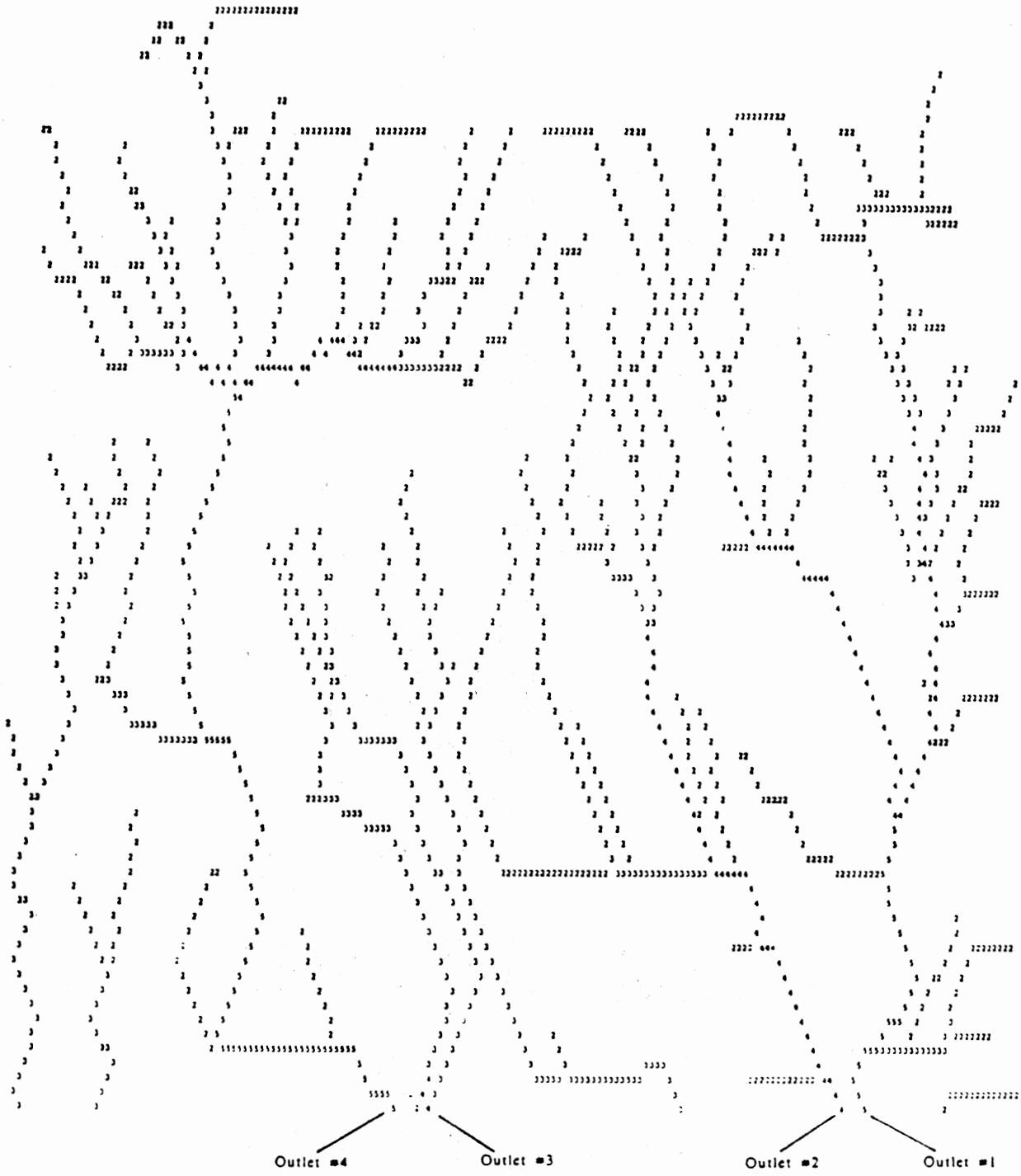

Figure 21. Rill networks for SH.

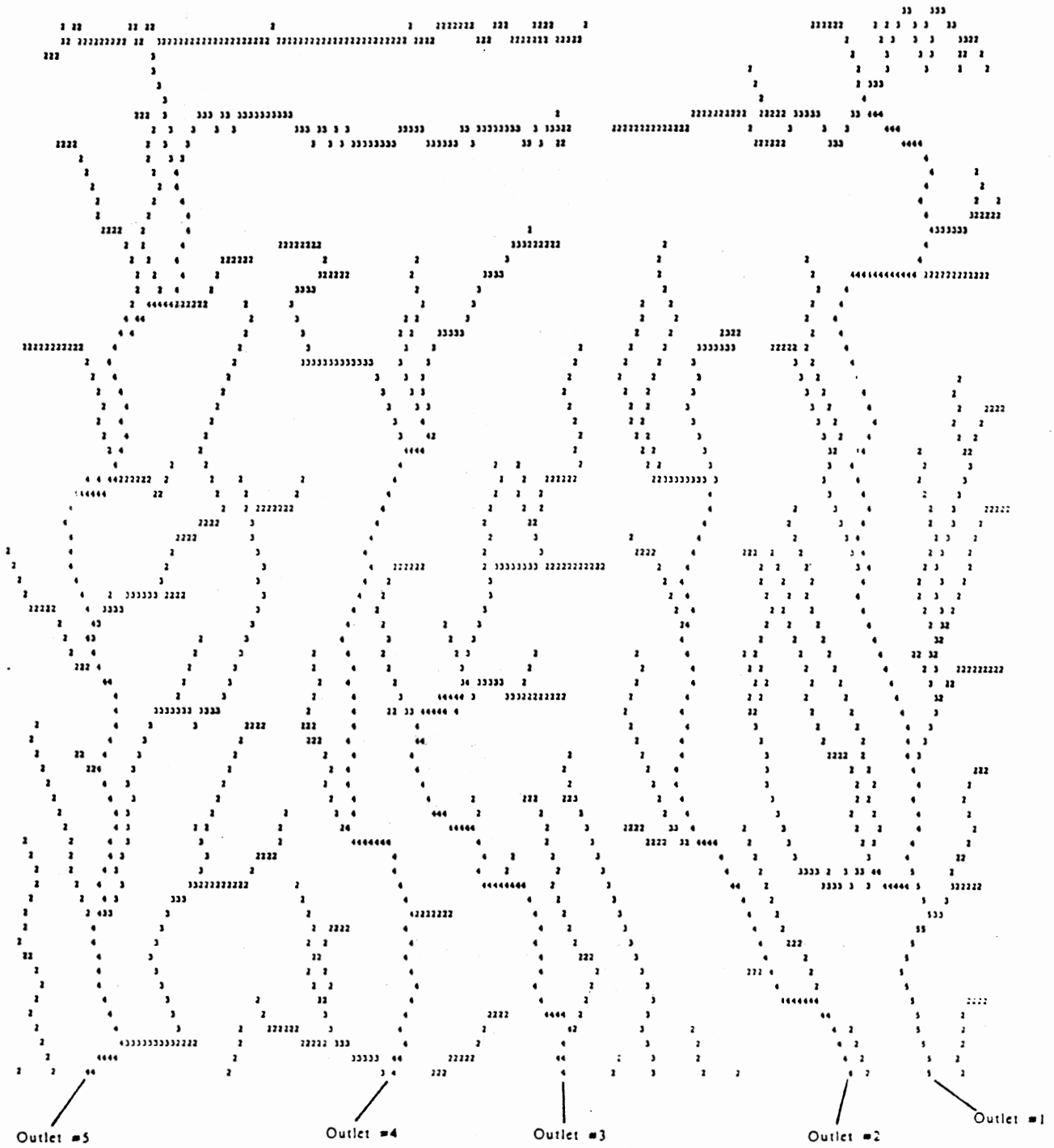

Figure 22. Rill networks for RL.

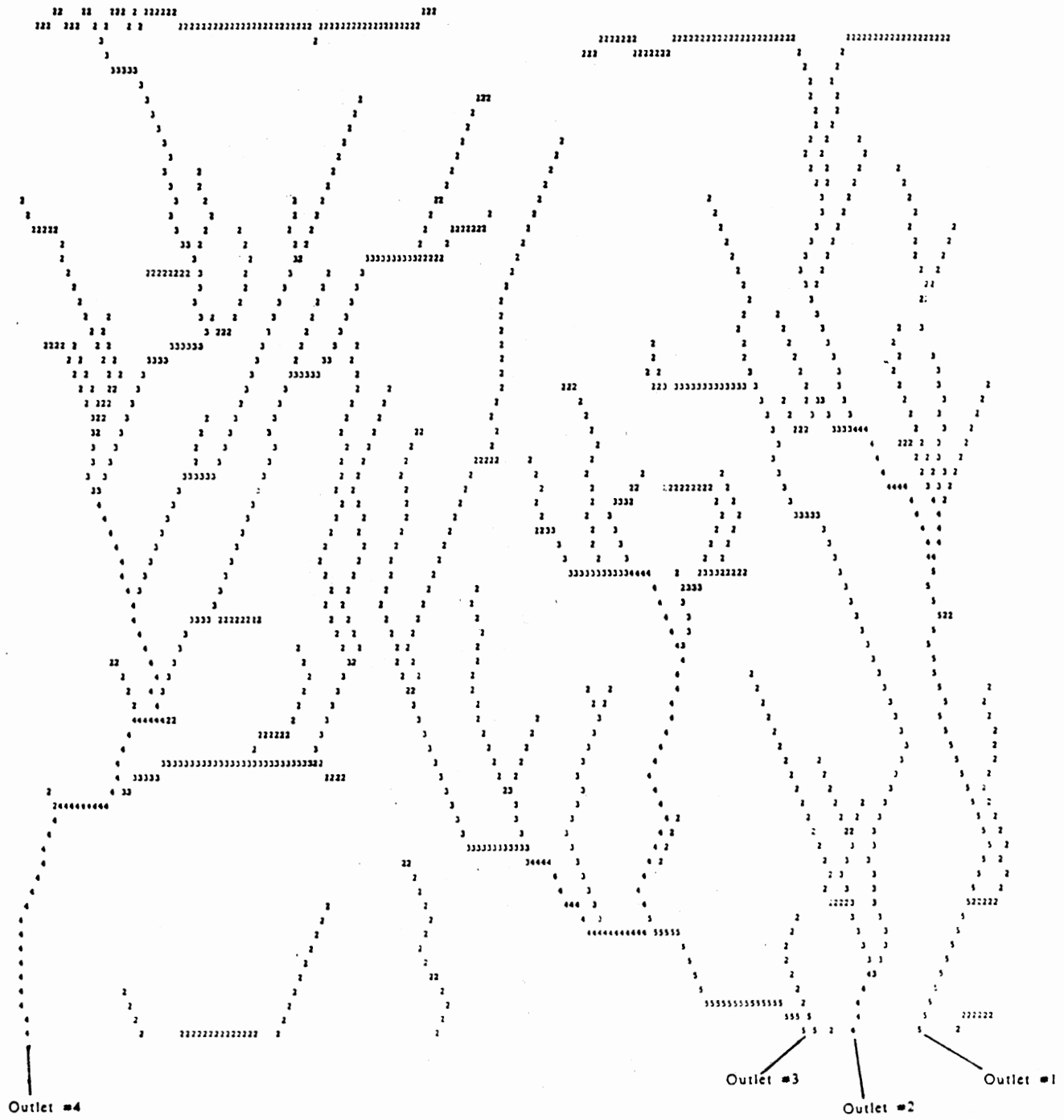

Figure 23. Rill networks for RH.

TABLE V

SUMMARY STATISTICS FOR DRAINAGE NETWORK SL

Outlet Channel (#)	Rill Order (#)	Count (#)	Average Length (m)	Average Area (sq m)	Average Slope (m/m)	Bifur. Ratio R_b	Length Ratio R_l	Area Ratio R_a
1	1	74	0.347	0.015	0.0695			
	2	20	0.695	0.092	0.0726	3.7	2.00	6.13
	3	4	1.434	0.272	0.0893	5.0	2.06	2.96
	4	1	5.521	2.793	0.0710	4.0	3.85	10.27
2	1	200	0.380	0.016	0.0835			
	2	37	0.639	0.106	0.0714	5.4	1.68	6.63
	3	11	1.299	0.443	0.0745	3.4	2.03	4.18
	4	3	2.373	1.962	0.0629	3.7	1.83	4.43
	5	1	3.245	7.121	0.0235	3.0	1.37	3.63
3	1	75	0.370	0.018	0.0790			
	2	21	0.793	0.128	0.0764	3.6	2.14	7.11
	3	6	0.422	0.290	0.0735	3.5	0.53	2.27
	4	1	5.039	3.203	0.0622	6.0	11.94	11.04
					Average	4.1	2.94	5.87

TABLE VI

SUMMARY STATISTICS FOR DRAINAGE NETWORK SH

Outlet Channel (#)	Rill Order (#)	Count (#)	Average Length (m)	Average Area (sq m)	Average Slope (m/m)	Bifur. Ratio R_b	Length Ratio R_l	Area Ratio R_a
1	1	119	0.396	0.018	0.0829			
	2	26	0.588	0.117	0.0736	4.6	1.48	6.65
	3	8	0.717	0.291	0.0743	3.3	1.22	2.49
	4	2	2.875	1.638	0.0975	4.0	4.01	5.63
	5	1	1.995	4.708	0.0347	2.0	0.69	2.87
2	1	57	0.321	0.017	0.0643			
	2	12	1.520	0.191	0.0800	4.8	4.74	11.44
	3	3	0.690	0.717	0.0739	4.0	0.45	3.75
	4	1	3.377	2.999	0.0687	3.0	4.89	4.18
3	1	26	0.447	0.031	0.0683			
	2	6	0.486	0.164	0.0847	4.3	1.09	5.22
	3	2	3.222	0.550	0.0619	3.0	6.63	3.35
	4	1	0.205	1.187	0.0221	2.0	0.066	2.16
4	1	114	0.322	0.016	0.0751			
	2	22	0.829	0.114	0.0939	5.2	2.57	7.26
	3	8	0.722	0.313	0.0767	2.8	0.87	2.75
	4	2	1.042	1.357	0.0119	4.0	1.44	4.34
	5	1	5.294	4.364	0.0589	2.0	5.8	3.22
					Average	3.5	2.52	4.67

TABLE VII

SUMMARY STATISTICS FOR DRAINAGE NETWORK RL

Outlet Channel (#)	Rill Order (#)	Count (#)	Average Length (m)	Average Area (sq m)	Average Slope (m/m)	Bifur. Ratio R_b	Length Ratio R_l	Area Ratio R_a
1	1	129	0.318	0.014	0.0704			
	2	25	0.666	0.109	0.0762	5.2	2.09	7.96
	3	8	1.043	0.430	0.0605	3.1	1.57	3.94
	4	2	2.967	2.030	0.0756	4.0	2.84	4.72
	5	1	1.445	4.501	0.0271	2.0	0.49	2.22
2	1	32	0.390	0.216	0.0757			
	2	9	0.730	0.119	0.0707	3.5	1.87	0.55
	3	3	0.541	0.335	0.0633	3.0	0.74	1.55
	4	1	4.232	1.756	0.0711	3.0	7.82	5.24
3	1	51	0.290	0.014	0.0687			
	2	12	0.573	0.094	0.0741	4.3	1.98	6.70
	3	3	0.575	0.390	0.0651	4.0	1.00	4.15
	4	1	3.284	1.840	0.0484	3.0	5.71	4.73
4	1	58	0.297	0.015	0.0760			
	2	9	0.325	0.094	0.0509	6.4	1.09	6.20
	3	3	1.091	0.313	0.0656	3.0	3.36	3.32
	4	1	4.730	1.879	0.0700	3.0	4.34	6.00
5	1	126	0.261	0.013	0.0539			
	2	22	0.735	0.121	0.0619	5.7	2.82	9.31
	3	5	1.864	0.531	0.0492	4.4	2.54	4.39
	4	1	7.117	5.014	0.0622	5.0	3.82	9.44
					Average	3.9	2.76	5.03

TABLE VIII

SUMMARY STATISTICS FOR DRAINAGE NETWORK RH

Outlet Channel (#)	Rill Order (#)	Count (#)	Average Length (m)	Average Area (sq m)	Average Slope (m/m)	Bifur. Ratio R_b	Length Ratio R_l	Area Ratio R_a
1	1	77	0.344	0.018	0.0655			
	2	12	0.920	0.163	0.0695	6.4	2.67	9.05
	3	4	0.860	0.542	0.0735	3.0	0.93	3.32
	4	2	0.798	1.210	0.1003	2.0	0.93	2.23
	5	1	3.276	3.064	0.0519	2.0	4.10	2.53
2	1	33	0.529	0.026	0.0713			
	2	6	0.727	0.137	0.0557	5.5	1.37	5.19
	3	2	2.780	0.892	0.0725	3.0	.82	6.51
	4	1	0.409	1.852	0.0212	2.0	0.15	2.08
3	1	81	0.494	0.023	0.0654			
	2	17	0.794	0.141	0.0822	4.8	1.61	6.13
	3	6	0.829	0.441	0.0653	2.8	1.04	3.13
	4	2	1.649	1.641	0.0683	3.0	1.99	3.72
	5	1	1.265	4.006	0.0209	2.0	0.77	2.44
4	1	131	0.389	0.018	0.0766			
	2	23	0.785	0.148	0.0735	5.7	2.02	8.36
	3	5	2.279	0.910	0.0733	4.6	2.90	6.15
	4	1	3.945	5.712	0.0534	5.0	1.73	6.28
					Average	3.7	1.86	4.79

channels near the boundary with those in the middle of the plot. The least significant difference (lsd) procedure (Steel and Torrie, 1980) was used. The results indicated that, at the 5% level of significance, the drainage network statistics for the outlet channels near the plot boundary were not significantly different from the network statistics for the outlet channels in the middle of the plot. Thus, the effects of the plot boundary on drainage network development are negligible.

As shown by Tables V through VIII, the average bifurcation ratios for runs SL, SH, RL and RH are 4.1, 3.5, 3.9 and 3.7 respectively. The variation within each run, however, can be large. For example, the bifurcation ratio for Run RH, Outlet Channel #1 varied between 2 and 6.4. It appears that the bifurcation ratio for this data set is not a function of rainfall rate nor surface roughness condition. The average bifurcation ratios for the rill networks lie within the range reported for natural streams by Yang (1971) and Rodríguez-Iturbe and Valdés (1979). For fourteen different river basins, Yang reported bifurcation ratios between 3.3 and 4.8. Rodríguez-Iturbe and Valdés summarized these ratios for natural streams to be between 3 and 5.

The average length ratios for runs SL, SH, RL and RH are given in Tables V through VIII as 2.9, 2.5, 2.8 and 1.9, respectively. The variation in these ratios within a test can again be large. For Run SL, the length ratio for Outlet Channel #3 varied between 0.53 and 11.94. No trend in

length ratios with rainfall rate or surface roughness is apparent. The average length ratios for the rill networks are close to the values reported for natural streams by Yang (1971). He reported length ratios between 1.9 and 2.6. Rodríguez-Iturbe and Valdés (1979) have summarized the range in length ratios for river basins as between 1.5 and 3.5.

The average area ratios are also given in Tables V through VIII. Values for runs SL, SH, RL and RH are 5.9, 4.7, 5.0 and 4.8, respectively. Similar to the other ratios, variations within a test can be large. The area ratio varied between 2.3 and 11.0 for Outlet Channel #3 of Run SL. Although the variation between runs is greater here, no trend is readily apparent. The average area ratios for the rill networks are again close to the range of 2.3 to 5.2 of natural stream values reported by Yang (1971). Rodríguez-Iturbe and Valdés (1979) have summarized the range in area ratios for river basins as between 3.0 and 5.0.

The figures given above indicate that the average stream ratios ($\bar{R}_B$, $\bar{R}_L$ and $\bar{R}_A$) obtained in this study generally followed patterns obtained in nature. Thus, the average drainage patterns appear to follow the well-established Horton's "laws of drainage composition."

The least significance difference (lsd) procedure (Steel and Torrie, 1980) was used to test each average stream ratio ($\bar{R}_B$, $\bar{R}_L$ and $\bar{R}_A$) for statistical significance: (1) for the rainfall rates, and (2) for the soil profile conditions. The results indicated that, for

each of $\bar{R}_B$, $\bar{R}_L$ and $\bar{R}_A$, and at 5% level of significance, there were no significant differences for the rainfall rates and for the soil profile conditions.

As shown by Tables V through VIII, the number of rills decreases as the rill order increases. Also, the drainage area increases with rill order. These observations are consistent with established geomorphic principles. The drainage density and channel frequency varied within the basin for each run (Table IX). This variation can be large in some cases. For example, the channel frequency for Run RH varied from 22 to 206 channels/m^2 while the drainage density for Run SL varied from 14.38 to 79.1 m^{-1}.

TABLE IX

VARIATION OF DRAINAGE DENSITY AND CHANNEL FREQUENCY WITHIN BASINS

Run ID	Drainage Density D_d (m^{-1})	Channel Frequency C_f (channels/m^2)
SL	14.38 - 79.1	25 - 188
SH	1.03 - 17.85	5 - 33
RL	2.31 - 23.82	3 - 91
RH	7.06 - 31.55	22 - 206

CHAPTER VI

SUMMARY AND CONCLUSIONS

The effects of rainfall intensity and soil surface condition on drainage network development in a laboratory environment were investigated. Two rainfall rates were used (relatively high and low rainfall rates) on two soil surface configurations (relatively rough and smooth surface profiles).

A premise for this study was the geometric similarity between large and small drainage basins (Leopold et al., 1964), thus enabling the results obtained from this study to be extendable to larger watersheds. For each rainfall rate and soil surface profile combination, drainage parameters were obtained. These parameters included the rill order, rill length, channel count and frequency, drainage area, drainage density, bifurcation ratio, length ratio and area ratio, which could be used in the quantitative description and characterization of a drainage basin. On the average, the drainage patterns obtained from this study followed the well-established Horton's "laws of drainage composition," i.e., the bifurcation ratio (R_B), length ratio (R_L) and area ratio (R_A) obtained from this study compared favorably with

those of natural streams (Rodríguez-Iturbe and Valdés, 1979; Yang, 1971).

Statistical tests were conducted on the average stream ratios ($\bar{R}_B$, $\bar{R}_L$ and $\bar{R}_A$) to determine if there were any significant differences in the results for the different rainfall rates and soil profile conditions. The least significant difference (lsd) procedure was used in the analysis. The results indicated that, at the 5% level of significance, there were no significant differences for each average stream ratio for the different rainfall rates and soil profile conditions.

Suggestions for Future Studies

1. Investigate the effects of other parameters such as slope and soil type on rill network development.
2. Investigate the temporal variability of drainage parameters in a laboratory environment.

REFERENCES

Alberts, E. E., J. M. Laflen and R. G. Spomer. 1986. Temporal Variation in Soil Erodibility Determined by Rainfall Simulation. ASAE Paper No.: 86-2040.

Allen, P. B. 1986. Drainage Density Versus Runoff and Sediment Yield. In Proceedings of the Fourth Federal Interagency Sedimentation Conference, Las Vegas, Nevada. Vol. I. pp. 3-38 to 3-44.

Band, L. E. 1986. Topographic Partition of Watersheds with Digital Elevation Models. Water Resources Research. 22(1): 15-24.

Bárdossy, A. and I Bogárdi. 1983. Network Design for the Spatial Estimation of Environmental Variables. Applied Mathematics and Computation. 12: 339-365.

Bárdossy, A., I Bogárdi and L. Duckstein. 1987. A Geostatistical Model of Reservoir Deposition. Water Resources Research. 23(3): 510-514.

Bath, M. 1974. Spectral Analysis in Geophysics. Elservier Scientific Publishing Company.

Beasley, D. B., L. F. Huggins and E. J. Monke. 1980. ANSWERS: A Model for Watershed Planning. Transactions of the ASAE. 23(4): 938-944.

Beveridge, G. S. G. and R. S. Schechter. 1970. Optimization: Theory and Practice. McGraw-Hill Book Company.

Bras, R. L. and I Rodríguez-Iturbe. 1985 Random Functions and Hydrology. Addison-Wesley Publishing Company.

Bryan, R. B. and S. Luk. 1981. Laboratory Experiments on the Variation of Soil Erosion Under Simulated Rainfall. Geoderma. 26: 245-265.

Carlston, C. W. 1963. Drainage Density and Streamflow. U. S. Geol. Survey Prof. Paper 422-C; 1-8.

Carr, J. R. , D. E. Myers and C. E. Glass. 1985 Cokriging - A Computer Program. Computers and Geosciences. 11(2): 111-127.

Chirlin, G. R. and E. F. Wood. 1982. On the Relationship Between Kriging and State Estimation. Water Resources Research. 18(2): 432-438.

Clark II, E.H., J.A. Haverkamp and W. Chapman. 1985. Eroding Soils. The Off-Farm Impacts. The Conservation Foundation. Washington, D.C.

Couger, G; B.N. Wilson, A. Ogunlela and C.T. Rice. 1989. Rill Identification from Point Elevation Data. ASAE Paper No. 89-2159, Presented at the ASAE Summer Meeting, Quebec City, Canada.

Currence, H. D. and W. G. Lovely. 1970. The Analysis of Soil Surface Roughness. Trans. of the ASAE. 13(6): 710-714.

Curtis, W. R. and W. R. Cole. 1972. Micro-topographic Profile Gage. Agricultural Engineering. 53: 17.

Davis, W. M. 1895. The Development of Certain English Rivers. Geog. Jour. 5: 127-146.

Delfiner, P. and J. P. Delhomme. 1973. Optimum Interpolation by Kriging. In Davis, J. C. and M. J. McCullagh (Editors). Display and Analysis of Spatial Data. Wiley and Sons, London. pp. 96-114.

Delhomme, J. P. 1978. Kriging in the Hydrosciences. Advances in Water Resources. 1(5): 251-266.

Dickinson, W. T., R. Pall and G. J. Wall. 1982. Seasonal Variations in Soil Erodibility. ASAE Paper No.: 82-2573.

Duck, P. W. and O. R. Burggraf. 1986. Spectral solutions for three-dimensional triple-deck flow over surface topography. Journal of Fluid Mechanics. 162: 1-22.

Ellison, W. D. and O. T. Ellison. 1947. Soil Erosion Studies--Part VI. Agricultural Engineering. September 1947.

Eyles, R. J. 1966. Stream Representation on Malayan Maps. Journal of Tropical Geography. 22: 1-9.

Fischler, M. A., J. M. Tenenbaum and H. C. Wolf. 1981. Detection of Roads and Linear Structures in Low-Resolution Aerial Imagery Using a Multisource Knowledge Integration Technique. Computer Graphics and Image Processing. 15: 201-223.

Flanagan, D. C., G. R. Foster and W. C. Moldenhauer. 1986. Storm Pattern Effect on Runoff, Sediment, and Nutrient Loss. ASAE Paper No.: 86-2019.

Foster, G. R. 1982. Modeling the Erosion Process. In Hydrologic Modeling of Small Watersheds. Haan, C. T., H. P. Johnson and D. L. Brakensiek (Editors). ASAE Monograph No. 5. pp. 297-380.

Foster, G. R. and L. D. Meyer. 1975. Mathematical Simulation of Upland Erosion by Fundamental Erosion Mechanics. In Present and Prospective Technology for Predicting Sediment Yields and Sources. ARS-S-40: 190-207.

Foster G. R. and W. H. Wischmeier. 1974. Evaluating Irregular Slopes for Soil Loss Prediction. Trans. of the ASAE. 17(2): 305-309.

Foster, G. R., L. F. Huggins and L. D. Meyer. 1984a. A Laboratory Study of Rill Hydraulics: I. Velocity Relationships. Trans. of the ASAE. 27(3): 790-796.

Foster G. R., L. F. Huggins and L. D. Meyer. 1984b. A Laboratory Study of Rill Hydraulics: II. Shear Stress Relationships. Trans. of the ASAE. 27(3): 797-804.

Foster, G. R., L. D. Meyer and C. A. Onstad. 1977. A runoff erosivity factor and variable slope length exponents for soil loss estimates. Trans. of the ASAE. 20(4): 683-687.

Foster, G. R., W. R. Osterkamp, L. J. Lane and D. W. Hunt. 1982. Effect of Discharge Rate on Rill Erosion. ASAE Paper No.: 82-2572.

Fowler, R. J. and J. J. Little. 1979. Automatic Extraction of Irregular Network Digital Terrain Models. Computer Graphics. 13(2): 199-207.

Freeze, R. A. 1980. A Stochastic-Conceptual Analysis of Rainfall-Runoff Processes on a Hillslope. Water Resources Research. 16(2): 391-408.

Gardiner, V. 1974. Drainage Basin Morphometry. British Geomorphological Research Group. Technical Bulletin No. 14.

Gilley, J. E., S. C. Finkner and G. E. Varvel 1986. Hydraulic and Soil Loss Variables on Eroding Areas. ASAE Paper No.: 86-2041.

Gold, C. M., T. D. Charters and J. Ramsden. 1977. Automated contour mapping using triangular element data structures and an interpolant over each irregular triangular domain. Computer Graphics. 11: 170-175.

Haan, C. T. 1977. Statistical Methods in Hydrology. Iowa State University Press. Ames, Iowa.

Haan, C. T. and B. N. Wilson. 1986. Another Look at the Joint Probability of Rainfall and Runoff. Proc. International Symposium on Flood Frequency and Risk Analyses. Louisiana State University, Baton Rouge, LA. May 14-17, 1986.

Hadley, R. F. and S. A. Schumm. 1961. Sediment Sources and Drainage Basin Characteristics in Upper Cheyenne River Basin. U. S. Geol Survey Water-Supply Paper 1531-B: 137-197.

Harral, B. B. and C. A. Cove. 1982. Development of an Optical Displacement Transducer for the Measurement of Soil Surface Profiles. Journal of Agricultural Engineering Research. 27: 421-429.

Henry, J. E., M. J. Sciarini and D. M. Van Doren, Jr. 1980. A Device for Measuring Soil Surface Profiles. Trans. of the ASAE. 23(6): 1457-1459.

Hirschi, M. C. and B. J. Barfield. 1986. KYERMO--A Physically Based Research Erosion Model. ASAE Paper No.: 86-2047.

Hirschi, M. C., B. J. Barfield and I. D. Moore 1984. Rillmeters for Detailed Measurement of Soil Surface Heights. ASAE Paper No.: 84-2534.

Horton, R. E. 1945. Erosional Development of Streams and their Drainage Basins; Hydrophysical Approach to Quantitative Morphology. Geol. Soc. America Bull. 56: 275-370.

Hudson, N. 1981. Soil Conservation. Cornell University Press. Ithaca, New York.

Jarvis, R. S. 1977. Drainage Network Analysis. Progress in Physical Geography. 1: 271-295.

Jaynes, D. B. and A. J. Clemmens. 1986. Accounting for Spatially Variable Infiltration in Border Irrigation Models. Water Resources Research. 22(8): 1257-1262.

Jenson, S. K. 1985. Automated Derivation of Hydrologic Basin Characteristics from Digital Elevation Model Data. In Proceedings Digital Representation of Spatial Knowledge: Auto-Carto 7. Washington, D. C.

Journel, A. G. and Ch. J. Huijbregts. 1978. Mining Geostatistics. Academic Press, New York.

Julian, P. R. 1967. Variance Spectrum Analysis. Water Resources Research. 3(3): 831-845.

Khorashahi, J., R. K. Byler and T. A. Dillaha. 1985. An Opto - Electronic Soil Profiler. ASAE Paper No.: 85-3041.

Knighton, D. 1984. Fluvial Forms and Processes. Edward Arnold Publishers.

Lavelle, J. W. and H. O. Mofjeld. 1987. Do Critical Stresses for Incipient Motion and Erosion Really Exist? Journal of Hydraulic Engineering (ASCE). 113(3): 370-385.

Lehrsch, G. A., F. D. Whisler and M. J. M. Römkens. 1988a. Spatial Variation of Parameters Describing Soil Surface Roughness. Soil Sci. Soc. Am. J. 52: 311-319.

Lehrsch, G. A., F. D. Whisler and M. J. M. Römkens. 1988b. Selection of a Parameter Describing Soil Surface Roughness. Soil Sci. Soc. Am. J. 52: 1439-1445.

Leopold, L. B., M. G. Wolman and J. P. Miller. 1964. Fluvial Processes in Geomorphology. W. H. Freeman and Company, San Francisco.

Mark, D. M. 1975. Computer Analysis of Topography: A Comparison of Terrain Storage Methods. Geografiska Annaler. 57: 179-188.

Mark, D. M. 1983. Relations Between Field Surveyed Channel Networks and Map-based Geomorphometric Measures Inez, Kentucky. Annals, Association of American Geographers. 73(3): 358-372.

Mark, D. M. 1984. Automated Detection of Drainage Networks from Digital Elevation Models. Cartographica. 21: 168-178.

McCool, D. K., M. G. Dossett and S. J. Yecha. 1981. A Portable Rill Meter For Field Measurement of Soil Loss. Proceedings of the International Symposium on Erosion and Sediment. Transport Measurement. June 1981. Florence, Italy. pp. 479-484.

McLain, D. H. 1976. Two Dimensional Interpolation from Random Data. Computer Journal. 19(2): 178-181.

Merva, G. E., R. D. Brazee, G. O. Schwab and R. B. Curry. 1970. Theoretical Considerations of Watershed Surface Description. Trans. of the ASAE. 13(4): 462-465.

Meyer, L. D. 1965. Mathematical Relationships Governing Soil Erosion by Water. Journal of Soil and Water Conservation. 20(4): 149-150.

Meyer, L. D. and E. J. Monke. 1965. Mechanics of Soil Erosion by Rainfall and Overland Flow. Trans. of the ASAE. 8(4): 572-577, 580.

Meyer, L. D. and W. H. Wischmeier. 1969. Mathematical Simulation of the Process of Soil Erosion by Water. Trans. of the ASAE. 12(6): 754-758, 762.

Meyer, L. D., D. G. DeCoursey and M. J. M. Romkens. 1976. Soil Erosion Concepts and Misconceptions. Proceedings of the Third Federal Inter-Agency Sedimentation Conference. Water Resource Council. March 22-23. Denver, Colorado.

Meyer, L. D., G. R. Foster and S. Nikolov. 1975. Effect of Flow Rate and Canopy on Rill Erosion. Trans. of the ASAE. 18(5): 905-911.

Mitchell, J. K. and B. A. Jones, Jr. 1973. Profile Measuring Device. Trans. of the ASAE. 16(3): 546-547.

Moore, I. D. and G. J. Burch. 1986a. Modelling Erosion and Deposition: Topographic Effects. Trans. of the ASAE. 29(6): 1624-1630, 1640.

Moore, I. D. and G. J. Burch. 1986b. Sediment Transport Capacity of Sheet and Rill Flow: Application of Unit Stream Power Theory. Water Resources Research. 22(8): 1350-1360.

Moore, I. D. and C. L. Larson. 1979. Estimating Micro-Relief Surface Storage from Point Data. Trans of the ASAE. 22(5): 1073-1077.

Moore, I. D., M. C. Hirschi and B. J. Barfield. 1983. Kentucky Rainfall Simulator. Trans. of the ASAE. 26(4): 1085-1089.

Morgan, K. M., D. R. Morris, G. B. Lee, R. W. Kiefer, G. D. Bubenzer and T. C. Daniel. 1980. Aerial Photography as an Aid to Cropland Erosion Analysis. Trans of the ASAE. 23(4): 907-909, 913.

Morisawa, M. 1957. Accuracy of Determination of Stream Lengths from Topographic Maps. Transactions, American Geophysical Union. 38(1): 86-88.

Morisawa, M. 1985. Rivers: Form and Process. Longman Inc., New York. pp. 137-155.

Morse, S. P. 1968. A Mathematical Model for the Analysis of Contour-Line Data. Journal of the Association for Computing Machinery. 15(2): 205-220.

Moss, A. J., P. Green and J. Hutka. 1982. Small Channels: Their Experimental Formation, Nature, and Significance. Earth Surface Processes and Landforms. 7: 401-415.

Moss, A. J., P. H. Walker and J. Hutka. 1980. Movement of Loose, Sandy Detritus by Shallow Water Flows: An Experimental Study. Sedimentary Geology. 25: 43-66.

Mutchler, C. K. and C.E. Carter. 1983. Soil Erodibility Variation During the Year. Trans of the ASAE. 26: 1102-1104, 1108.

Myers, D. E. 1982. Matrix Formulation of Co-Kriging. Mathematical Geology. 14(3): 249-257.

Neibling, W. H., G. R. Foster, R. A. Nattermann, J. D. Nowlin and P. V. Holbert. 1981. Laboratory and field testing of a programmable plot-sized rainfall simulator. In Erosion and Sediment Transport Measurement. Proceedings of the Florence Symposium International Association of Hydrological Sciences. Publication No. 133. pp. 405-414.

Newland, D. E. 1975. An Introduction to Random Vibrations and Spectral Analysis. Longman Group Limited, London.

Novak, M. D. 1985. Soil Loss and Time to Equilibrium for Rill and Channel Erosion. Trans. of the ASAE. 28(6): 1790-1793.

O'Callaghan, J. F. and D. M. Mark. 1984. The Extraction of Drainage Networks from Digital Elevation Data. Computer Vision, Graphics and Image Processing. 28: 323-344.

Ogunlela, A., B. N. Wilson, C. T. Rice and G. Couger. 1989. Rill Network Development and Analysis Under Simulated Rainfall. ASAE Paper No. 89-2112, Presented at the ASAE Summer Meeting, Quebec City, Canada.

Onstad, C. A., J. K. Radke and R. S. Young. 1981. An outdoor portable rainfall erosion laboratory. In Erosion and Sediment Transport Measurement. Proceedings of the Florence Symposium. International Association of Hydrological Sciences. Publication No. 133. pp. 415-422.

Palacios-Vélez, O. L. and B. Cuevas-Renaud. 1986. Automated River-Course, Ridge and Basin Delineation from Digital Elevation Data. Journal of Hydrology. 86: 299-314.

Park, S. W., J. K. Mitchell and J. N. Scarborough. 1981. Soil Erosion Simulation on Small Watersheds. ASAE Paper No.: 81-2527.

Peucker, T.K. and D. H. Douglas. 1975. Detection of surface-specific points by local parallel processing of discrete terrain elevation data. Computer Graphics and Image Processing. 4: 375-387.

Peucker, T. K., R. J. Fowler, J. J. Little and D. M. Mark. 1978. The Triangulated Irregular Network. Proc. ASP-ACSM Symposium on DTM's, St. Louis, Mo. pp. 516-540.

Podmore, T. H. and L. F. Huggins. 1980. Surface Roughness Effects on Overland Flow. Trans of the ASAE. 23(6): 1434-1439, 1445.

Podmore, T. H. and L. F. Huggins. 1981. An Automated Profile Meter for Surface Roughness Measurements. Trans of the ASAE. 24(3): 663-665, 669.

Radke, J. K., M. A. Otterby, R. A. Young and C. A. Onstad. 1981. A Microprocessor Automated Rillmeter. Trans. of the ASAE. 24(2): 401-404, 408.

Rao, S. S. 1984. Optimization: Theory and Applications. Wiley Eastern Limited.

Rhind, D. 1975. A Skeletal Overview of Spatial Interpolation Techniques. Computer Applications. 2: 293-309.

Rice, C., B. N. Wilson and M. Appleman. 1988. Soil Topography Measurements Using Image Processing Techniques. Computers and Electronics in Agriculture. 3: 97-107.

Rodríguez-Iturbe, I. and J. B. Valdés. 1979. The Geomorphologic Structure of Hydrologic Response. Water Resources Research. 15(6): 1409-1420.

Rogers, W. F. and V. P. Singh. 1986. Some Geomorphic Relationships and Hydrograph Analysis. Water Resources Bulletin. 22(5): 777-784.

Rohlf, R. A. and M. E. Meadows. 1980. Dynamic Mathematical Modeling of Rill Erosion. Proceedings of the Symposium on Watershed Management. ASCE. Boise, Idaho. pp. 13-26.

Romkens, M. J. M., S. Singaryar and C. J. Gantzer. 1982. An Automated Noncontact Surface Profile Meter. ASAE Paper No.: 82-2620.

Sayler, M. A. and K. J. Fornstrom. 1986. Critical Tractive Force for Modeling Furrow Irrigation Erosion. ASAE Paper No.: 86-2086.

Schafer, R. L. and W. G. Lovely. 1967. A Recording Soil Surface Profile Meter. Agricultural Engineering. 48: 280-282.

Scheidegger, A. E. 1967. A Stochastic Model for Drainage Patterns into an Intramontane Trench. Bulletin, International Association of Scientific Hydrology 12: 15-20.

Schumm, S. A. 1983. Chp. 4. Fluvial Geomorphology. Stream Mechanics Short Course. Colorado State University. June 6-17, 1983.

Schumm, S. A. and H. R. Khan. 1972. Experimental Study of Channel Patterns. Geological Society of America Bulletin. 83: 1755-1770.

Schwab, G. O., R. K. Frevert, T. W. Edminister and K. K. Barnes. 1966. Soil and Water Conservation Engineering. John Wiley and Sons.

Seginer, I. 1969. Random Walk and Random Roughness Models of Drainage Networks. Water Resources Research. 5(3): 591-607.

Sharma, M. L., G. A. Gander and C. G. Hunt. 1980. Spatial Variability of Infiltration in a Watershed. Journal of Hydrology. 45: 101-122.

Shreve, R. L. 1966. Statistical Law of Stream Numbers. Jour. Geology. 74: 17-37.

Simanton, J. R., C. W. Johnson, J. W. Nyhan and E. M. Romney. 1985. Rainfall Simulation on Rangeland Erosion Plots. In Erosion on Rangelands: Emerging Technology and Data Base. Lane, L. J. (Editor). Proceedings of the Rainfall Simulator Workshop. Tucson, Arizona. pp. 11-17.

Spomer, R. G. and A. T. Hjelmfelt, Jr. 1986. Concentrated Flow Erosion on Conventional and Conservation Tilled Watersheds. Trans of the ASAE. 29(2): 489-493.

Steel, R. G. D. and J. H. Torrie. 1980. Principles and Procedures of Statistics. A Biometrical Approach. McGraw-Hill Book Company.

Strahler, A. N. 1964. Quantitative Geomorphology of Drainage Basins and Channel Networks. In Chow, V. T. (Editor). Handbook of Applied Hydrology. McGraw-Hill, New York. pp. 4-39 to 4-76.

Toriwaki, J. and T. Fukumura. 1978. Extraction of Structural Information from Grey Pictures. Computer Graphics and Image Processing. 7: 30-51.

Tubbs, L. J. and D. A. Haith. 1981. Simulation Model for Agricultural Non-point-source Pollution. Journal WPCF. 53(8): 1425-1433.

United States Department of Agriculture (USDA). Soil Conservation Service. 1985. Soil and Water Conservation Research and Education Progress and Needs. A report from the Soil Conservation Service to Research and Education Agencies and Organizations. March 1985.

Warrick, A. W. and D. E. Myers. 1987. Optimization of Sampling Locations for Variogram Calculations. Water Resources Research. 23(3): 496-500.

Warrick, A. W. and D. R. Nielsen. 1980. Spatial Variability of Soil Physical Properties in the Field. In Hillel, D. Applications of Soil Physics. Academic Press.

Wiberg, P. L. and J. D. Smith. 1987. Calculations of the Critical Shear Stress for Motion of Uniform and Heterogeneous Sediments. Water Resources Research. 23(8): 1471-1480.

Williams, J. R. 1975. Sediment-yield prediction with universal equation using runoff energy factor. In Present and Prospective Technology for Predicting Sediment Yields and Sources. ARS-A 40: 244-251.

Wilson, B. N. 1986. Erosion Modeling Using Minimization

Wilson, B. N. 1986. Erosion Modeling Using Minimization Principles. ASAE Paper No. 86-2044.

Wilson, B. N. and B. J. Barfield. 1986. A Detachment Model for Non-Cohesive Sediment. Trans of the ASAE. 29(2): 445- 449.

Wilson, B. N. and C. Rice. 1987. Large-Scale Laboratory Apparatus for Erosion Studies. ASAE Paper No.: 87-2096.

Wilson, J. P. 1986. Estimating the topographic factor in the Universal Soil Loss Equation for watersheds. Journal of Soil and Water Conservation. 41(3): 179-184.

Wischmeier, W. H. and D. D. Smith. 1978. Predicting Rainfall Erosion Losses--A guide to Conservation Planning. Agriculture Handbook No. 537. USDA--Science and Education Administration.

Wu, T. H., K. W. Bedford, M. E. Mossaad, K. L. McCurdy and E. M. Ali. 1980. A Stochastic Model of Soil Erosion. Project Completion Report No. 711523. Contract No. A - 056 - OHIO. State of Ohio. Water Resources Center. The Ohio State University.

Yang, C. T. 1971. Potential Energy and Stream Morphology. Water Resources Research. 7(2): 311-322.

Yates, S. R. and A. W. Warrick. 1987. Estimating Soil Water Content Using Cokriging. Soil Sci. Soc. Am. J. 51(1): 23-30.

Yost, R. S., G. Uehara and R. L. Fox. 1982a. Geostatistical Analysis of Soil Chemical Properties of Large Land Areas. I. Semi-variograms. Soil Sci. Soc. Am. J. 46: 1028-1032.

Yost, R. S., G. Uehara and R. L. Fox. 1982b. Geostatistical Analysis of Soil Chemical Properties of Large Land Areas. II. Kriging. Soil Sci. Soc. Am. J. 46: 1033-1037.

Young, R. A. and C. A. Onstad. 1978. Characterization of Rill and Interrill Eroded Soil. Trans. of the ASAE. 21(6): 1126-1130.

Zevenbergen, L. W. and C. R. Thorne. 1987. Quantitative Analysis of Land Surface Topography. Earth Surface Processes and Landforms. 12: 47-56.

Zingg, A. W. 1940. Degree and Length of Land Slope as it Affects Soil Loss in Runoff. Agricultural Engineering. 21: 59-64.

Zobeck, T. M. and C. A. Onstad. 1986. Tillage and Rainfall Effects on Random Roughness. ASAE Paper No.: 86-2014.

VITA

Ayodele Olanrewaju Ogunlela

Candidate for the Degree of

Doctor of Philosophy

Thesis: EROSIONAL DRAINAGE NETWORK: DEVELOPMENT AND ANALYSIS UNDER SIMULATED RAINFALL

Major Field: Agricultural Engineering

Biographical:

Personal Data: Born in Ibadan, Nigeria, August 24, 1958, the son of Daniel Folorunsho and Victoria Wuraola Ogunlela.

Education: Graduated from Ibadan Boys' High School, Ibadan, Nigeria, in June 1975; received Bachelor of Science Degree in Agricultural Engineering from the University of Ibadan, Ibadan, Nigeria, in June 1980; received Master of Science Degree in Agricultural Engineering from Iowa State University, Ames, Iowa, in May 1985; completed requirements for the Doctor of Philosophy Degree at Oklahoma State University in December 1989.

Professional Experience: Lecturer, Department of Civil Engineering, Federal Polytechnic, Ilaro, Nigeria, September 1981 to July 1982; Graduate Research Assistant, Department of Agricultural Engineering, Iowa State University, Ames, Iowa, August 1983 to December 1984; Teaching Assistant, Department of Agricultural Engineering, Oklahoma State University, September 1985 to December 1985, and September 1986 to December 1986; Graduate Research Assistant, Department of Agricultural Engineering, Oklahoma State University, January 1986 to November 1988.

Professional and Honorary Organizations: Associate Member, American Society of Agricultural Engineers; member, Alpha-Epsilon, Honor Society of Agricultural Engineering.